Sexual Dimorphism of the Thoracic Vertebrae in a Modern Cretan Population:

A Comparison of the Individual Vertebrae in Terms of Accuracy in Estimating Sex

LAURA GAMBARO

A thesis submitted in partial fulfilment of the requirements of Bournemouth University for the degree of Master of Philosophy

October 2013

Bournemouth University

Abstract

Estimation of sex is one of the first steps when developing a biological profile for recovered human remains. Several studies have been concerned with sexual dimorphism in the human vertebrae in general, yet few are concerned specifically with the thoracic vertebrae. This thesis examines the presence and extent of sexual dimorphism in the thoracic vertebrae of a documented Greek population from the island of Crete, and establishes a method for sex assessment.

A total of 16 linear measurements were taken from all twelve thoracic vertebrae, using a sample of 70 adult individuals. Out of the 16 measurements, the minimum number of dimorphic variables in a vertebra was eleven. The univariate discriminant function analysis yielded results with up to 89.4% total accuracy. Using a stepwise method of discriminant function analysis, two variables in T1 predicted sex with 90.6% total accuracy.

In comparison to previous research on other vertebrae, the current study yielded similar results in terms of accuracy and significance of individual variables. Nevertheless, comparative data for thoracic vertebrae are only available for T12. The applicability of this method to other collections cannot be drawn, as no similar studies exist. It is concluded that the thoracic vertebrae of the Greek population are sexually dimorphic and that the method used in this study shows great potential. Nevertheless, it needs to be tested in other populations in order to further evaluate its applicability.

TABLE OF CONTENTS

LIST OF TABLES

LIST OF FIGURES

Acknowledgement

First and foremost, I wish to thank Prof. M. Michalodimitrakis and Dr. E. Kranioti for allowing me access to their collection. A special "thank you" to Dr. Kranioti, who endured endless questioning sessions, not only in regards to statistics, and helped me to find back on track on several occasions.

I would also like to express my gratitude to the people at Bournemouth University: Dr. M. Smith for his patience and input, and Prof. H. Schutkowski for his knowledge and wise words. Without their support, I would have not been able to complete my thesis. Finally, a very special "thank you" to Louise Pearson, who always seemed to have the solution in times of crisis.

I am especially happy to thank Dr. D. Nathena, who has not only became a friend, but helped me in ways she does not even know.

Another big "thank you" to my friends and family: My parents, for their belief and support, and my friends for tolerating my mood swings for so long. Σ' αγαπάω, μωρό μου. Είσαι ήρωας!

Thank you all!

1 Introduction

The main focus of forensic anthropology lies in the identification of unknown human remains as well as in the interpretation of the evidence related to death (Klepinger 2006).

In recent deaths, identification may be a quite simple task but in some cases, the remains are recovered in an advanced state of decomposition, are incomplete, burned or otherwise severely mutilated. In these cases, identification relies on the biological profile gathered through the examination of the skeletal remains.

In a forensic setting, the identification process of an individual includes estimation of age, stature, ancestry, and sex. Knowing sex is of particular importance as possible matches can be decreased by 50% (İşcan & Loth 1997). However, the reliability of sex determination depends greatly on the available bones and on their condition. The two approaches used to determine sex can rely on the inspection and evaluation of morphological traits, and/or on the metric assessment of skeletal measurements. In cases where the pelvis or skull is available and intact, the examination of the morphological characteristics can predict sex with accuracies up to 95% (Purkait & Chandra 2004). Unfortunately, recovered remains are often incomplete, broken or have been exposed to extreme environmental conditions, making it impossible to examine visual markers. It is therefore necessary to further develop metric methods, especially for bones that do not show directly observable traits, such as the vertebrae (Hou et al. 2011).

Previous research on vertebrae has showed promising results in determining sex, reaching accuracies up to 94.2% (see Hou et al. 2011). Nevertheless, most of the thoracic vertebrae have so far been neglected in previous research.

As no similar study has been carried out on the Greek population, the present study investigates 70 individuals from a Cretan documented collection, and aims to identify and determine the degree of sexual dimorphism in all twelve thoracic vertebrae. In addition, if sexual dimorphism is found to exist, the gathered data shall provide aid in the identification of sex, as well as population-specific osteometric data for future studies.

2 Thematic Research

2.1 History of Forensic Anthropology

Forensic anthropology's origin in the United States can be traced back to 1849, to the murder of George Parkman. Oliver Wendell Holmes and Jeffries Wyman, both anatomy professors at Harvard University during that time, were asked to assist in an investigation regarding a dismembered body and a burnt head in a furnace. Holmes and Wyman used the dentures found in the furnace to identify Parkman's remains (Ingle 1991). Three decades later, Thomas Dwight, a Harvard anatomy professor, became the first American anatomist researching issues relative to forensic anthropology (Ubelaker 2006). A notable contribution was his publication “The Identification of the Human Skeleton, a Medicolegal Study” in 1878 (Thomas 2003). This publication might be the reason for Dwight being credited as the "father" of forensic anthropology in the United States. Another important figure in this early era was Harris Hawthorne Wilder, a professor of zoology at Smith College in 1892, with a great interest in human anatomy. The duality of interests resulted in two publications concerned with new developments in human identification: One was facial reconstruction on skulls, and the other was dermatoglyphics, the study of fingerprints (Stewart 1982). Besides the Parkman murder in 1849, the case of Adolph Louis Luetgert is frequently mentioned in regards to the history of forensic anthropology. George A. Dorsey, a PhD student of anthropology at Harvard, served as an expert witness during this so-called Luetgert case in 1897. Adolph Louis Luetgert was accused of killing his wife and dissolving her remains with the use of acid in a vat at his sausage factory. Four small fragments were recovered, which Dorsey identified as human, originating from the foot, hand, and rib. Due to his testimony, Luegert was convicted of murder (Quintyn 2010).

A later key player was Alex Hrdlička, who became the first curator of the physical anthropology division at the Smithsonian Institution in Washington, DC. Hrdlička (1869-1943) is probably best known as the founder of the American Journal of Physical Anthropology, and the American Association of Physical Anthropologists. Furthermore, his expertise in various legal cases led to the establishment of a continuous collaboration between the Smithsonian Institute and the Federal Bureau of Investigations (Brickley & Ferllini 2007). The first physical anthropologist with a full-time teaching position in the United States was Earnest A. Hooton (1887-1954). While working at Harvard, he trained several of the future presidents of the American Association of Physical Anthropologists (Spencer 1981). Another important figure during the period of Hrdlička and Hooton was T.

Wingate Todd. Born in England and trained as an anatomist, he moved to the United States in 1912 to take Dr. Carl Hamann's teaching position at the Western Reserve University. As the Ohio state law allowed professors to retain cadavers dissected by medical students, Hamann and Todd were able to begin an anatomical collection. Until his death in 1938, Todd had built and researched a collection of 3000 documented individuals (Tersigni-Tarrant & Shirley 2013).

During the period of 1950 to 1960, the departments of anthropology began to include physical anthropology in their graduate programs. Most of these programs were organized by former students of Hooton, with the exception of the University of Pennsylvania, which was formalized by Wilton M. Krogman, a former student of T. Wingate Todd (Spencer 1981). Krogman produced the first textbook in forensic anthropology, The Human Skeleton in Forensic Medicine in 1962. Focusing on the practical application of human osteology to forensics, his work soon became a primary reference in the field of forensic anthropology (Tersigni-Tarrant & Shirley 2013). One of Krogman's students was William M. Bass. After his graduation from Pennsylvania, Bass taught at the University of Tennessee where he founded the first forensic anthropology research facility in the U.S., better known as "The Body Farm". Finally, forensic anthropology was officially incorporated in the field of forensic medicine in 1972 through incorporation of physical anthropology into the disciplines acknowledged by the American Academy of Forensic Sciences. ABFA (the American Board of Forensic Anthropology) was formed five years later with the task to "encourage the study of, improve the practice of, establish and enhance standards for, and advance the science of forensic anthropology and to encourage and promote adherence to high standards of ethics, conduct, and professional practice in forensic anthropology".

The roots of forensic anthropology in Europe can be traced back to 1755 where Jean-Joseph sue, instructor of art anatomy at the Louvre in Paris, published measurements taken from cadavers. Even though his intention was to provide artists with accurate data regarding body proportions, his work lead to additional research on stature calculation. Matthieu-Joseph-Bonaventure Orfila added to Sue's database with a publication of his own measurements. For many years, the two databases became the sources used by the medicolegal community regarding evaluation of stature. A century later, Paul Broca, a surgeon and anthropologist, founded the world's first official organization of physical anthropology, the Société d'Anthropologie de Paris. Broca is also credited as the developer of the osteometric board, stereograph, and goniometer. Other contributors during this time were Etienne Rollet and Leonce Manouvrier. An early English contribution was made by Karl Pearson's regression

theory. He used Rollet's long-bone cadaver length data presenting them in regression equations (Ubelaker 2006).

Not all countries recognize forensic anthropology as a discipline, and where recognized, the variation between the groups of practitioners is remarkable. While most forensic anthropologists in Britain, Denmark and Portugal are based in academic institutions, Spain and Hungary employ specialists in government organizations. Until today, the U.K. remains the only European country with an official accreditation for forensic anthropologists (Brickley & Ferllini 2007). The Council for Registration of Forensic Practitioners (CRFP), established in 2001, developed an accreditation system that allowed eligible practitioners to register. Nevertheless, CRFP ceased operating in 2009, just few years after its establishment, ending also the accreditation for forensic anthropologists in the UK (Kranioti & Paine 2011). A new accreditation system has been ratified in June 2013, supported by the Royal Anthropological Institute (RAI) serving as the overall governing body. The system is similar to the one followed by the American Board of Physical Anthropologists and includes 3 accreditation levels.

2.2 Uses and Application of Forensic Anthropology

When confronted with skeletal remains, the forensic anthropologist is faced with four initial questions: Determination of sex, estimation of age and stature, and the assessment of ancestry. The following chapters will provide an overview of the methods used for these tasks:

2.2.1 Estimation of sex

Determining sex is usually the first step in the development of a biological profile, as sex is necessary in order to make ancestry, age and stature estimations. Nearly all bones of the human body have been used to develop methods for sex estimation, with varying results. Generally, the pelvic girdle, skull and long bones are the preferred anatomic regions when estimating sex. Sexual dimorphism and estimation of sex is discussed in detail in Chapter 3.

2.2.2 Assessment of ancestry

When determining ancestry, the skull remains the most reliable part of the human skeleton (İşcan 1988) as it has several features that assist as indicators in regards to ancestry. But

even though the identification of ancestry continues to be a central focus in forensic anthropology, the utility within science has been questioned (Pickering 2009). Nevertheless, in a multi-ethnic society - such as the United States - ancestry must be declared on numerous documents and identification papers, using the terms "Asian", "Black", "American Indian", "White/Caucasian" or "Unknown". Even though such identification can help to narrow down the search of a missing person, such a statement can also cause confusion. İşcan (1988) points out that terms such as "Asian" completely ignore the fact that 30% of the inhabitants of Asia are in fact "Caucasoid". Generally, the skull provides by far the most informative visual traits in regards to ancestry assessment (Klepinger 2006).

2.2.3 Estimation of age

The most challenging of the four identifiers is the estimation of age at death (İşcan 1988). The physiological age is usually assessed first and then correlated with the chronological age. Next to the teeth, the stage of epiphyseal union is probably the most important indicator when estimating age, keeping in mind that different epiphyses provide different levels of accuracy. While the different stages of ossification or development and formation of the teeth can provide valuable information in regards to age in sub-adults, the estimation of age in adults is a much more difficult task as the morphological variations are subtle. One of the most reliable methods here is the Suchey-Brooks method, which compares the symphyseal surfaces of the pubis of the os coxae in order to categorize them in one of six age groups (Brooks & Suchey 1990). Similar methods have been developed using the auricular surface of the ilium (Lovejoy et al. 1985, Buckberry & Chamberlain 2002), and the sternal end of the 4th rib (İşcan et al. 1984). Another method used to determine age in adults is quantitative bone histology (Kerley et al. 1978, Stout et al. 1994). The technique is destructive, but there are methods that are minimally invasive. Given the appropriate expertise, quantitative bone histology is one of the more accurate methods for estimating age (Franklin 2010).

2.2.4 Estimation of stature

Stature is usually estimated by comparing the lengths of certain bones to tables of published data or through the use of regression formulae (İşcan 1988). Another method reconstructs stature by summing up the measurements from the different skeletal parts, which contribute to height, adding a correction factor for the soft tissue (Fully1956). Before estimating stature, sex, age and ancestry must be determined as stature varies with these variables. The femur, tibia, fibula, humerus, ulna and radius are the most commonly used bones for stature estimation and various formulae have been developed for these bones. An approach was

made to explore femoral osteon geometry in relation to height. Unfortunately, the results did not show any significance (Britz et al. 2009).

2.2.5 Other applications

Although traditionally, forensic anthropologists were mainly involved in the reconstruction of the biological profile of an individual and the investigation of possible trauma and pathology, current applications are more complicated. Forensic anthropologists today may be involved in mass grave investigations and asked to give an opinion on possible torture, or are challenged with highly fragmented and decomposed individuals where the task may be to separate human from animal remains, associating body parts, etc. Furthermore, image analysis and facial recognition from video surveillance cameras (Tome et al. 2013), facial approximation (Stephan et al. 2006), gait analysis (Lynnerup & Vedel 2005, Larsen et al. 2008) and vein pattern analyses (Lee 2012) are only a few of the many new tasks a forensic anthropologist may be challenged with.

2.3 Anatomy of the Vertebral Column

Before an examination of the thoracic vertebrae can be initiated, a more in-depth understanding of the morphology of the vertebral column is necessary. The following chapter intends to provide an overview.

The adult vertebral column consists of 26 bones, and is - from top to bottom - divided into five distinct sections: cervical, thoracic, lumbar, sacrum and the coccyx. Every section consists of a group of individual vertebrae:

- 7 cervical vertebrae
- 12 thoracic vertebrae
- 5 lumbar vertebrae
- 5 sacral vertebrae
- 3-5 coccygeal vertebrae

The vertebrae are numbered from the cervical spine to the lumbar spine:

- Cervical vertebrae are the vertebrae of the cervical spine and are named beginning from the first cervical vertebrae with C1 to C7.
- Thoracic vertebrae are the vertebrae of the thoracic spine. They are referred to as T1 to T12.
- Lumbar vertebrae are the vertebrae of the lumbar spine from L1 to L5.

Looking at the spine from a lateral view, it is apparent that the individual sections of the spine are formed differently: The cervical and lumbar spine has a ventral curvature, while the thoracic spine and sacrum bend dorsally. This results in the appearance of a double S-shaped curvature. This special form of the human spine fulfils the purpose of minimizing and distributing the shocks that occur naturally in walking upright (White & Folkens 2005). With the exception of the first and second cervical vertebrae, and the fused vertebrae of the sacrum and coccyx, two adjacent vertebrae are always connected together by a disc, which is located between the two vertebral bodies. The disc itself consists of connective tissue with a relatively rigid outer ring and an elastic soft inner core. Tasks of the intervertebral discs are the muting of bumps and concussions as well as the flexible connection of the individual vertebrae.

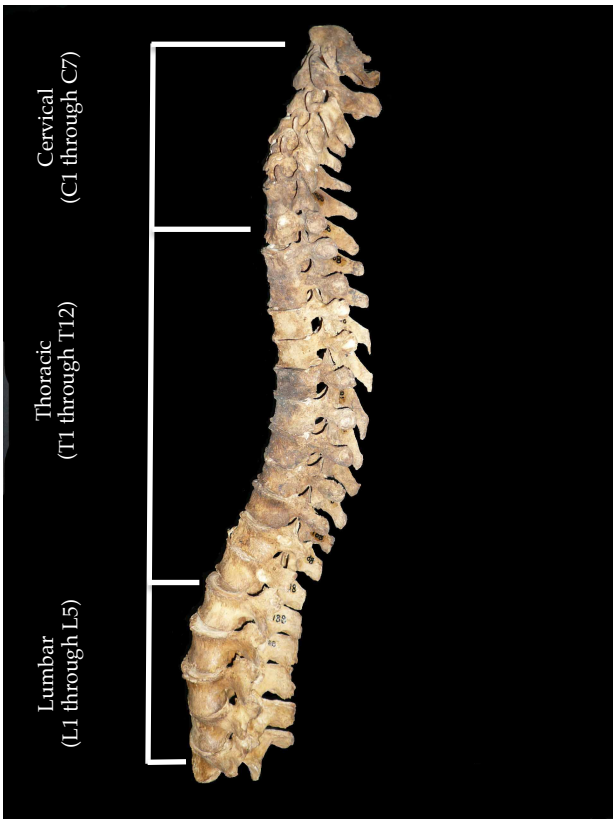

Figure 1: Curvature of the spine, lateral view (author's image)

Even if the individual vertebrae in the different areas of the spine appear somewhat different from each other, the general structure remains the same in all sections: Each vertebra (with exception of C1) consists of a vertebral body, adjoined by the bony vertebral arch. This results in a cavity in the centre of the vertebrae. The totality of these cavities forms the spinal canal, which holds the spinal cord. On each side of the vertebral arch arises a transverse process and on the back the spinous process. These bony projections serve as insertion points for ligaments and muscles. To ensure a stable contact of each vertebra with its adjacent vertebrae, they are linked together by facet joints. Two processes, the pedicles, are located on either side of the superior part of the vertebral body, and connect to the vertebral arch. In the case of the axis, the pedicles connect to the odontoid process, while the atlas lacks pedicles completely (White & Folkens 2005, Standring & Gray 2005).

2.3.1 The Cervical Spine

This part of the vertebral column consists of seven vertebrae, located in the neck area. The cervical vertebrae are positioned most superiorly, have large transverse foramina, and smaller (oval or heart shaped) bodies when compared to the thoracic or lumbar vertebrae. They can easily be recognized by the foramen in their transverse processes (see Figure 4). Compared to the bones of the lumbar spine, they are relatively small and delicate. Nevertheless, the delicate structure is sufficient to support the weight of the head.
The vertebrae are numbered from the skull down. The first two cervical vertebrae, which are directly below the skull, differ in structure from the remaining vertebrae. The first cervical vertebra, which is also called atlas (see Figure 2), does not have a vertebral body. It is, simplified, only a bony ring. Together with C2 (also called axis), it forms the atlanto-axial joint allowing lateral rotation of the axis and the skull. The atlas does not have a spinous process, but a posterior tubercle at the midpoint of the posterior arch. The masses lateral of the ring provide support for the articular facets. These superior articular facets allow articulation with the base of the skull (White & Folkens 2005, Standring & Gray 2005).

Figure 2: Atlas, superior view (author's image)

Figure 3: Dens of the Axis, anterior view (author's image)

The mobility of the skull results from the specific articulation of the atlas with the second cervical vertebra, the axis (see Figure 3). The axis is built almost exactly like every other vertebra. Its distinctiveness however is a projection, a bony prominence facing towards the skull called odontoid process or "dens" which is Latin for „tooth“. This „dens“ projects into the vertebral foramen of the first cervical vertebra. Through this connection, turning movements of the head are possible. In order to prevent the „dens“ and first cervical vertebra

to shift against each other, the "tooth" is held in position by a strong ligament on the inside of the atlas (White & Folkens 2005, Standring & Gray 2005).

Figure 4: Cervical vertebra, superior view (author's image)

2.3.2 The Thoracic Vertebrae

The thoracic part of the vertebral column is composed of twelve vertebrae, named according to their anatomical position, the thorax. As the thoracic vertebrae form a transition between the cervical and the lumbar vertebrae, the lower four thoracic vertebrae show more features of a lumbar vertebra. The bodies are larger, and the transverse and spinous processes appear more robust. The main characteristics of the thoracic vertebrae are the costal articular facets (foveae) lateral to the body and transverse processes in order to articulate with the ribs. Through this second contact point, the rib is stabilized. Typical for the thoracic vertebrae are the very flat superior and inferior articular facets, the long spinous processes, and the prominent transverse processes (White & Folkens 2005). The spinal canal is filled almost completely by the spinal cord. In the lower thoracic area, just like in the cervical spine, a "thickening" of the spinal cord can be found. The nerves to the legs pass through this section. T1 (the first thoracic vertebra) has a whole articular facet for the rib on either side of the vertebral body, and half a facet (or demi-facet) inferiorly for the upper half of the second rib (see Figure 5). The vertebral body is similar to that of a cervical vertebra. Within the thoracic vertebrae, T1 can easily be recognized by the long and thick spinous process, which is directed almost horizontally (Standring & Gray 2005).

Figure 5: T1, superior view (author's image)

T10 provides a complete articular facet on either side, placed superiorly on the vertebral body (see Figure 6). T11 is in appearance closer to a lumbar vertebra. The large articular facets for the heads of the ribs are placed on either side of the vertebral body. The tubercles of the ribs connect to facets on the transverse processes of the thoracic vertebrae, with exception of T11 and T12. The spinous and transverse processes are very short and do not provide articular facets (Standring & Gray 2005). The twelfth thoracic vertebra (T12) has a similar appearance as T11, but the inferior articular facets assume the appearance of the lumbar vertebrae (White and Folkens 2005).

Figure 6: T10, lateral view (author's image)

2.3.3 The Lumbar Vertebrae

The five lumbar vertebrae carry most of the body weight. Therefore, they are built relatively large. The lumbar vertebrae have massive bodies with robust transverse and spinous processes, and are quite easy to identify. They also contain mammillary and accessory processes on their bodies, which are sites of attachment of deep back muscles (see Figure 7). The lumbar vertebrae - like the thoracic and cervical vertebrae - increase in size from superior to inferior, and are the largest of all (unfused) vertebrae. The spinal cord ends in the upper part of the lumbar region, usually at the level of the first or second lumbar vertebra. However, the nerves of the legs and pelvis continue from the lower end of the vertebral canal of the lumbar spine. The nerves leave the spinal canal on different levels. Due to the increased load in this particular area, signs of wear such as joint deterioration or herniated discs are not uncommon (White & Folkens 2005, Standring & Gray 2005).

Figure 7: Lumbar vertebra, superior view (author's image)

2.3.4 The Sacrum and the Coccyx

The sacrum is located at the base of the spine and consists of five vertebrae, which begin to fuse between ages 16-18 (see Figure 8). The sacrum composes, together with the right and left os coxae, the pelvic girdle, and is - by definition - classified as part of the vertebral column. The sacrum articulates superiorly with L5, laterally with the ilium, and inferiorly with the coccyx (Klepinger 2006, White & Folkens 2005).

The coccyx of humans corresponds to the tail skeleton of other vertebrates, and articulates with the sacrum. It consists of three to five fused vertebrae, and serves as an attachment point for a number of ligaments and muscles (White & Folkens 2005, Standring & Gray 2005).

Figure 8: Sacrum, anterior view (author's image)

3 Sexual Dimorphism

As mentioned earlier, determining sex is usually the first step in the development of a biological profile, and nearly all bones of the human body have been used to develop methods for this purpose. The following chapters shall provide an overview on these methods, as well as the different bones investigated.

3.1 Methods

A first approach in understanding sexual dimorphism in humans was to determine gross morphological features, such as the pelvic brim, the supraorbital ridges or the shape of the forehead and mastoid process. The observed differences in these visual features are compared in order to establish the differences between males and females. The most distinguishing visual difference between males and females can be seen in the architecture of the pelvic girdle. This is simply due to the fact that females are able to bare children, and males are not (Pickering & Bachman 2009).

A solely morphological approach in sexing skeletal remains can be somewhat problematic, as an accurate classification relies on the experience of the examiner (Spradley & Lantz 2011). The condition of the remains as well as the degree of sexual dimorphism in different populations may further complicate identification. If skeletal remains are damaged or incomplete, a morphological analysis of the preferred bones may not be carried out as it is based on specific visual landmarks in order to determine sex. In such cases, osteometry is used, as a large number of studies have been developed for this method on almost every bone of the human body.

One of the first osteometric studies was carried out by Washburn (Washburn 1948). Using the length of the ischium, and the length of the pubis, he calculated the ischio-pubic index that gave him accuracy rates of up to 90% in determining sex correctly. Other osteometric studies by Pons (1955), Thieme & Schull (1957), DeVilliers (1968) and Singh (1974) followed, yet until one concern remains until today: The appearance of sexual dimorphism varies greatly between populations. As any standard osteometric study produces a discriminant function formula specific to that dataset, it should only be applied to this known population.

3.2 Sexual dimorphism in the human skeleton

Even though most skeletal elements show a certain degree of sexual dimorphism, some bones are better estimators of determining sex than others. If an entire skeleton is present for estimating sex, many different methods and processes are available, and positive identification may not be such a difficult task. On the other hand, determining sex in individuals who have not yet reached maturity is a far more complex task. Taylor and Twomey (1984) performed three studies, using different measurement techniques, in order to prove that female spine grows more in length than the male spine between the ages of nine and 13. But even though their studies prove sexual dimorphism in children, the age of the individuals was known. No accurate method has yet been developed in order to determine sex of an unknown individual who has not yet reached skeletal maturity.

3.2.1 Pelvis

The most reliable bone to determining sex in adults is the os coxae and can achieve approximately 90% accuracy when used alone. The methods used are through visual observation of morphological traits or metric analysis (Bytheway & Ross 2010). The visual morphologic method developed by Phenice (1969) remains one of the most accurate. Using the ventral arc, the subpubic concavity, and the medial aspect of the ischio-pubic ramus, Phenice achieved an accuracy of 95%. Even though research focused more on morphological characteristics, a study by Schulter-Ellis et al. (1985), using two metric variables, showed that sex was determined correctly in 98% of the cases. A more recent study by Patriquin et al. (2005) examined a collection of 400 South African individuals using nine measurements, and reached an overall accuracy of 86% in determining sex correctly. The most dimorphic measurements were the ischial length in whites, and the acetabular diameter in blacks. The findings reiterated the necessity of population and ancestry specific standards. Another study by Bytheway and Ross (2010) used the left os coxae of 200 individuals from the Terry Collection and identified thirty-six landmarks, which were then digitized. The gathered shape variables were then used in the multivariate analyses. Results reached from accuracies between 98%-100%. In general, the high accuracy in adult pelvises can be explained due to basic biological differences in males and females.

3.2.2 Skull

Next to the pelvis, the skull is a very reliable indicator of sex, and the single most studied bone in forensic anthropology (Krogman & İşcan 1986). Krogman (1955) published a study, presenting 14 morphological traits, which could be used to distinguish male from female skulls. More traditional studies are concerned with morphological traits while more recent studies incorporate analytical methods to metric data. As features may depend on occupation, race or nutrition, the morphological approach tends to be unreliable. Even though males are generally larger and more robust compared to females, sexual dimorphism in the human skull is not as significant in terms of morphology. Nevertheless, there are morphological traits such as the mastoid process, the mental eminence, or the supra-orbital margin and ridge, which can be useful indicators in determining sex (Buikstra & Ubelaker 1994). Spradley and Jantz (2011) compared the effectiveness in determining sex of cranial and postcranial elements. The results showed that the postcranial elements performed better than the skull, which did not exceed accuracies of 90%. A study of Deshmukh and Devershi (2006) using 74 adult skulls of Indian origin supports these findings. Using 16 parameters, their results showed an overall accuracy of 87% in classifying males and females correctly.

3.2.3 Long Bones

The postcranial skeleton has been well studied in terms of sex estimation, even in incomplete skeletal remains. One of the most studied bones in these terms is the humerus. As osteometric methods are population specific - in terms of sex identification - researchers have tried to conduct studies in order to establish standards for individual populations. Few studies exist on sex identification based on visual traits. Rogers (1999) used four morphological features of the posterior, distal humerus to determine sex. The method was developed using individuals from the Toronto Grant Collection, and was afterwards tested on 93 individuals from the Bass Collection, and 35 individuals from the University of New Mexico. The study reports an accuracy of 92%. Worth mentioning is the fact that the research did not include African-American individuals. This fact may explain the high accuracies as sexual dimorphism is more easily discerned within discrete populations than between members of differing populations. Rogers' (1999) technique was later re-evaluated by Falys et al. (2005), using 351 humeri from a documented collection of St. Bride's, London. The results yielded an overall accuracy of 79%.

A metric study of long bones of the upper limb found the humeral length to be the most discriminatory indicator for estimating sex (Holman & Bennett 1991). The sample consisted of 302 individuals of the Terry collection, and five measurements of the long bones of the

upper limb were chosen. Accuracies resulted between 85%-92%. In comparison, a study of 143 individuals from the Anatomical Institutes in Munich and Cologne, found the head diameter to be the most discriminant value, achieving 93% accuracy in combination with the epicondylar breadth (Mall et al. 2001).

An analysis of Berrizbeitia (1989) including 1108 radii from the Terry Collection resulted in 96% accuracy, measuring the maximum and minimum diameters of the head. Another study of the Terry Collection was carried out by Holman and Bennett (1991). The result of the 2 measurements (maximum length and semistyloid breadth) analysed provided accuracy rates in predicting sex correctly between 72% for males and 92% for females. A more recent study by Barrier and L'Abbé (2008) used a South African sample of 400 radii determined the minimum midshaft diameter as the best discriminatory variable (86%). When applying all measurements, the classification accuracy reached 88%.

Using three measurements from the proximal epiphysis of the ulna, Purkait (2001) classified sex correctly in 85% of the cases, applying only one measurement.
A later study by Barrier et al. (Barrier et al. 2008) took eight measurements from 400 ulnae of a South African sample. Cross-validated results showed accuracies between 83%-89%.

As the femur is basically the heaviest and longest bone of the human skeleton it is often recovered and in good condition. For these reasons, there are numerous existing studies in terms of sexual dimorphism in the femur. An early study by Dittrick and Myers Suchey (1986) analysed the femora of 370 prehistoric individuals, focusing on two femoral measurements: Maximum head diameter and bicondylar width. The results showed an overall accuracy of 90%. It has to be mentioned that sex was previously assessed using traits of the os pubis, questioning the accuracy of the outcome. King (King et al. 1998) determined the combination of the maximum head diameter and bicondylar breadth to be the best indicator when determining sex from the femur, yielding 94.2% accuracy. When using only one variable, bicondylar breath showed the best performance with an accuracy of 93.3%. The study also concluded that Thais differ greatly from whites and blacks in metric terms. This conclusion underlines once again the necessity of population-specific methods for sex identification.

A study performed with 280 adult Indian femora estimated sex using four measurements, taken from the femoral head, subject to discriminant function analysis (Purkait 2003). The maximum vertical and horizontal diameter showed to be the best single discriminator each reaching an accuracy of 92.1%. His following study introduced a method using three

dimensions. This method reached an even greater accuracy. Using the combination of these three measurements, sex was predicted correctly in 86.4% of the cases (Purkait 2005). Brown (Brown et al. 2007) used the method as defined by Purkait (2005) and tested it on a collection of 200 Indo-European and African American adult femora from the Terry Collection. The head diameter alone predicted sex correctly in 85.5% of the cases, in combination with the proximal end of the femur, the accuracy increased to 90%.

İşcan et al. (1984) used the tibial length, and circumference, antero-posterior, and transverse measurements at the nutrient foramen level to determine sex. An average of 80% accuracy was reached using the circumference alone. If other dimensions were added, the accuracy increased about 4%. In a following study, Holland (1991) examined 100 individuals from the Hamann-Todd Collection, applying five measurements to the proximal end of the left tibiae. The outcome of the linear regression equations achieved classification accuracies between 86%-95%. A test sample of another 20 individuals from the Hamann-Todd collection allowed correct classification of sex in 85%-100% of the cases. Applying the method on a prehistoric sample, previously sexed using the crania, the classification range was also between 85%-100%.

In a study carried out by Kieser et al. (1992), 100 tibiae of Caucasoids and 102 tibiae of South African blacks were examined, taking five measurements on the proximal end of each tibia as previously defined by Holland (1991). Through multivariate analysis, and stepwise discriminant function analysis, they were able to correctly identify sex and allocate to the individual group with an accuracy range between 84.6%-92%.

The fibula is one of the least studied bones in forensic anthropology. This may be due to the fact that it is rarely recovered intact due to its fragility (the proximal end being filled with spongy bone). Nevertheless, Sacragi and Ikeda (1995) carried out a study using a collection of 71 Japanese individuals and found the distal end of the fibula as a reliable source in determining sex. Using five measurements, sex was correctly identified in 90.6% of the cases.

3.2.4 Other Bones

Tague (2007) examined the costal process of the first sacral vertebra for sexual dimorphism. His sample consisted of 197 individuals of male and female American blacks and whites from the Hamann-Todd and Terry Collections. Besides the finding that measurements taken

from males were significantly larger than the ones taken from females, females also showed to generally have a longer costal process.

Robling and Ubelaker (1997) examined the metatarsals of 110 individuals from the Terry Collection using 6 measurements. As a result, sex was classified correctly between 83 to 100%. Mountrakis et al. (2010) used 186 individuals from the Athens collection defining seven measurements, which were taken from all metatarsals. The accuracy ranged between 77.9%-87.3%, while the right metatarsal I showed to be the best indicator when determining sex.

Several studies have been concerned with the issue of determining sex from measurements in metacarpals, and differ mainly in terms of the specific metacarpals used, the origin of the population sample. Most studies examined the metacarpals only, with few exceptions: In addition to the metacarpals, Scheuer and Elkington (1993) included the first proximal phalanx in their research, while Smith (1996), as well as Case and Ross (2007) also included all phalanges.

In their study, Scheuer and Elkington (1993) defined six measurements for each of the metacarpals; interarticular length, medio-lateral width of the base, antero-posterior width of the base, medio-lateral width of the head, antero-posterior width of the head, and maximum midshaft diameter. Using a cadaveric sample of 60 individuals of British ancestry, Scheuer and Elkington (1993) predicted sex correctly with accuracy rates between 74%-94%, while metacarpal I showed to be the best predictor. Barrio (Barrio et al. 2006) used a sample of 79 individuals from the Complutense University of Madrid, and applied 8 dimensions previously defined by Scheuer and Elkington (1993), Falsetti (1995), and Smith (1996). The accuracy ranged between 81% for the right metacarpals IV and V, to 91% for the left metacarpal II.

In a recent study, Manolis et al. (2009) applied seven dimensions, previously defined by Smith (1996), Falsetti (1995), Scheuer and Elkington (1993), and Musgrave and Harneja (1978), to a Greek population (n=151) from the Athens Collection. Accuracies ranged between 79.6%-88.9% for the left, and 80.2%-88.9% for the right metacarpals, with the highest discriminations found in the left metacarpal I, and the right metacarpal V.

A study of a Turkish collection of 78 females and 173 males using the 4th right rib resulted in up to 89% accuracy (Kocak et al. 2003). An Italian study of the talus and calcaneus using a sample of 118 northern Italian skeletons, classified sex correctly with up to 96% accuracy

(Talus). Interesting was the fact that most southern Italian males were misclassified as females when the validity of the discriminant function equations were used in an independent sample of individuals of different origin (northern AND southern Italy), confirming the population-specificity of discriminant function equations (Gualdi-Russo 2007).

3.2.5 Sexual Dimorphism of the Cretan Collection

In Greece, there are currently two modern collections available for research purposes: The Athens collection, and the Cretan collection. Both collections consist of Greek individuals, the distinctions Athens or Cretan is mainly made to identify the two collections.

The Athens collection consists of 225 individuals born in different parts of Greece. 114 of the 225 individuals have complete records of age, sex, cause of death, occupation and place of birth (Kranioti 2009). A detailed description of the Cretan collection is provided in Chapter 4.1.

Since its establishment, the Cretan collection has served as the source of several population-specific studies: Kranioti et al. (2008) studied the craniofacial characteristics, taking 16 dimensions of a total of 90 males and 88 females in order to investigate sexual dimorphism in the Greek population. Results yielded accuracy rates up to 88.2%.

In 2009, Kranioti & Michalodimitrakis (2009) created a sex identification technique applying six defined variables (maximum length, vertical head diameter, midshaft maximum diameter, midshaft minimum diameter, mid- shaft circumference, and epicondylar breadth) on a sample of 168 left humeri. The means in males and females differed significantly, and sex was correctly identified in up to 92.9% of the cases.

Another study of the humeri used a total of 97 individual radiographs, defining eleven landmarks on the proximal and distal parts. Multivariate discriminant function analysis provided results with up to 89.7% accuracy (Kranioti, Bastir et al. 2009).

The same year, another study by (Kranioti, Vorniotakis et al. 2009) measured and radiographed 36 males and 34 female femora. The stepwise discriminant function yielded an accuracy rate of 92.9% in determining sex. The generated formula was then used in order to develop a sex identification software by incorporating it into a Java application. The

software was then tested with a sample of 36 femoral radiographs, producing an accuracy rate of 91.7%.

Steyn et al. (2009) investigated the occurrence of healed trauma in the Cretan collection, as well as the Pretoria Bone and Raymond Dart collections. Fractures of the rib, femur and radius were the most common in the Greek collection, while 46% of the females and 42% of the males showed to have at least one fracture.

Papaioannou et al. (2012) estimated sex from the scapula and the clavicle of 147 individuals from the Cretan collection, recommending the used methods in cases, which exhibit above 95% probability of correct classification.

In summary, the results of aforementioned studies clearly show the high level of sexual dimorphism in the Greek population. Thus, it is reasonable to assume that sexual dimorphism will be present in the vertebral column, an element not yet studied in this population.

3.3 Sexual Dimorphism of the Vertebrae

Whether the results are obtained by directly visible structural features or gathered through metric data; determining sex depends upon presence or absence of anatomical markers. Almost every bone of the human skeleton has been examined in order to evaluate sexual dimorphism, most of them focusing on bones that already have obvious visual markers, such as the pelvis or the skull. The majority of osteometric studies involve bones with obvious size differences. But as mentioned earlier, forensic anthropologists are often required to estimate sex of unknown individuals from just a few bones. The study of sexual dimorphism in less frequently used bones is therefore of importance (Wescott 2000). Regarding the study of vertebrae, the cervical and lumbar vertebrae have so far received far more attention.

3.3.1 Early development

Taylor and Twomey (1984) conducted three different studies, all demonstrating the presence of sexual dimorphism in the vertebral column. The first study examined thoracolumbar spines of 1427 children in the aged 5-19, divided in age groups. The second study examined the mid-vertebral height and maximum transverse diameter of T6 and T9 from 166 radiographs. The third study measured mid-vertebral height and transverse diameter of the

lumbar spine from 105 skeletal samples. The combined results showed significant sex related changes in individuals until the age of 13; A greater growth in vertebral height in females, and, due to the effect of testosterone on muscle development, a greater growth of the transverse diameter in males (Taylor &Twomey 1984). Gilsanz et al. (1994) came to a similar conclusion, measuring the density of the cortical and cancellous bone and dimensions of lumbar vertebral bodies in 196 children and adolescents between the ages of 4-20, divided into groups according to the stage of sexual development. The findings showed that the cross-sectional areas of the bodies were approximately 17% greater in males than in females and added that this difference in vertebral body size increased with development, peaking at sexual maturity (Gilsanz et al. 1994).

3.3.2 Sexual dimorphism in the adult vertebrae

Even though not all vertebrae of the human spine have been studied, existing publications have so far provided valuable results investigating sexual dimorphism in adults. Liguoro et al. (1994) compared the cervical vertebral bodies from radiographs, and confirmed sexual dimorphism. Particularly the vertebral body of the second cervical vertebra showed significant differences according to sex. Another morphometric study by Kibii (Kibii et al. 2010) confirmed Liguoro's (Liguoro 1994) findings. The study explored the morphometric variations of the 7th cervical vertebra in a collection consisting of 240 Zulu, white and black South Africans. The results showed that measurements taken from males are generally larger than the ones taken from females. Nevertheless, the study also concluded that sexual dimorphism is more apparent within the same population group.

MacLaughlin and Oldale (1992) examined the accuracy with which sex may be predicted from vertebral body diameters of 205 adult skeletons from the Spitalfields Collection. Three measurements (anterior and posterior transverse diameters and antero-posterior diameter) were used on T11, T12 and L1, and found to be sexually dimorphic predicting sex with accuracies ranging between 70%-87%. The highest result from a single measurement was achieved by the anterior transverse diameter predicting sex correctly in 86.9% of the cases for T12, and 83.2% of the cases for T11. The posterior transverse diameter achieved the highest accuracy for L1 with 82.2%. Knowing that the collection was from the 18th century, it is questionable if this method is applicable to modern individuals.

A study by Marino (Marino 1995) examined 100 first cervical vertebrae (C1) from the Terry Collection, and 100 individuals from the Hamann-Todd collection. Both samples were equally divided by sex and ancestry. The eight measurements taken resulted in an accuracy

range between 75%-85% for the Terry Collection, and 60%-77% when applied to the Hamann-Todd Collection. In a separate control test, the measurements were applied to 34 archaeological specimens using the Terry equations. The control samples were correctly identified with accuracy between 60-85%. The study concluded that accuracy increased as sample size decreased, being an indicator of population-specific discrepancies.

Using the second cervical vertebra, Wescott (Wescott 2000) estimated sex with 83% accuracy using 8 dimensions taken from 400 individuals from the Hamann-Todd and Terry Collections. Wescott found all 8 variables to be sexually dimorphic but the maximum sagittal length (XSL) showed by far to be the best single variable classifying sex correctly with an accuracy of 83.4%. His findings suggest, that - like Marino's study - the results of the Hamann-Todd and Terry collections do not differ significantly. The slight difference could eventually be explained due to the fact that the Terry collection sample consists of Caucasians only. Unfortunately, the effect of ancestry between the results of these collections was not tested.

Using the same variables as Wescott (plus one additional), Marlow (Marlow & Pastor 2011) studied the second cervical vertebrae of 153 individuals from the Spitalfields Collection. Marlow's findings confirmed the ones from Wescott, namely that metric analysis of the second cervical vertebra can accurately determine sex. The findings showed a similar result with 83% accuracy but also raised another issue: As the results were similar, showing the maximum sagittal length (XSL) to be most dimorphic, this is also a measurement relying on intact spinous processes. Unfortunately, if a vertebra were to be damaged, it is likely to be in this region making it impossible to apply this variable. The conclusion was, that even though Wescott's (Wescott 2000) method proves to be valuable and that sex can be determined effectively through this method, it is not suitable if the spinous process is damaged, as the most reliable variable needs to be excluded from the analysis.

Pastor (Pastor 2005) examined sexual dimorphism at the junction of the 12th thoracic (T12) and the 1st lumbar vertebra. He used a total of 53 vertebral pairs from the Spitalfields Collections, taking 12 measurements and found 7 of the 12 traits for T12 and 8 of the 12 traits for L1 to be sexually dimorphic. The study was then carried out on 124 individuals from the Terry Collection, applying the initial 12 measurements plus two additional. The results showed overall accuracies between 77-92% using one or several measurements combined.

Yu (Yu et al. 2008) took thirty-three linear measurements and two ratios from the 12th thoracic vertebra (T12) from 102 individuals, reconstructed with computer tomographic images. Out of these linear traits, they found 23 to be sexually dimorphic. Using only one variable, sex was predicted correctly with an accuracy range between 62.7-85.3%. Using additional equations and the stepwise method of discriminant function analysis, the coronal diameter of the superior endplate of the vertebral body, the ratio of anterior to middle height of the body, and the length of the left mammillary process and pedicle achieved an accuracy of 90%. The high result may be due to fact that the population used consisted of Koreans only.

Another recent study by Hou et al. (2012) obtained 30 linear measurements (most of them previously defined by Yu et al.), from 141 three-dimensional reconstructed T12 models of Chinese origin. 28 of the measurements proved to be dimorphic, as the discriminant function equations predicted sex with an accuracy range between 56.4-90.1%. Using again the stepwise approach, four variables predicted sex correctly in 94.2% of the cases.

Zheng et al. (2012) developed a technique to assess sex from measurements taken from the first lumbar vertebra. Using a sample of 210 Chinese males and females, Zheng et al. took 23 linear measurements and two ratios. Using the stepwise method of discriminant function analysis, three measurements (upper end-plate width, left pedicle height, and middle end-plate depth) achieved the highest accuracy with 88.6% when combined.

Several osteometric studies have identified sexual dimorphism for populations from specific geographical regions, producing discriminant function formulae for this population. As the appearance of sexual dimorphism varies greatly between the populations, the formulae should therefore only be applied to this same population. Until now, no study has been carried out exploring sexual dimorphism in vertebrae of the Greek population. The necessity for standards for this population should therefore be acknowledged.

4 Material and Method

4.1 Material

The skeletal collection for this study consists of 210 individuals selected from the cemeteries of St. Konstantinos and Pateles, Heraklion, Crete. The Department of Forensic Sciences of the University of Crete was given permission by the local District Attorney, as well as the health department to analyse a limited number of unearthed remains in order to carry out a population-based osteometric study.
After the burial, it is common practice in Greece to remove the remains from the graves after a few years. The exhumed bones are then gathered, cleaned, placed in individual boxes, and stored in a designated room (ossuary) provided by the city, or in family tombs. In some cases, living members cannot afford the rental fee to keep the remains in these tombs or the ossuary. In these cases, the bones are then gathered and cremated. A permit to use the unclaimed bones for study purposes has to be obtained by the families of the deceased, the district attorney, as well as the health department.

The individuals of this collection were born in Crete between 1867 and 1956, and died between 1968 and 1998. Death certificates including age, sex, height, marital status, and cause of death can be obtained from the City Hall of Heraklion census archives for part of the skeletal material. Sex was apparent for all individuals as the names are clearly indicated on the boxes that contained the remains (for more information on the collection see Kranioti et al. 2008).
A minimum of 70 individuals was necessary for the proposed study in order to gather sufficient data for the statistical analysis. The individuals were selected from the 210 available skeletons according to the following criteria

1. Completeness of the thoracic vertebrae
2. Good preservation
3. Lack of severe pathological alteration in the vertebral column

A number of people who may have migrated from Turkey, islands and mainland Greece are excluded from the study.

4.2 Method

4.2.1 Data Collection

A total of 70 individuals from a contemporary Cretan collection were examined. For this study, all 12 thoracic vertebrae were measured. Unless where one or more vertebrae were missing, fused, showed other severe pathology or were not macerated, all possible measurements were recorded. Excluding one or more measurements from a single vertebra did not exclude the other measurements. The exclusion of a single or multiple vertebrae did not exclude the individual. Data was collected where possible.

Overall, the sample includes measurements from individuals ranging in age from 29-90 years (see Table 1). Every vertebra was examined, and a maximum of 16 measurements were taken to the nearest 0.01mm using a Mitutoyo digital sliding calliper. As stated in protocols of previous studies (Marino 1995, Wescott 2000, Marlow & Pastor 2011), only one side, the right side (from an anterior view), was recorded, unless this was not possible due to severe damage on the vertebra. In these cases, the left side was measured or the measurement was not recorded at all. Side differences were not tested, as previous studies have not found significant variation in terms of accuracy (see Yu et al. 2008, Hou et al. 2012).

Table 1: Sample means and ranges

	N	Mean Age	Min. Age	Max. Age
Male	38	68.6	50	87
Female	32	72.7	29	90
Total	70	70.3		

4.2.2 Definition of Measurements

The following measurements were recorded:

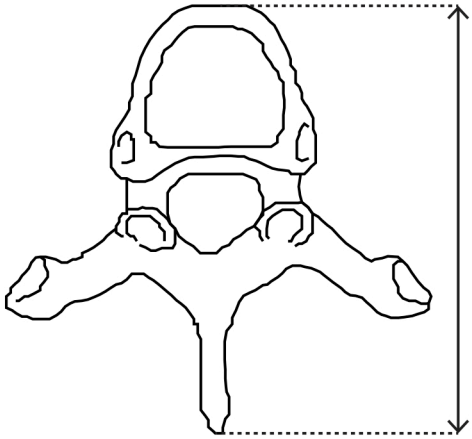

XLV (1)

Maximum Length of Vertebra

Sagittal length measured from the anterior superior edge of the vertebral body to the posterior edge of the spinous process

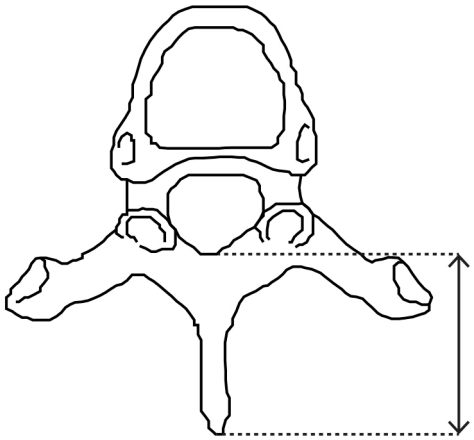

XLS (2)

Maximum Length of Spinous Process

Sagittal length measured from the anterior superior edge to the most posterior edge of the spinous process

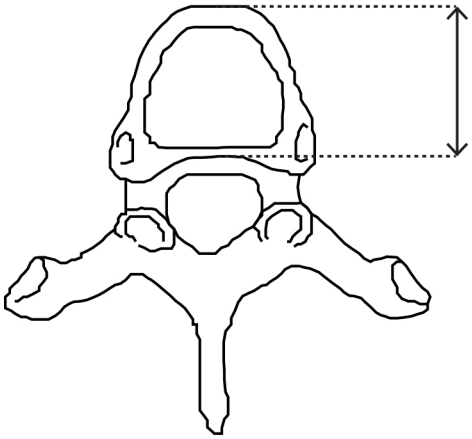

XLVBs (3)

Maximum Length of Vertebral Body - Superior

Sagittal length measured from the anterior superior edge to the posterior superior edge of the vertebral body

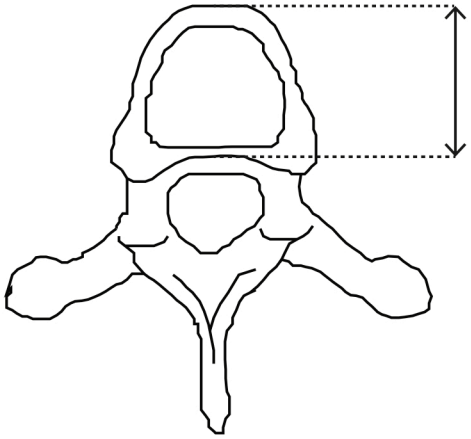

XLVBi (4)

Maximum Length of Vertebral Body - Inferior

Sagittal length measured from the anterior inferior to the posterior inferior point of the vertebral body

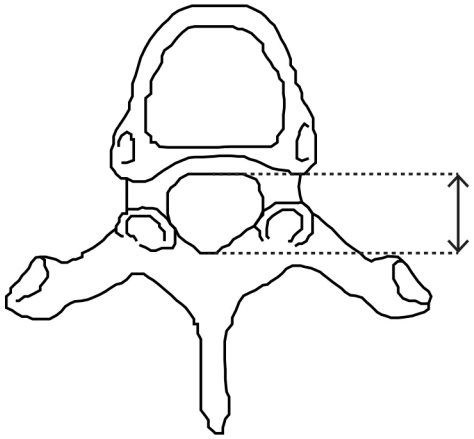

XDFs (5)

Maximum Diameter of Foramen - Sagittal

Sagittal length measured from the posterior border of the vertebral body towards the most anterior point of the spinous process

XHBp (6)

Maximum Height of Vertebral Body - Posterior

Height measured from the posterior superior edge to the posterior inferior edge of the vertebral body

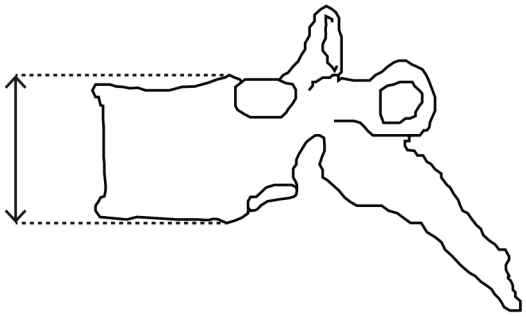

XHBa (7)

Maximum Height of Vertebral Body - Anterior

Height measured from the anterior superior edge to the anterior inferior edge of the vertebral body

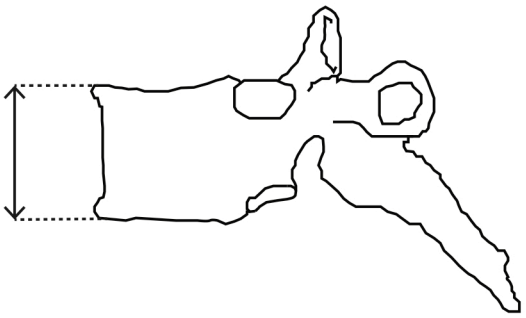

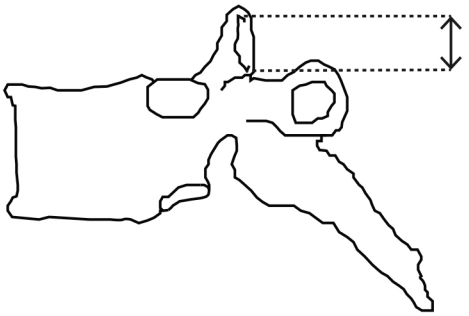

XHFs (8)

Maximum Height of Facet Plane - Superior

Height measured from the most superior point to the most inferior point of the superior articular facet plane (right facet)

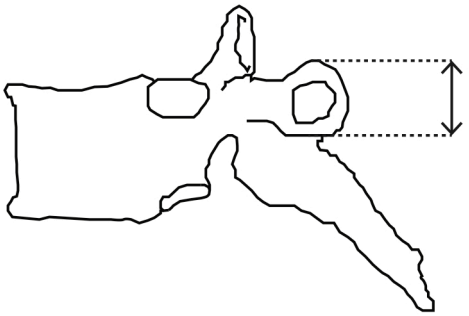

XHTP (9)

Maximum Height of Transverse Process

Height measured from the most superior to the most inferior point of the transverse process (right transverse process)

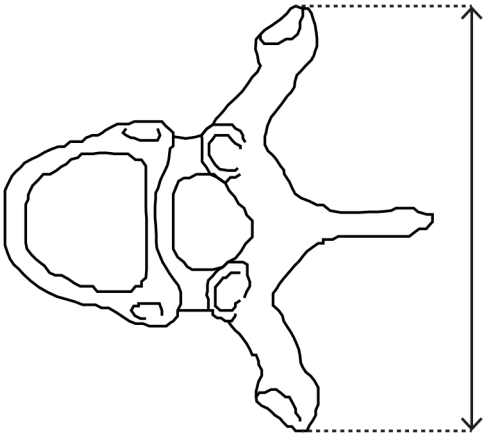

XBV (10)

Maximum Breadth of Vertebra

Transverse length measured from the most distal borders from the left to the right lateral transverse processes

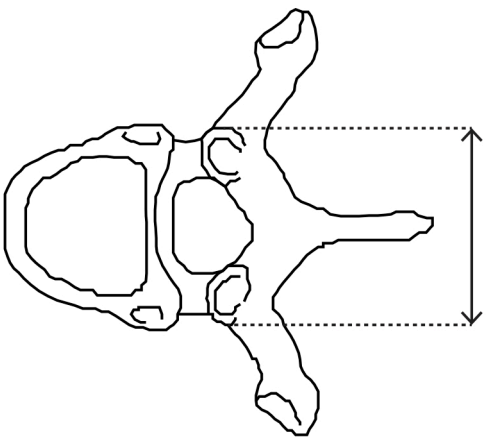

XDSF (11)

Maximum Distance of Facets - Superior

Transverse length measured from the lateral distal borders of the superior articular facets

XBFs (12)

Maximum Breadth of Facet - Superior

Transverse length measured from the lateral edges of the superior articular facet plane (right facet)

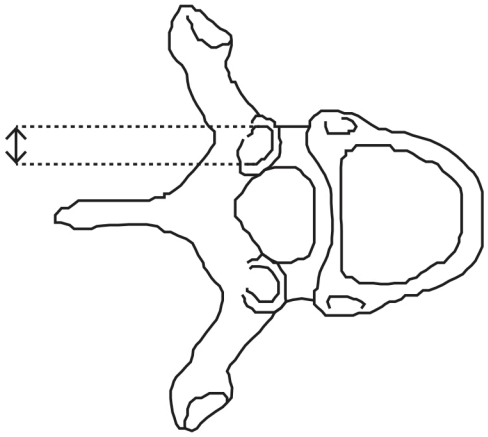

XDFc (13)

Maximum Diameter of Foramen

Transverse length measured from the proximal lateral borders of the pedicles

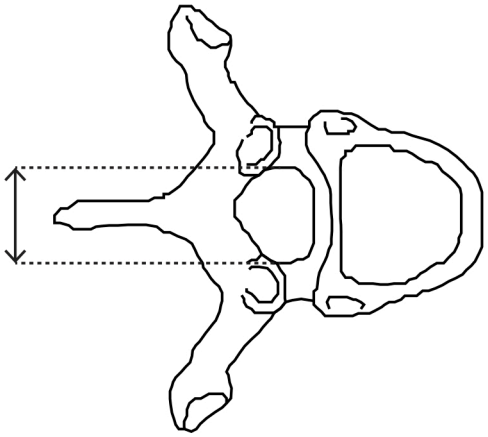

XBP (14)

Maximum Breadth of Pedicle

Transverse length measured from the lateral borders of the pedicle (right pedicle)

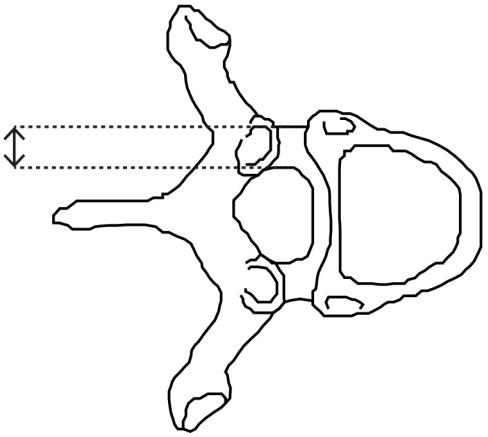

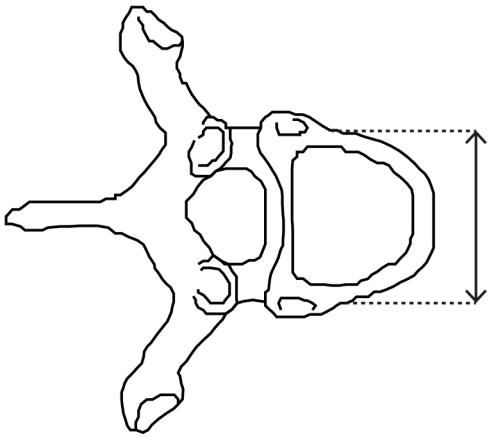

XBVBs (15)

Maximum Breadth of Vertebral Body - Superior

Transverse length measured from the lateral borders of the superior vertebral body, excluding the superior costal facets

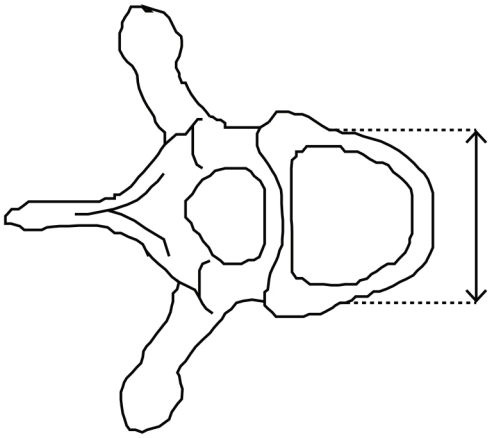

XBVBi (16)

Maximum Breadth of Vertebral Body - Inferior

Transverse length measured from the lateral borders of the inferior vertebral body, excluding the inferior costal facets

Figure 9: Line Drawings of thoracic vertebrae (1-3, 5, 10-15 superior view, 4, 16 inferior view, 6-9 lateral view)

Most measurements used in this study have been described in previous literature, some resulting in high prediction accuracies. These measurements were included in order to test their applicability for the thoracic vertebrae, as well as for comparative purposes. Measurements XHFs and XHTP were devised for this study in order to test their accuracy. Ratios used in previous studies were ignored, as they did not achieve reliable results. The following table provides an overview of these measurements, their origin, and original abbreviations:

Table 2: Literature sources of previously used measurements*

	Marino 1995	Wescott 2000	Yu et al. 2008	Kibii et al. 2010	Marlow & Pastor 2011	Zheng et al. 2012	Hou et al. 2012
XLV		XSL			XSL		sVL
XLS			SL			SPL	SL
XLVBs			sBDs			EPDu	sBDs
XLVBi			iBDs	BAP		EPDl	iBDs
XDFs	LVF	LVF	FDs	CAP	LVF	SCD	FDs
XHBp			BHp			VBHp	BHp
XHBa			BHa	CCH		VBHa	BHa
XHFs							
XHTP							
XBV			TDm			TDm	TDm
XDSF	MxDS	SFB			SFB		sAD
XBFs	WSF	SFT			SFT		
XDFc			FDc	CT	WVF		FDc
XBP			IPW				IPW
XBVBs			sBDcm			EPWu	sBDc
XBVBi			iBDcm	CCW		EPWl	iBDc

*Explanation of abbreviations for Table 2:

Marino (1995):
Maximum length of the vertebral foramen (LVF), maximum distance between the lateral edges of the superior facets (MxDS), maximum width of (right) superior facet (WSF)

Wescott (2000):
Maximum sagittal length (XSL), length of vertebral foramen (LVF), maximum breadth across the superior facets (SFB), superior facet transverse diameter (SFT)

Yu et al. (2008):
Spinal process length (SL), central sagittal diameter of endplate on superior plane (sBDs), central sagittal diameter of endplate on inferior plane (iBDs), sagittal diameter of vertebral foramen on median plane (FDs), posterior height of vertebral body (BHp), anterior height of vertebral body (BHa), maximum distance between transverse processes (TDm), coronal diameter of vertebral foramen (FDc), width of vertebral pedicle (lPW), maximum coronal diameter of endplate on superior plane (sBDc), maximum coronal diameter of endplate on inferior plane (iBDc)

Kibii et al. (2010):
Cervical body anteroposterior diameter (BAP), cervical canal anteroposterior diameter (CAP), cervical centrum height (CCH), cervical canal transverse diameter (CT), cervical centrum width (CCW)

Marlow & Pastor (2011):
Maximum sagittal length (XSL), length of vertebral foramen (LVF), maximum breadth across superior facets (SFB), superior facet transverse diameter (SFT), width of vertebral foramen (WVF)

Zheng et al. (2012):
Spinous process length (SPL), upper end-plate depth (EPDu), Lower end-plate depth (EPDl), spinal canal depth (SCD), posterior height of vertebral body (VBHp), anterior height of vertebral body (VBHa), maximum distance between transverse processes (TDm), upper end-plate width (EPWu), lower end-plate width (EPWl)

Hou et al. (2012):
Sagittal length of the vertebra on superior plane (sVL), spinal process length (SL), central sagittal diameter of endplate on superior plane (sBDs), central sagittal diameter of endplate on inferior plane (iBDs), sagittal diameter of vertebral foramen on median plane (FDs), posterior height of vertebral body (BHp), anterior height of vertebral body (BHa), maximum distance between transverse processes (TDm), distance between superior articular processes (sAD), coronal diameter of vertebral foramen (FDc), width of vertebral pedicle (lPW), coronal diameter of endplate on superior plane (sBDc), coronal diameter of endplate on inferior plane (iBDc)

4.3 Statistical Analysis

The statistical analyses were performed using Statistical Product and Service Solutions (SPSS version 19). The variables in this study were defined according to the measurements recorded on each vertebra. Subsequently, a screening and cleaning of the data was carried out in order to avoid errors in the analyses. Meaning, any missing values were checked, and all minimum and maximum values were visually screened to see if the individual values were within the range of possible scores. After screening for errors, the descriptive statistical analysis provided the standard deviations, means and ranges, and the test for analysis of variance (ANOVA) indicated if the 16 dimensions differed significantly in the mean scores between males and females of the Cretan collection. The threshold of significance in this study was set at a p value of 0.05.

4.3.1 Discriminant Function Analysis

Discriminant function analysis has become a standard tool in forensic anthropology and is primarily used to sort binomial characteristics between groups, in this case the level of sexual dimorphism within a population based on the observed characteristics. Discriminant function analysis allows the identification of those variables competent at separating groups, and determines, which variables provide the highest discrimination between the groups (Barrier 2007). When a single measurement is used independently to determine sex, the analysis is referred to as univariate discriminant function analysis. However, when a combination of measurements is used, the method is termed multivariate discriminant function analysis and can either be stepwise or direct. A discriminant score is assigned to each case. The scores differ between cases, depending on the single variable or the combination of variables in the function. The unstandardized coefficient (or raw coefficient) is necessary to calculate the discriminant function equations, while the F-ratios, Wilks' lambda, Eigenvalues and degrees of freedom (df) provide an overview of the statistical significance (Burns & Burns 2008). A discriminant function is built with the following formula:

$$\mathbf{p = a_1 * x_1 + a_2 * x_2 + \ldots + a_n * x_n + b}$$

$\mathbf{a_1}$ to $\mathbf{a_n}$ represent the discriminant coefficients, $\mathbf{x_1}$ to $\mathbf{x_n}$ the discriminant variables and **b** the constant. In order to determine a case either male or female, **p** (the product) will be compared to the sectioning point, which derives from the mean male and female

discriminant scores. A higher value than the sectioning point will be assigned male, a value below will be assigned female. The stepwise discriminant function analysis selects a combination of variables, using forward entry and backward elimination, which exposes the most accurate predictors in discriminating sex, and produces the unstandardized coefficients, the group centroids, and the constant (Burns & Burns 2008, Navsa 2010).

The same method applies when calculating the discriminant formula for a single variable. In these cases, where only one variable is used for the analysis, another method of determining sex can be applied by using demarking points. A demarking point refers to the average of the group's means, and provides the possibility to estimate sex without calculating the discriminant function formula. Any value below the point would be considered female, any value above would be considered male (Kranioti 2009).

4.3.2 Cross-validation

The purpose of cross-validation is to estimate the accuracy of prediction. The leave-one-out cross-validation removes one individual from its subset or group at a time, and the discriminant function is calculated using all other subsets until all cases have been left out once. All individuals are classified this way, and the number of correctly classified individuals is then divided by the total sample number, producing the final cross-validated classification accuracy (Dirkmaat 2012). The closer the accuracies are together, the higher the reliability of the discriminant function (Kranioti 2009).

4.3.3 Posterior probability

Posterior probability scores display the effectiveness of how a function has classified the individual, and are achieved by calculating the total number of specimens classified versus the number of correctly classified cases. In short: Posterior probabilities calculate the likelihood of a case being reassigned to its original group. As all sectioning points have been set to zero, a score near zero would mean that there is almost a 50% probability that this classification is wrong. Scores farther from zero would therefore provide a more dependable estimate (Osipov et al. 2013). Discriminant scores below 0 indicate female, scores above 0 indicate male. The x-axis indicates the value of the calculated discriminant score; the y-axis provides the probability of correct classification. In Figure 10, for example, the calculated value of the discriminant score is 1, the probability of correct classification is above 90% for the individual to be male. For forensic applications, a 95% posterior probability of correct classification is considered the cut-off point for admission in court (Aitken et al. 2010).

Posterior probabilities were also calculated for single variables with accuracy rates above 80%, and are presented in Appendix C. The diagram created using Excel for Mac. Posterior probabilities were calculated using a sub-program of SPSS 19.

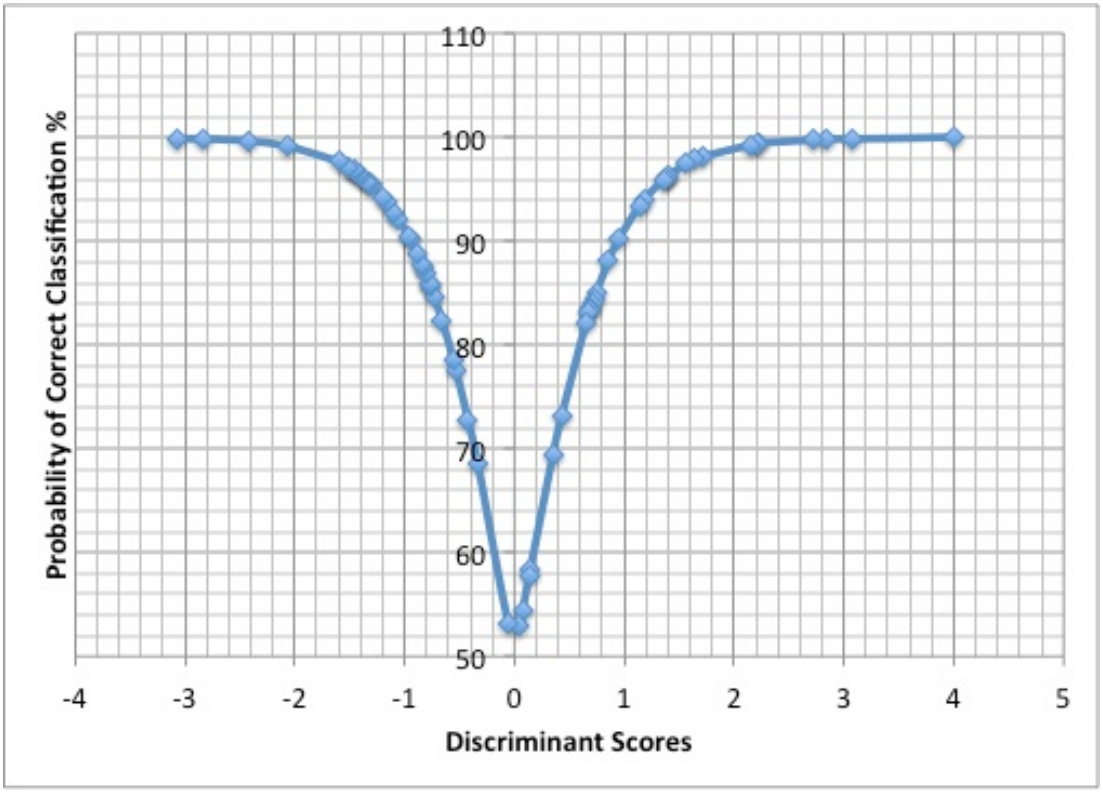

Figure 10: Posterior probability graph

4.3.4 Intra-Observer Error/Estimation of Error

Twenty individuals were randomly selected and re-measured in order to determine the absolute mean error, the absolute technical error of measurement (TEM), and the relative TEM, which expresses the error between the two measurements as a percentage. Variations on the technique execution cause variability on the measurements and are therefore responsible for a higher incidence of error. Relative TEM results above the 5% mark would demonstrate an inconsistency in execution of the applied technique.

The calculation is done by first defining the deviation between the original and re-taken measurement. In a second step, the deviation is raised to the second power, and the result is applied to the following formula (Perini et al. 2005):

Absolute TEM $= \sqrt{\frac{\Sigma\, di^2}{2n}}$

Where

$\sum di^2$ = sum of deviations raised to the second power

n = number of individuals measured

i = number of deviations

The absolute TEM is then applied to a second formula:

Relative TEM $= \frac{TEM}{VAV} \times 100$

Where

VAV = Variable Average Value (the calculated arithmetic mean of the mean between the first and the second measurement)

Relative TEM = the Technical Error of Measurement expressed in %

An inter-observer test was not carried out, as the method is well described and has been used in previous studies (Liguoro et al. 1994, Kibii et al. 2010, MacLaughlin & Oldale 1992, Marino 1995, Wescott 2000, Marlow & Pastor 2011, Pastor 2005).

5 Results

The test of intra-observer error showed that no variable has exceeded the 4.9% mark, values up to 5% are considered acceptable. The results of the analyses are presented in Appendix A.

5.1 First thoracic vertebra (T1)

ANOVA (analysis of variance) tests were carried out and provided descriptive statistics including standard deviations, means, and F-ratios of all the variables from males and females for T1. The compiled statistics determine the level of significance between the categorical groups and are shown in Table 3.

Table 3: Descriptive statistics, F-ratios and p-values for the variables measured on T1

	Males (n=36)		**Females** (n=29)			
Variable*	**Mean**	**SD**	**Mean**	**SD**	**F-ratio**	**p-value**
XLV	66.29	3.25	59.72	3.13	66.46	0.00
XLS	36.16	2.32	32.85	2.77	27.05	0.00
XLVBs	16.55	1.22	14.62	1.09	43.90	0.00
XLVBi	17.05	1.63	14.92	0.80	39.90	0.00
XDFs	15.08	1.03	13.90	1.06	20.55	0.00
XHBp	17.35	0.96	15.71	1.06	42.21	0.00
XHBa	15.85	1.31	14.66	1.12	14.98	0.00
XHFs	12.37	1.90	11.69	1.76	2.21	0.14
XHTP	14.04	1.12	12.75	0.96	24.21	0.00
XBV	79.28	3.64	70.02	3.97	95.82	0.00
XDSF	48.60	4.05	44.78	3.37	16.30	0.00
XBFs	14.75	2.25	13.80	1.64	3.56	0.06
XDFc	21.63	1.67	19.63	1.64	23.32	0.00
XBP	8.69	1.21	7.33	0.93	24.69	0.00
XBVBs	26.78	2.24	24.31	2.26	19.18	0.00
XBVBi	34.81	2.37	30.95	3.04	32.69	0.00

*For the meaning of acronyms see pages 30 to 34

In T1, fourteen of the sixteen dimensions proved to be highly significant between the sexes at level of $p<0.001$. XBV (maximum breadth of vertebra) showed to be the most

discriminating measure for T1 with an F-ratio value of 95.82, followed by XLV (maximum length of vertebra) with an F-ratio value of 66.46. A direct analysis was performed individually on all fourteen measurements; the results including the demarking points can be seen in Table 4.

Table 4: Discriminant function equations and demarking points for T1 using one measurement

Variable	F-ratio	Unstandardized Coefficient	Constant	Demarking Point		
XLV	66.462	0.313	-19.832	Female<	62.95	>Male
XLS	27.047	0.396	-13.745	Female<	34.50	>Male
XLVBs	43.904	0.859	-13.481	Female<	15.59	>Male
XLVBi	39.902	0.750	-12.081	Female<	15.98	>Male
XDFs	20.548	0.959	-13.956	Female<	14.49	>Male
XHBp	42.205	0.997	-16.574	Female<	16.52	>Male
XHBa	14.983	0.813	-12.451	Female<	15.25	>Male
XHTP	24.213	0.951	-12.814	Female<	13.40	>Male
XBV	95.820	0.264	-19.821	Female<	74.58	>Male
XDSF	16.302	0.267	-12.490	Female<	46.63	>Male
XDFc	23.323	0.604	-12.522	Female<	20.63	>Male
XBP	24.688	0.916	-7.395	Female<	8.01	>Male
XBVBs	19.175	0.444	-11.401	Female<	25.56	>Male
XBVBi	32.692	0.371	-12.273	Female<	32.90	>Male

A stepwise analysis was then carried out on the fourteen significant measurements; the results are shown in Table 5. Only two variables were selected: XBV (maximum breadth of vertebra) and XLV (maximum length of vertebra), which previously also showed the highest univariate F-ratios.

Table 5: Stepwise discriminant function statistics for T1, sectioning point is set to zero, results are cross-validated

Step	Variable		Exact F	df	Unstandardized Coefficient	Group Centroids
1	XBV	Max. Breadth	81.867	1.58	0.158	M=1.169
2	XLV	Max. Length	49.278	2.57	0.173	F=-1.429
	(Constant)					-22.877
	Accuracy male					91.7%
	Accuracy female					89.3%
	Accuracy total					90.6%

The following example shall explain the process of calculating the formulae:

P = **unstandardized coefficient of XBV * XBV + unstandardized coefficient of XLV * XLV + constant**

The values for the unstandardized coefficients for this example derive from the T1 stepwise analysis and are presented in Table 5. We assume that the maximum breadth of vertebra (XBV) for the first thoracic vertebra of an unknown individual measures 71.57mm, and the maximum length of vertebra (XLV) measures 62.13mm. The coefficient for XBV (0.158) is multiplied by the value of its corresponding variable (71.75), added to the coefficient for XLV (0.173) that is multiplied by its corresponding variable (62.13), and so on. The constant is added in the end. In this example, the calculation would be executed as follows:

P = **0.158 * 71.75 + 0.173 * 62.13 - 23.007**

or

10.75 + 11.31 - 23.01 = -0.95

This result (-0.95) is now compared to the sectioning point, which derives from the average of the two male and female centroids. The average is calculated as follows:

((male centroid - female centroid)/ 2) + female centroid = sectioning point

In this case, the sectioning point equals -0.13. As the value of the discriminant score (-0.95) is below the value of the sectioning point, the individual would be classified as female.

The accuracies for the cross-validated data for T1, with values above 70%, are presented in Table 6. For tables with a complete overview of the results (original and cross-validated) see Appendix B. Confidence levels for single and combined measurements with total accuracy above 80% are presented in Appendix D.

The highest accuracy rate was obtained using the stepwise function (90.6%), selecting XBV and XLV combined. XBV showed the highest accuracy rate of a single variable with a value of 87.7%, followed by XLV with 87.5% accuracy, cross-validated.

Table 6: Cross-validated classification accuracies for T1

Function		Male		Female		Average
	N	Count	%	Count	%	Accuracy
Stepwise (XBV, XLV)	64	36	91.7	28	89.3	90.6
XLV	64	36	88.9	28	85.7	87.5
XLS	64	36	75.0	28	71.4	73.4
XLVBs	65	36	77.8	29	82.8	80.0
XLVBi	64	36	75.0	28	89.3	81.3
XDFs	65	36	63.9	29	69.0	66.2
XHBp	64	36	77.8	28	82.1	79.7
XHBa	65	36	63.9	29	75.9	69.2
XHTP	65	36	75.0	29	79.3	76.9
XBV	65	36	88.9	29	86.2	87.7
XDSF	63	34	61.8	29	82.8	71.4
XDFc	65	36	69.4	29	75.9	72.3
XBP	64	35	71.4	29	79.3	75.0
XBVBs	64	35	71.4	29	69.0	70.3
XBVBi	64	35	77.1	29	72.4	75.0

The posterior probabilities for the stepwise discriminant scores are calculated in Figure 11.

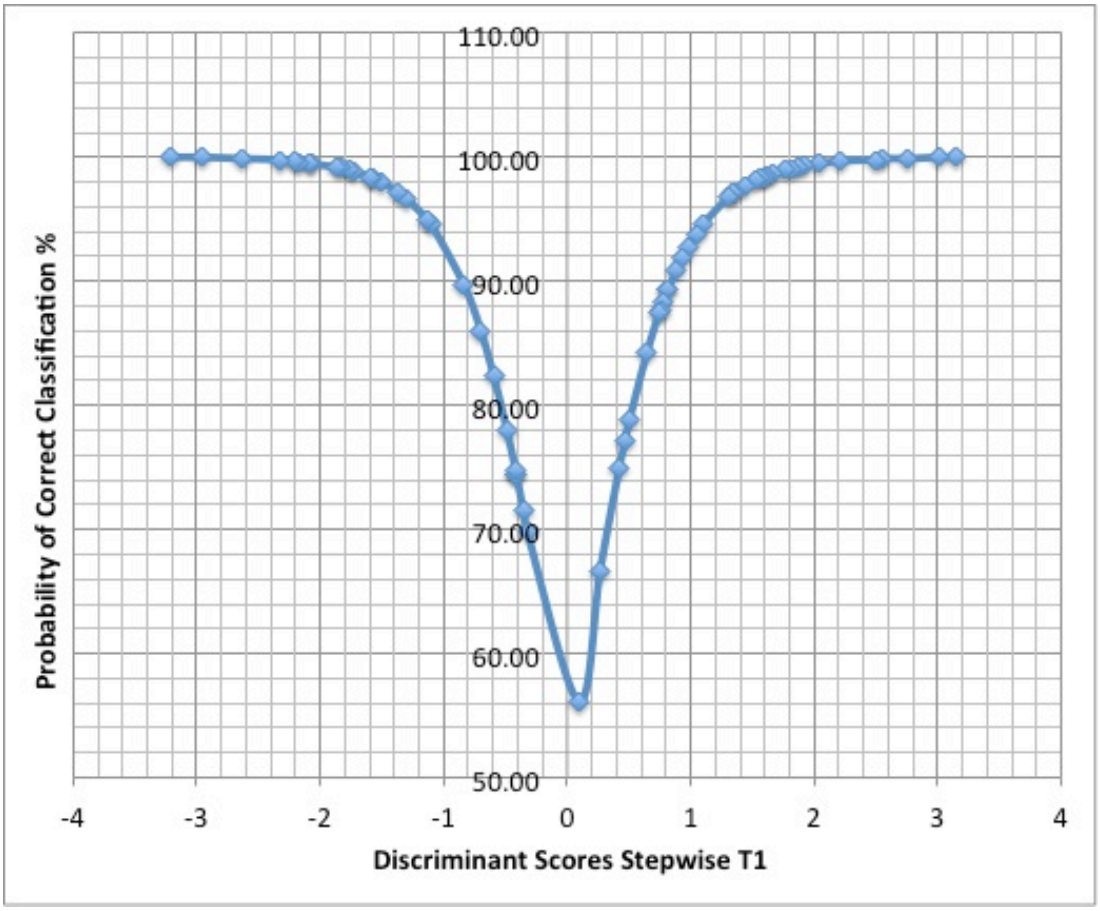

Figure 11: Posterior probabilities for T1 stepwise function

5.2 Second thoracic vertebra (T2)

The compiled descriptive statistics for T2 are presented in Table 7. Besides means and standard deviations, the analysis of variance test provided an overview of the level of significance for each dimension, as well as the associated F-ratios.

Table 7: Descriptive statistics, F-ratios and p-values for the variables measured on T2

	Males (n=35)		Females (n=30)			
Variable	**Mean**	**SD**	**Mean**	**SD**	**F-ratio**	**p-value**
XLV	68.91	3.21	62.43	4.08	46.50	0.00
XLS	38.08	3.07	35.03	3.87	11.54	0.00
XLVBs	17.48	1.62	15.61	1.63	20.70	0.00
XLVBi	18.58	1.80	16.70	1.47	20.15	0.00
XDFs	15.15	1.13	14.48	1.06	6.05	0.02
XHBp	18.11	1.06	16.75	1.18	22.51	0.00
XHBa	17.41	1.42	16.06	1.33	15.03	0.00
XHFs	11.84	1.29	11.03	1.47	5.44	0.02
XHTP	15.51	1.38	13.69	1.42	27.54	0.00
XBV	73.92	4.27	64.47	4.50	75.24	0.00
XDSF	41.68	2.80	36.42	3.83	39.70	0.00
XBFs	12.72	1.72	11.38	1.45	10.77	0.00
XDFc	18.58	1.50	16.89	1.30	23.17	0.00
XBP	6.92	1.00	6.15	0.90	10.52	0.00
XBVBs	27.49	1.87	25.01	2.23	22.86	0.00
XBVBi	35.76	2.12	31.29	2.24	67.22	0.00

All sixteen measurements in T2 proved to be dimorphic, fourteen at level <0.01. As in T1, XBV scored the highest F-ratio with a value of 75.24, followed by XBVBi with a value of 67.22, and XLV with a value of 46.50 (Table 7). The results of the direct analysis, performed individually on all sixteen variables, are presented in Table 8. and include the demarking points. The demarking points provide another possibility to estimate sex without calculating the discriminant function formula. Any value above the demarking point would be considered female, any value below would be considered male.

Table 8: Discriminant function equations and demarking points for T2 using one measurement

Variable	F-ratio	Unstandardized Coefficient	Constant	Demarking Point		
XLV	46.499	0.275	-18.131	Female<	65.66	>Male
XLS	11.544	0.288	-10.576	Female<	36.62	>Male
XLVBs	20.701	0.615	-10.239	Female<	16.54	>Male
XLVBi	20.148	0.604	-10.700	Female<	17.64	>Male
XDFs	6.050	0.910	-13.510	Female<	14.82	>Male
XHBp	22.506	0.895	-15.650	Female<	17.42	>Male
XHBa	15.029	0.725	-12.167	Female<	16.73	>Male
XHFs	5.436	0.729	-8.366	Female<	11.43	>Male
XHTP	27.543	0.714	-10.479	Female<	14.61	>Male
XBV	75.241	0.228	-15.891	Female<	69.33	>Male
XDSF	39.704	0.304	-11.948	Female<	39.01	>Male
XBFs	10.768	0.622	-7.537	Female<	12.04	>Male
XDFc	23.170	0.708	-12.596	Female<	17.73	>Male
XBP	10.523	1.047	-6.874	Female<	6.54	>Male
XBVBs	22.859	0.489	-12.879	Female<	26.24	>Male
XBVBi	67.215	0.459	-15.456	Female<	33.53	>Male

The stepwise analysis selected three variables: XBVBi, XLV, and XDSF. Variable XBV was not selected, although it previously showed the highest univariate F-ratio (see Table 7).

Table 9: Stepwise discriminant function statistics for T2, sectioning point set to zero, results are cross-validated

Step	Variable		Exact F	df	Unstandardized Coefficient	Group Centroids
1	XBVBi	Max. Breadth of Body Inf.	57.678	1.54	0.221	M=1.177
2	XLV	Max. Length	37.944	2.53	0.146	F=-1.459
	XDSF	Max. Dist. of Facets Sup.	30.872	3.52	0.142	
	(Constant)					-22.635
	Accuracy male					93.5%
	Accuracy female					84.6%
	Accuracy total					89.5%

The highest total accuracy for a single variable was obtained by XBV, scoring 83.1% cross-validated, followed by XDSF, and XBVBi with 82.5% and 81.3%, respectively. The stepwise analysis including XBVBi, XLV, and XDSF reached an accuracy rate of 89.5% when combined. Table 10 shows the accuracy rates of the stepwise analysis, and the variables with accuracies above 70%.

Table 10: Cross-validated classification accuracies for T2

Function		Male		Female		Average
	N	Count	%	Count	%	Accuracy
Stepwise (XBVBi, XLV, XDSF)	57	31	93.5	26	84.6	89.5
XLV	59	32	84.4	27	74.1	79.7
XLS	60	32	62.5	28	67.9	65.0
XLVBs	63	35	71.4	28	85.7	77.8
XLVBi	63	34	61.8	29	89.7	74.6
XDFs	65	35	65.7	30	60.0	63.1
XHBp	62	34	73.5	28	82.1	77.4
XHBa	63	34	70.6	29	62.1	66.7
XHFs	63	35	62.9	28	67.9	65.1
XHTP	65	35	77.1	30	70.0	73.8
XBV	65	35	82.9	30	83.3	83.1
XDSF	63	35	85.7	28	78.6	82.5
XBFs	63	35	68.6	28	67.9	68.3
XDFc	65	35	74.3	30	76.7	75.4
XBP	65	35	65.7	30	63.3	64.6
XBVBs	63	34	73.5	29	72.4	73.0
XBVBi	64	34	82.4	30	80.0	81.3

The posterior probabilities for the stepwise discriminant scores of T2 are presented in Figure 12. The diagram demonstrates the levels of probability when a sample is classified through its discriminant score.

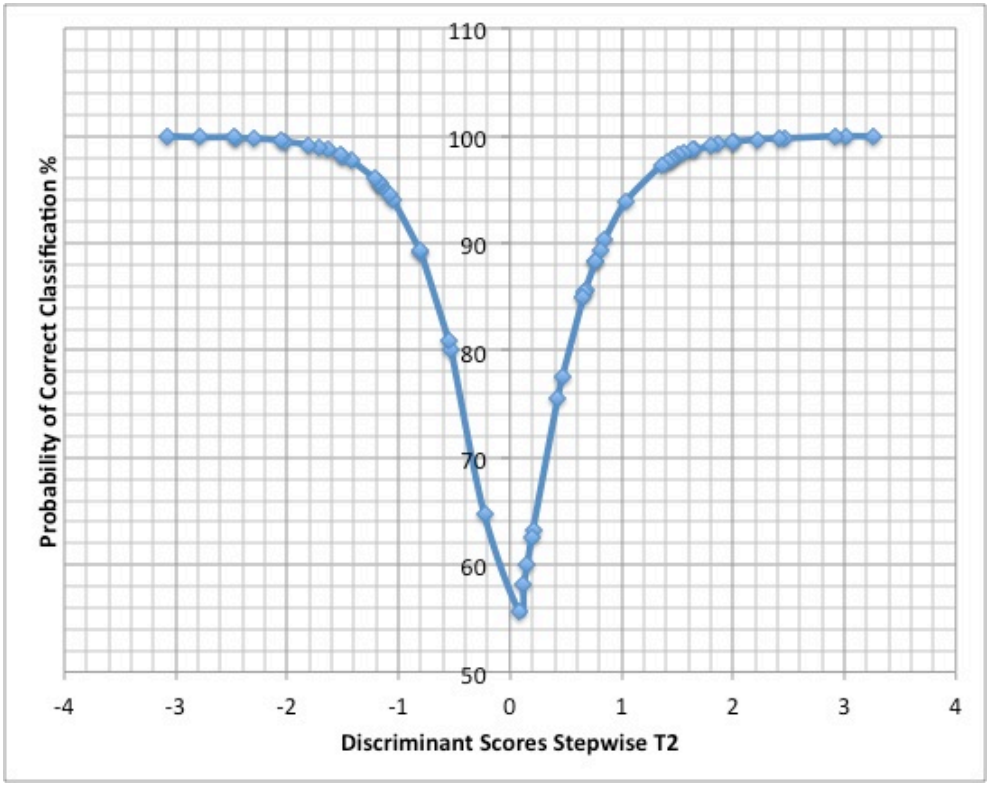

Figure 12: Posterior probabilities for T2 stepwise function

5.3 Third thoracic vertebra (T3)

The descriptive statistics of the 3rd thoracic vertebra are presented in Table 11. Thirteen dimensions were significantly different between the sexes at level <0.01, and three dimensions at level <0.05.

Table 11: Descriptive statistics, F-ratios and p-values for the variables measured on T3

	Males (n=36)		**Females** (n=31)			
Variable	**Mean**	**SD**	**Mean**	**SD**	**F-ratio**	**p-value**
XLV	70.73	4.69	63.93	3.97	36.55	0.00
XLS	39.90	5.37	36.20	4.77	7.96	0.01
XLVBs	19.20	1.97	17.02	1.24	27.49	0.00
XLVBi	20.42	1.82	18.05	1.31	35.55	0.00
XDFs	15.31	1.18	14.57	1.11	6.90	0.01
XHBp	18.42	1.15	17.20	1.28	16.11	0.00
XHBa	17.52	1.16	16.51	1.30	10.46	0.00
XHFs	11.71	1.67	10.83	1.12	5.88	0.02
XHTP	15.76	1.45	13.63	1.32	38.86	0.00
XBV	67.30	3.45	59.47	3.89	75.30	0.00
XDSF	36.31	2.30	32.70	2.39	38.40	0.00
XBFs	11.52	1.20	10.47	1.15	12.36	0.00
XDFc	17.53	1.56	15.86	1.10	24.78	0.00
XBP	5.49	0.92	4.72	0.81	12.92	0.00
XBVBs	26.90	1.83	23.82	1.76	47.10	0.00
XBVBi	34.99	2.22	30.39	2.02	77.71	0.00

XBVBi and XBV showed to be the most discriminating variables with F-ratios of 77.71 and 75.30, respectively. As all variables proved to be dimorphic at relevant levels, the subsequent direct analysis included sixteen measurements. The compiled statistics are presented in Table 12, demarking points are calculated for all variables.

Table 12: Discriminant function equations and demarking points for T3 using one measurement

Variable	F-ratio	Unstandardized Coefficient	Constant	Demarking Point		
XLV	36.553	0.229	-15.454	Female<	67.21	>Male
XLS	7.962	0.196	-7.481	Female<	38.02	>Male
XLVBs	27.494	0.599	-10.893	Female<	18.10	>Male
XLVBi	35.546	0.621	-12.005	Female<	19.22	>Male
XDFs	6.904	0.871	-13.031	Female<	14.93	>Male
XHBp	16.107	0.826	-14.754	Female<	17.81	>Male
XHBa	10.456	0.813	-13.872	Female<	17.02	>Male
XHFs	5.881	0.693	-7.830	Female<	11.26	>Male
XHTP	38.859	0.717	-10.589	Female<	14.69	>Male
XBV	75.304	0.274	-17.455	Female<	63.35	>Male
XDSF	38.403	0.428	-14.814	Female<	34.47	>Male
XBFs	12.362	0.846	-9.344	Female<	11.00	>Male
XDFc	24.782	0.732	-12.256	Female<	16.68	>Male
XBP	12.916	1.147	-5.884	Female<	5.11	>Male
XBVBs	47.101	0.556	-14.158	Female<	25.35	>Male
XBVBi	77.712	0.469	-15.415	Female<	32.70	>Male

The stepwise analysis (presented in Table 13) included XBVBi, and XBV, which previously also showed the highest F-ratios.

Table 13: Stepwise discriminant function statistics for T3, sectioning point set to zero, results are cross-validated

Step	Variable		Exact F	df	Unstandardized Coefficient	Group Centroids
1	XBVBi	Max. Breadth of Body inf.	54.822	1.54	0.276	M=1.010
2	XBV	Max. Breadth	34.742	2.53	0.147	F=-1.252
	(Constant)					-18.291
	Accuracy male					83.3%
	Accuracy female					90.0%
	Accuracy total					86.4%

Overall, XBV showed the highest dimorphic value, reaching a prediction accuracy of 89.4% when used alone, followed by XBVBi with a prediction accuracy of 86.6%. The stepwise selection of XBVBi and XBV combined predicting sex correctly in 86.4% of the cases (see Table 14).

Table 14: Cross-validated classification accuracies for T3

Function		Male		Female		Average
	N	Count	%	Count	%	Accuracy
Stepwise (XBVBi, XBV)	66	36	83.3	30	90.0	86.4
XLV	61	33	81.8	28	75.0	78.7
XLS	61	33	63.6	28	67.9	65.6
XLVBs	65	35	71.4	30	80.0	75.4
XLVBi	66	36	75.0	30	80.0	77.3
XDFs	67	36	58.3	31	67.7	62.7
XHBp	64	35	68.6	29	75.9	71.9
XHBa	63	34	61.8	29	58.6	60.3
XHFs	63	34	55.9	29	65.5	60.3
XHTP	67	36	77.8	31	87.1	82.1
XBV	66	36	88.9	30	90.0	89.4
XDSF	65	35	80.0	30	86.7	83.1
XBFs	64	35	71.4	29	72.4	71.9
XDFc	67	36	72.2	31	83.9	77.6
XBP	66	35	62.9	31	71.0	66.7
XBVBs	65	35	77.1	30	80.0	78.5
XBVBi	67	36	86.1	31	87.1	86.6

The posterior probabilities for the stepwise discriminant score of T3 are calculated and presented in Figure 13.

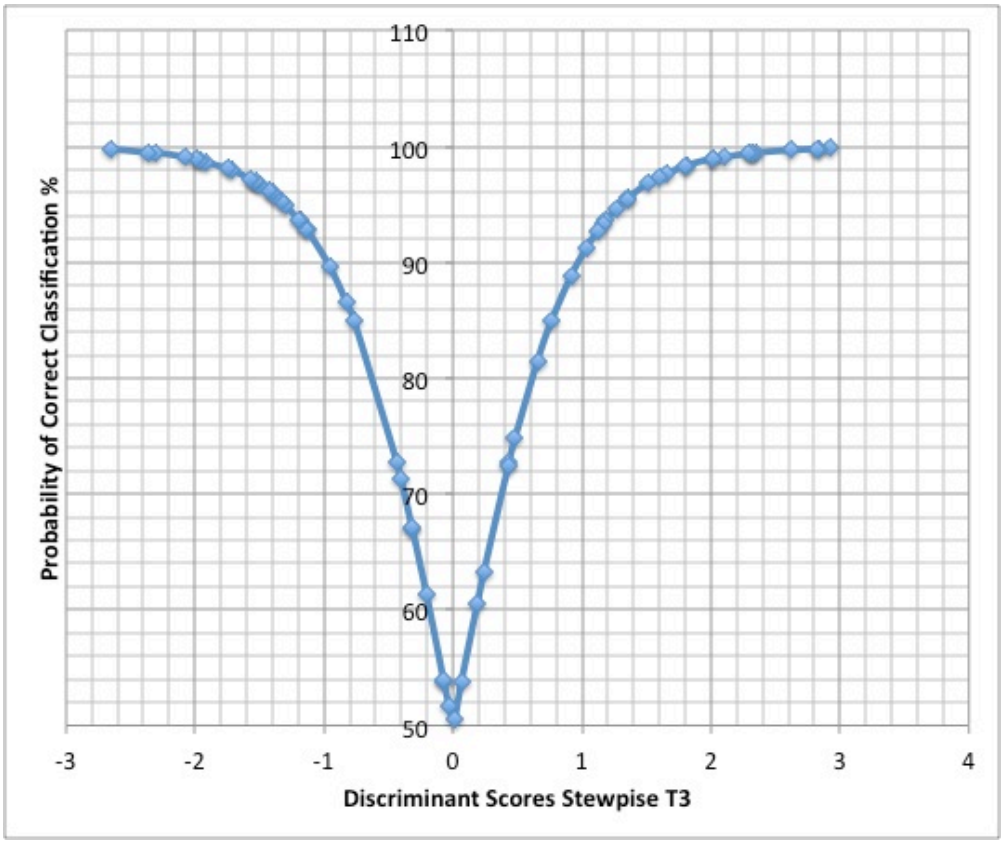

Figure 13: Posterior probabilities for T3 stepwise function

5.4 Fourth thoracic vertebra (T4)

The compiled results of the descriptive statistics and ANOVA, presented here in Table 15, showed fifteen of the sixteen measurements of T4 to be significantly dimorphic between the sexes. The only variable not showing significance (at level <0.05) was XHFs.

Table 15: Descriptive statistics, F-ratios and p-values for the variables measured on T4

	Males (n=34)		**Females** (n=29)			
Variable	**Mean**	**SD**	**Mean**	**SD**	**F-ratio**	**p-value**
XLV	73.52	3.78	66.73	3.75	48.28	0.00
XLS	44.63	4.50	39.99	5.79	12.17	0.00
XLVBs	21.27	2.00	18.60	1.25	37.69	0.00
XLVBi	21.93	2.01	19.28	1.20	34.43	0.00
XDFs	15.35	1.24	14.60	1.23	5.70	0.02
XHBp	18.96	1.34	17.56	1.31	15.54	0.00
XHBa	17.78	1.30	16.81	1.43	7.52	0.01
XHFs	11.12	1.14	10.90	1.39	0.45	0.51
XHTP	15.58	1.28	13.70	1.33	32.68	0.00
XBV	64.46	4.05	57.76	4.35	40.00	0.00
XDSF	34.31	2.86	31.37	2.18	19.83	0.00
XBFs	11.46	1.37	10.39	1.30	9.66	0.00
XDFc	16.87	1.72	15.44	0.96	15.84	0.00
XBP	4.88	1.00	4.15	0.87	9.43	0.00
XBVBs	26.44	2.02	23.71	1.78	31.08	0.00
XBVBi	34.85	2.25	30.54	1.62	70.67	0.00

XBVBi showed the highest F-ratio with 70.67, followed by XLV with a value of 48.28 and XBV with a value of 40.00 (see Table 15). The subsequent direct analysis was performed on the fifteen significant measurements. The compiled results, as well as the individual demarking points are presented in Table 16.

Table 16: Discriminant function equations and demarking points for T4 using one measurement

Variable	F-ratio	Unstandardized Coefficient	Constant	Demarking Point		
XLV	48.281	0.265	-18.708	Female<	70.25	>Male
XLS	12.168	0.195	-8.311	Female<	42.39	>Male
XLVBs	37.688	0.587	-11.770	Female<	19.92	>Male
XLVBi	34.432	0.594	-12.299	Female<	20.61	>Male
XDFs	5.700	0.811	-12.162	Female<	14.97	>Male
XHBp	15.536	0.752	-13.798	Female<	18.26	>Male
XHBa	7.520	0.738	-12.800	Female<	17.29	>Male
XHTP	32.684	0.767	-11.292	Female<	14.65	>Male
XBV	40.003	0.239	-14.644	Female<	61.01	>Male
XDSF	19.833	0.389	-12.820	Female<	32.84	>Male
XBFs	9.655	0.746	-8.185	Female<	10.92	>Male
XDFc	15.843	0.704	-11.411	Female<	16.15	>Male
XBP	9.432	1.065	-4.842	Female<	4.52	>Male
XBVBs	31.079	0.522	-13.152	Female<	25.06	>Male
XBVBi	70.668	0.505	-16.578	Female<	32.68	>Male

A stepwise analysis was carried out on the fifteen significant measurements; the results are shown in Table 17. Only two variables were selected: XBV (maximum breadth of vertebra) and XLV (maximum length of vertebra), which previously also showed the highest univariate F-ratios.

Table 17: Stepwise discriminant function statistics for T4, sectioning point set to zero, results are cross-validated

Step	Variable		Exact F	df	Unstandardized Coefficient	Group Centroids
1	XBVBi	Max. Breadth of Body Inf.	53.339	1.51	0.354	M=1.067
2	XLV	Max. Length	35.721	2.5	0.141	F=-1.289
	(Constant)					-21.424
	Accuracy male					81.3%
	Accuracy female					88.5%
	Accuracy total					84.5%

The accuracies are presented in Table 18. XLV showed to be the most discriminant single dimension, predicting sex correctly in 85.0% of the cases when used alone. The second highest single predictor was XBVBi with a prediction accuracy of 83.3%. The stepwise procedure using XBVBi and XLV combined could increase the accuracy rate to 84.5%.

Table 18: Cross-validated classification accuracies for T4

Function		Male		Female		Average
	N	Count	%	Count	%	Accuracy
Stepwise (XBVBi, XLV)	58	32	81.3	26	88.5	84.5
XLV	60	33	87.9	27	81.5	85.0
XLS	60	33	66.7	27	70.4	68.3
XLVBs	62	34	73.5	28	89.3	80.6
XLVBi	56	30	76.7	26	84.6	80.4
XDFs	62	33	63.6	29	62.1	62.9
XHBp	57	32	62.5	25	72.0	66.7
XHBa	59	33	60.6	26	65.4	62.7
XHTP	63	34	73.5	29	79.3	76.2
XBV	63	34	82.4	29	82.8	82.5
XDSF	61	33	57.6	28	85.7	70.5
XBFs	62	34	55.9	28	67.9	61.3
XDFc	63	34	67.6	29	79.3	73.0
XBP	63	34	58.8	29	65.5	61.9
XBVBs	62	34	73.5	28	78.6	75.8
XBVBi	60	32	81.3	28	85.7	83.3

The posterior probabilities for the stepwise selection are presented in Figure 14.

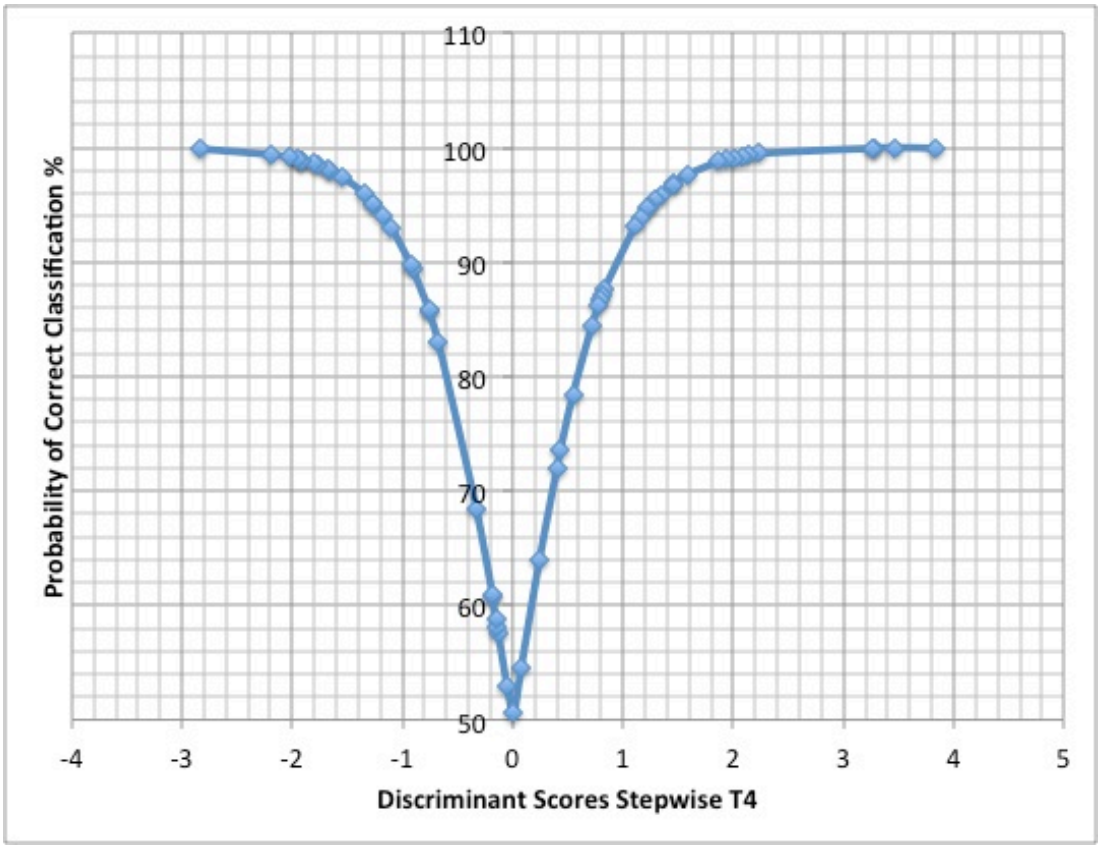

Figure 14: Posterior probabilities for T4 stepwise function

5.5 Fifth thoracic vertebra (T5)

Carrying out the analysis of variance test (ANOVA), provided descriptive statistics for means, F-ratios, and standard deviations for T5 (see Table 19).

Table 19: Descriptive statistics, F-ratios and p-values for the variables measured on T5

	Males (n=36)		**Females** (n=29)			
Variable	**Mean**	**SD**	**Mean**	**SD**	**F-ratio**	**p-value**
XLV	75.32	3.61	67.98	4.04	48.43	0.00
XLS	46.84	5.00	42.83	5.04	8.64	0.01
XLVBs	22.66	1.92	19.97	1.21	37.68	0.00
XLVBi	23.35	2.12	20.70	1.49	30.90	0.00
XDFs	15.71	1.41	14.79	1.21	7.48	0.01
XHBp	19.84	1.56	18.17	1.40	17.69	0.00
XHBa	18.11	1.71	17.06	1.38	6.30	0.02
XHFs	11.27	1.08	10.54	1.33	5.27	0.03
XHTP	15.56	1.39	13.67	1.40	29.37	0.00
XBV	64.98	3.51	58.70	3.92	46.35	0.00
XDSF	33.19	2.79	29.88	1.91	26.24	0.00
XBFs	11.09	1.40	10.00	1.03	10.78	0.00
XDFc	16.92	1.75	15.18	1.12	20.73	0.00
XBP	4.64	1.01	4.13	0.83	4.60	0.04
XBVBs	26.96	1.89	24.02	1.58	39.98	0.00
XBVBi	35.54	2.31	31.20	1.76	67.92	0.00

Out of sixteen variables, eleven proved to be sexually dimorphic at level <0.01, and five at level <0.05. XBVBi scored the highest F-ratio with 67.92, followed by XLV with a value of 48.43, and XBV with a value of 46.35 (see Table 19). Direct analyses of all sixteen measurements provided the individual demarking points and are presented in Table 20.

Table 20: Discriminant function equations and demarking points for T5 using one measurement

Variable	F-ratio	Unstandardized Coefficient	Constant	Demarking Point		
XLV	48.426	0.263	-18.971	Female<	71.65	>Male
XLS	8.641	0.199	-8.988	Female<	44.91	>Male
XLVBs	37.679	0.605	-13.007	Female<	21.31	>Male
XLVBi	30.896	0.539	-11.923	Female<	22.01	>Male
XDFs	7.479	0.757	-11.573	Female<	15.24	>Male
XHBp	17.686	0.669	-12.791	Female<	19.01	>Male
XHBa	6.302	0.635	-11.211	Female<	17.58	>Male
XHFs	5.266	0.837	-9.161	Female<	10.90	>Male
XHTP	29.366	0.717	-10.559	Female<	14.62	>Male
XBV	46.346	0.271	-16.820	Female<	61.73	>Male
XDSF	26.238	0.407	-12.939	Female<	31.54	>Male
XBFs	10.784	0.798	-8.469	Female<	10.55	>Male
XDFc	20.732	0.666	-10.752	Female<	16.06	>Male
XBP	4.599	1.065	-4.697	Female<	4.38	>Male
XBVBs	39.982	0.569	-14.589	Female<	25.49	>Male
XBVBi	67.918	0.479	-16.115	Female<	33.37	>Male

The stepwise analysis selected XLV and XBVBi, the two variables with the highest univariate F-ratios. The selection and associated coefficients and group centroids are presented in Table 21.

Table 21: Stepwise discriminant function statistics for T5, sectioning point set to zero, results are cross-validated

Step	Variable		Exact F	df	Unstandardized Coefficient	Group Centroids
1	XLV	Max. Length	39.618	1.46	0.162	M=0.974
2	XBVBi	Max. Breadth of Body Inf.	28.634	2.45	0.277	F=-1.252
	(Constant)					-20.883
	Accuracy male					83.3%
	Accuracy female					90.0%
	Accuracy total					86.5%

Eleven of the sixteen variables reached accuracies above 70%. XLV scored the highest rate in predicting sex correctly with 86.8% when used alone, followed by XBVBi with an accuracy rate of 81.3%. The stepwise analysis, which selected these two measurements as best indicators, reached an overall prediction rate of 86.5% using XLV and XBVBi combined.

Table 22: Cross-validated classification accuracies for T5

Function		Male		Female		Average
	N	Count	%	Count	%	Accuracy
Stepwise (XLV, XBVBi)	52	30	83.3	22	90.0	86.5
XLV	53	30	86.7	23	87.0	86.8
XLS	55	31	58.1	24	62.5	60.0
XLVBs	58	33	72.7	25	80.0	75.9
XLVBi	61	33	72.7	28	78.6	75.4
XDFs	62	34	52.9	28	75.0	62.9
XHBp	58	33	81.8	25	72.0	77.6
XHBa	58	33	69.7	25	72.0	70.7
XHFs	57	32	56.3	25	64.0	59.6
XHTP	65	36	77.8	29	72.4	75.4
XBV	65	36	83.3	29	75.9	80.0
XDSF	59	34	70.6	25	84.0	76.3
XBFs	57	32	59.4	25	60.0	59.6
XDFc	62	34	73.5	28	82.1	77.4
XBP	63	35	65.7	28	64.3	65.1
XBVBs	58	32	75.0	26	80.8	77.6
XBVBi	64	36	75.0	28	89.3	81.3

The posterior probabilities for the stepwise discriminant scores are calculated and presented in Figure 15. Posterior probabilities for individual variables scoring above 80% are shown in Appendix C.

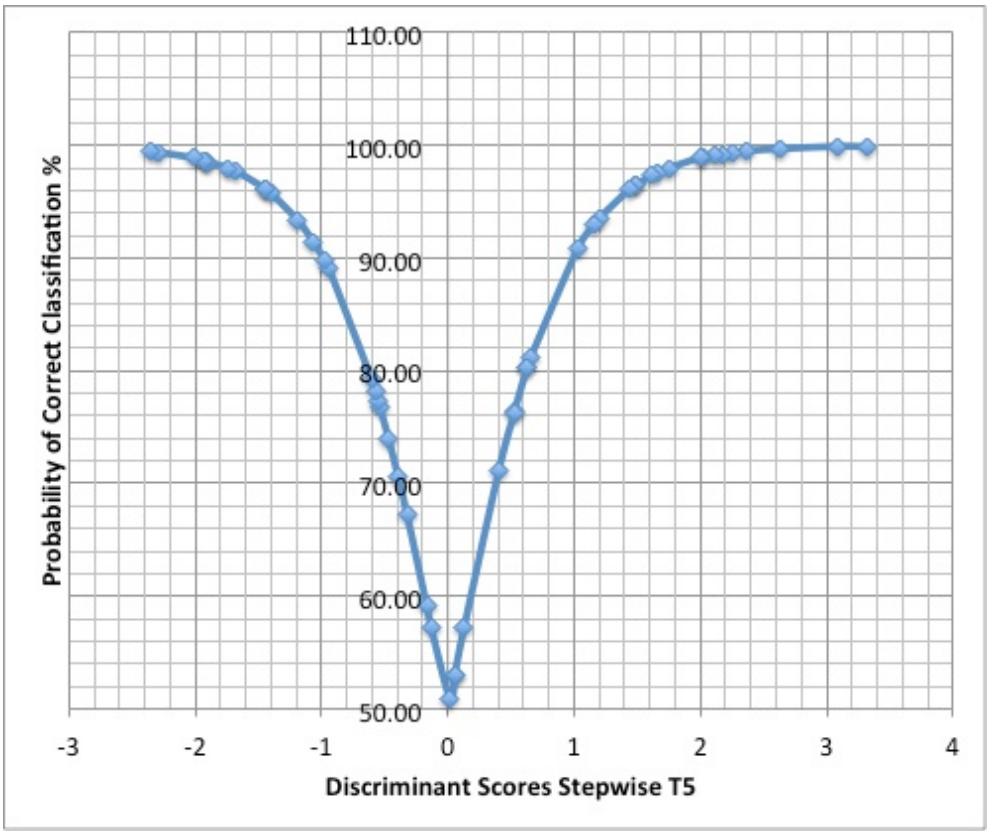

Figure 15: Posterior probabilities for T5 stepwise function

5.6 Sixth thoracic vertebra (T6)

In T6, all variables showed to be significant in determining sex, thirteen at level <0.01, and three at level <0.05. The compiled ANOVA statistics are presented in Table 23.

Table 23: Descriptive statistics, F-ratios and p-values for the variables measured on T6

	Males (n=37)		Females (n=29)			
Variable	**Mean**	**SD**	**Mean**	**SD**	**F-ratio**	**p-value**
XLV	77.69	3.44	69.55	4.25	68.50	0.00
XLS	50.48	5.02	45.11	4.91	17.84	0.00
XLVBs	24.21	2.07	21.52	1.46	33.74	0.00
XLVBi	25.14	2.06	22.09	1.59	38.70	0.00
XDFs	15.52	1.40	14.86	1.09	4.27	0.04
XHBp	20.61	1.31	18.59	1.49	30.22	0.00
XHBa	18.73	1.39	17.19	1.07	22.98	0.00
XHFs	11.33	1.20	10.50	1.30	6.81	0.01
XHTP	15.35	1.71	13.29	1.02	32.67	0.00
XBV	66.25	3.76	59.05	3.37	65.32	0.00
XDSF	32.97	2.71	29.63	2.16	28.30	0.00
XBFs	11.07	1.32	10.00	1.34	9.78	0.00
XDFc	16.61	1.77	15.27	1.13	12.14	0.00
XBP	4.84	1.06	4.31	0.92	4.45	0.04
XBVBs	27.77	2.05	24.69	1.77	39.42	0.00
XBVBi	36.67	2.55	31.84	2.16	65.55	0.00

XLV and XBVBi showed the highest univariate F-ratios with values of 68.50 and 65.55, respectively. A direct analysis was then performed individually on all sixteen measurements, and the demarking points were calculated. Results are presented in Table 24.

Table 24: Discriminant function equations and demarking points for T6 using one measurement

Variable	F-ratio	Unstandardized Coefficient	Constant	Demarking Point		
XLV	68.503	0.262	-19.420	Female<	73.65	>Male
XLS	17.839	0.201	-9.682	Female<	47.82	>Male
XLVBs	33.743	0.547	-12.597	Female<	22.88	>Male
XLVBi	38.697	0.531	-12.689	Female<	23.62	>Male
XDFs	4.271	0.785	-11.949	Female<	15.18	>Male
XHBp	30.224	0.719	-14.201	Female<	19.60	>Male
XHBa	22.979	0.794	-14.344	Female<	17.96	>Male
XHFs	6.812	0.805	-8.833	Female<	10.92	>Male
XHTP	32.674	0.692	-9.990	Female<	14.33	>Male
XBV	65.321	0.279	-17.570	Female<	62.54	>Male
XDSF	28.296	0.402	-12.665	Female<	31.30	>Male
XBFs	9.776	0.751	-7.967	Female<	10.54	>Male
XDFc	12.136	0.653	-10.461	Female<	15.93	>Male
XBP	4.452	0.997	-4.600	Female<	4.58	>Male
XBVBs	39.415	0.518	-13.671	Female<	26.22	>Male
XBVBi	65.548	0.42	-14.498	Female<	34.29	>Male

The stepwise analysis determined XLV and XBVBi as best combined indicators when predicting sex (see Table 25).

Table 25: Stepwise discriminant function statistics for T6, sectioning point set to zero, results are cross-validated

Step	Variable		Exact F	df	Unstandardized Coefficient	Group Centroids
1	XLV	Max. Length	55.947	1.53	0.168	M=1.016
2	XBVBi	Max. Breadth of Body Inf.	35.954	2.52	0.221	F=-1.312
	(Constant)					-19.959
	Accuracy male					87.5%
	Accuracy female					88.8%
	Accuracy total					88.1%

The stepwise selection of XLV and XBVBi combined predicted sex correctly in 88.1% of the cases. Nevertheless, single variables seemed to perform better results. The highest single accuracy rate was reached by XLV scoring 88.5% when used alone, followed by XBV (84.8%), and XBVBi (84.4%). An overview of the accuracy performances scoring above 70% is presented in Table 26.

Table 26: Cross-validated classification accuracies for T6

Function		Male		Female		Average
	N	Count	%	Count	%	Accuracy
Stepwise (XLV, XBVBi)	59	32	87.5	27	88.9	88.1
XLV	61	34	88.2	27	81.5	82.2
XLS	62	35	71.4	27	77.8	74.2
XLVBs	63	35	74.3	28	71.4	73.0
XLVBi	61	35	75.0	25	84.0	78.7
XDFs	64	36	55.6	28	64.3	59.4
XHBp	59	34	82.4	25	76.0	79.7
XHBa	63	36	75.0	27	74.1	74.6
XHFs	62	35	60.0	27	66.7	62.9
XHTP	65	36	72.2	29	86.2	78.5
XBV	66	37	83.8	29	86.2	84.8
XDSF	64	36	72.2	28	75.0	73.4
XBFs	62	35	65.7	27	70.4	67.7
XDFc	65	37	64.9	28	78.6	70.8
XBP	65	37	54.1	28	53.6	53.8
XBVBs	63	35	77.1	28	82.1	79.4
XBVBi	64	35	82.9	29	86.2	84.4

Posterior probabilities for the stepwise selection of T6 are presented in Figure 16, and indicate the probability of correct classification if the discriminant scores of XLV and XBVBi combined are calculated.

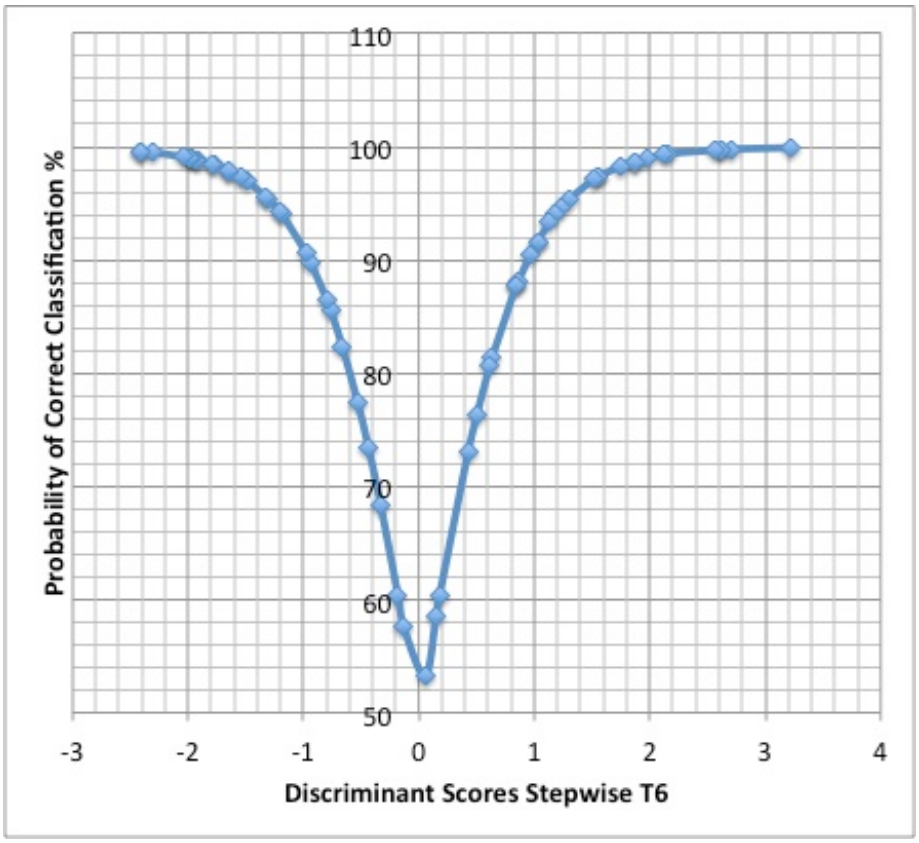

Figure 16: Posterior probabilities for T6 stepwise function

5.7 Seventh thoracic vertebra (T7)

Descriptive statistics and ANOVA of T7 show that all dimensions but XHFs are sexually dimorphic in T7, thirteen at level <0.01. The compiled statistic of the 37 males and 28 females is presented in Table 27.

Table 27: Descriptive statistics, F-ratios and p-values for the variables measured on T7

	Males (n=37)		Females (n=28)			
Variable	**Mean**	**SD**	**Mean**	**SD**	**F-ratio**	**p-value**
XLV	78.49	4.08	70.86	4.64	44.47	0.00
XLS	49.62	4.56	45.01	5.69	11.92	0.00
XLVBs	25.81	2.13	22.95	1.56	31.82	0.00
XLVBi	26.83	2.14	23.52	1.95	38.13	0.00
XDFs	15.51	1.52	14.81	1.08	4.12	0.05
XHBp	21.09	1.42	19.05	1.60	25.68	0.00
XHBa	19.24	1.39	17.62	1.35	20.43	0.00
XHFs	11.05	1.21	10.63	1.02	1.94	0.17
XHTP	14.49	1.25	12.88	0.81	35.10	0.00
XBV	66.54	4.06	58.85	3.29	66.31	0.00
XDSF	32.84	2.85	30.06	2.08	18.09	0.00
XBFs	11.08	1.35	10.15	1.25	7.24	0.01
XDFc	16.78	1.75	15.34	1.29	13.00	0.00
XBP	5.39	1.12	4.41	0.99	12.99	0.00
XBVBs	29.12	2.31	25.63	1.80	38.83	0.00
XBVBi	37.42	2.73	32.57	2.17	59.61	0.00

With an F-ratio value of 66.31, XBV showed to be the best single predictor, followed by XBVBi with a value of 59.61, and XLV with a value of 44.47. The consecutive direct analysis provided demarking points for the individual variables, and is presented in Table 28.

Table 28: Discriminant function equations and demarking points for T7 using one measurement

Variable	F-ratio	Unstandardized Coefficient	Constant	Demarking Point		
XLV	44.472	0.232	-17.454	Female<	74.52	>Male
XLS	11.920	0.198	-9.467	Female<	47.38	>Male
XLVBs	31.822	0.519	-12.803	Female<	24.38	>Male
XLVBi	38.126	0.486	-12.345	Female<	25.18	>Male
XDFs	4.118	0.742	-11.282	Female<	15.15	>Male
XHBp	25.682	0.669	-13.565	Female<	20.08	>Male
XHBa	20.429	0.727	-13.472	Female<	18.42	>Male
XHFs	1.941	0.879	-9.562	Female<	10.84	>Male
XHTP	35.100	0.920	-12.685	Female<	13.68	>Male
XBV	66.313	0.267	-16.866	Female<	62.69	>Male
XDSF	18.088	0.393	-12.429	Female<	31.45	>Male
XBFs	7.235	0.763	-8.166	Female<	10.62	>Male
XDFc	13.000	0.637	-10.295	Female<	16.06	>Male
XBP	12.991	0.936	-4.661	Female<	4.90	>Male
XBVBs	38.833	0.471	-13.07	Female<	27.40	>Male
XBVBi	59.605	0.399	-14.095	Female<	34.99	>Male

The stepwise analysis selected XBV and XHTP as best combination when predicting sex. Coefficients, group centroids and the constant are presented in Table 29, the sectioning point is set to zero.

Table 29: Stepwise discriminant function statistics for T7, sectioning point set to zero, results are cross-validated

Step	Variable		Exact F	df	Unstandardized Coefficient	Group Centroids
1	XBV	Max. Breadth	53.428	1.51	0.163	M=1.016
2	XHTP	Max. Height of Transv. Proc.	34.989	2.5	0.555	F=-1.325
	(Constant)					-17.908
	Accuracy male					77.8%
	Accuracy female					92.9%
	Accuracy total					84.4%

Overall, XBV reached the highest accuracy rate, determining sex correctly in 87.5% of the cases when used alone, followed by XBVBi with 83.1% and XDSF with 80.6% accuracy. The stepwise combination of XBV and XHTP predicted sex correctly in 84.4% of the cases; results are presented in Table 30.

Table 30: Cross-validated classification accuracies for T7

Function		Male		Female		Average
	N	Count	%	Count	%	Accuracy
Stepwise (XBV, XHTP)	64	36	77.8	28	92.9	84.4
XLV	59	35	80.0	24	75.0	78.0
XLS	59	35	68.6	24	58.3	64.4
XLVBs	60	36	77.8	24	75.0	76.7
XLVBi	60	34	79.4	26	69.2	75.0
XDFs	63	36	50.0	27	59.3	54.0
XHBp	57	34	76.5	23	69.6	73.7
XHBa	60	34	73.5	26	76.9	75.0
XHFs	59	35	40.0	24	58.3	47.5
XHTP	65	37	67.6	28	89.3	76.9
XBV	64	36	83.3	28	92.9	87.5
XDSF	62	35	77.1	27	85.2	80.6
XBFs	59	35	57.1	24	66.7	61.0
XDFc	63	36	66.7	27	81.5	73.0
XBP	64	37	62.2	27	66.7	64.1
XBVBs	60	36	72.2	24	87.5	78.3
XBVBi	65	37	81.1	28	85.7	83.1

Figure 17 shows the posterior probabilities for the discriminant scores of the T7 stepwise selection.

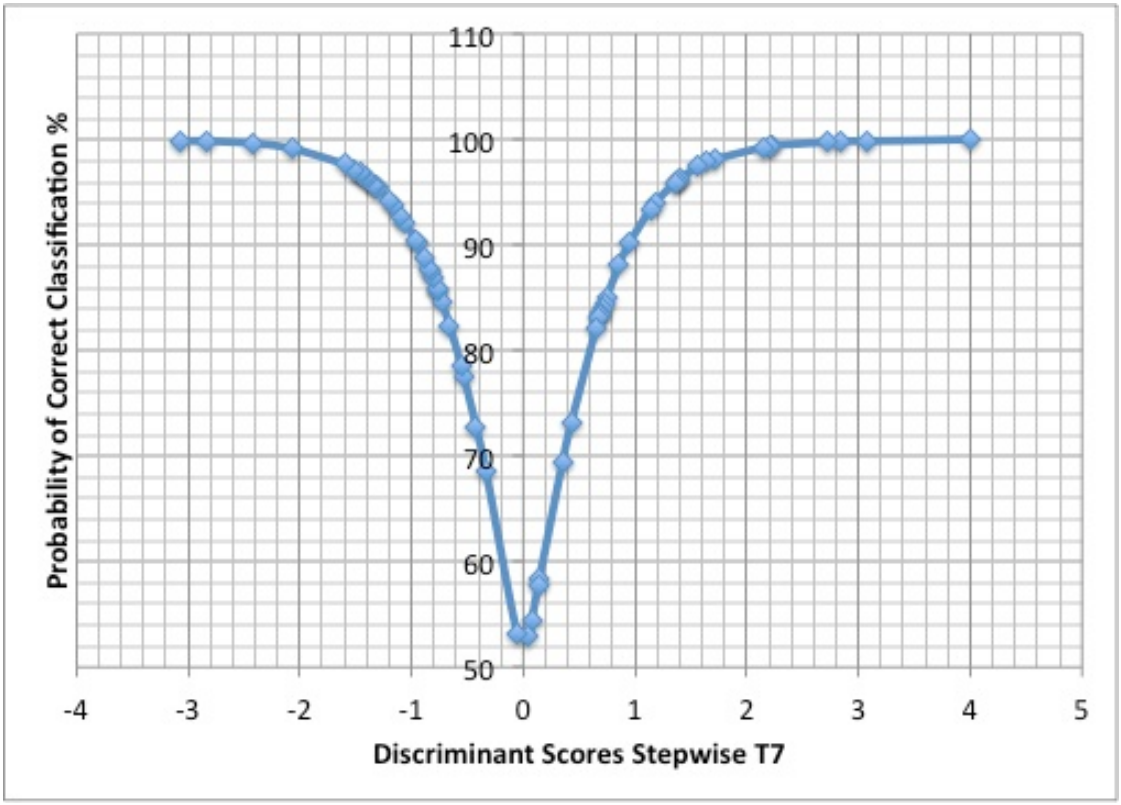

Figure 17: Posterior probabilities for T7 stepwise function

5.8 Eight thoracic vertebra (T8)

The compiled statistics from the analysis of variance test for T8 is presented in Table 31. Out of sixteen variables, fifteen showed to be significant in predicting sex, fourteen at level <0.01 (see Table 31). The only variable not showing any significance was XHFs.

Table 31: Descriptive statistics, F-ratios and p-values for the variables measured on T8

	Males (n=36)		**Females** (n=26)			
Variable	**Mean**	**SD**	**Mean**	**SD**	**F-ratio**	**p-value**
XLV	78.17	3.62	71.23	4.64	39.59	0.00
XLS	45.80	3.26	41.73	5.15	13.03	0.00
XLVBs	27.60	2.17	24.33	1.95	34.74	0.00
XLVBi	28.01	2.39	24.78	2.04	29.24	0.00
XDFs	15.54	1.28	14.61	1.05	9.00	0.00
XHBp	21.46	1.43	19.44	1.67	23.83	0.00
XHBa	19.39	1.42	18.05	1.66	11.10	0.00
XHFs	11.32	1.77	10.79	1.29	1.54	0.22
XHTP	13.88	1.08	12.53	0.99	25.34	0.00
XBV	65.07	4.28	58.32	3.93	39.70	0.00
XDSF	33.50	2.65	30.12	2.16	26.99	0.00
XBFs	11.64	1.47	9.96	1.02	22.56	0.00
XDFc	16.86	1.73	15.63	1.35	8.81	0.00
XBP	5.60	1.19	4.83	0.98	6.91	0.01
XBVBs	30.47	2.25	27.40	2.02	28.26	0.00
XBVBi	38.78	2.85	34.41	2.45	39.86	0.00

XBVBi, XBV, and XLV scored the highest F-ratio values with, 39.86, 39.70 and 39.59, respectively (see Table 31). The subsequent direct analysis of the fifteen significant variables provided the demarking points for each variable, and is presented in Table 32.

Table 32: Discriminant function equations and demarking points for T8 using one measurement

Variable	F-ratio	Unstandardized Coefficient	Constant	Demarking Point		
XLV	39.594	0.245	-18.414	Female<	74.66	>Male
XLS	13.031	0.240	-10.555	Female<	43.69	>Male
XLVBs	34.741	0.480	-12.608	Female<	25.98	>Male
XLVBi	29.242	0.444	-11.830	Female<	26.42	>Male
XDFs	9.004	0.839	-12.710	Female<	15.07	>Male
XHBp	23.831	0.651	-13.414	Female<	20.46	>Male
XHBa	11.099	0.656	-12.344	Female<	18.71	>Male
XHTP	25.340	0.960	-12.784	Female<	13.21	>Male
XBV	39.698	0.242	-15.035	Female<	61.63	>Male
XDSF	26.988	0.405	-13.027	Female<	31.83	>Male
XBFs	22.556	0.763	-8.366	Female<	10.80	>Male
XDFc	8.811	0.630	-10.304	Female<	16.25	>Male
XBP	6.905	0.901	-4.758	Female<	5.22	>Male
XBVBs	28.256	0.464	-13.536	Female<	28.93	>Male
XBVBi	39.861	0.372	-13.729	Female<	36.55	>Male

The stepwise analysis for T8 included XBV and XLVBs. Table 33 shows the selected variables, associated coefficients and group centroids. Sectioning point is set to zero

Table 33: Stepwise discriminant function statistics for T8, sectioning point set to zero, results are cross-validated

Step	Variable		Exact F	df	Unstandardized Coefficient	Group Centroids
1	XBV	Max. Breadth	36.307	1.49	0.15	M=0.881
2	XLVBs	Max. Length of Body Sup.	23.579	2.48	0.249	F=-1.072
	(Constant)					-15.806
	Accuracy male					78.8%
	Accuracy female					79.2%
	Accuracy total					78.9%

Single variable XBVBi, with a value of 82.3%, reached the highest accuracy rate in determining sex in T8. No other variable - or combination of variables - exceeded this value. The stepwise selection of XBV and XLVBs combined predicted sex correctly in 80.7% of the cases, 78.9% cross-validated, followed by single variables XLV and XDSF with accuracy rates of 78.6% and 78.3%, respectively. An overview of the results with performances above 70% is presented in Table 34. A complete table is available in Appendix B.

Table 34: Cross-validated classification accuracies for T8

Function		Male		Female		Average
	N	Count	%	Count	%	Accuracy
Stepwise (XBV, XLVBs)	57	33	78.8	24	79.2	78.9
XLV	56	32	81.3	24	75.0	78.6
XLS	56	32	75.0	24	70.8	73.2
XLVBs	58	34	76.5	24	75.0	75.9
XLVBi	58	33	69.7	25	72.0	70.7
XDFs	60	35	62.9	25	72.0	66.7
XHBp	56	32	71.9	24	66.7	69.6
XHBa	59	34	67.6	25	72.0	69.5
XHTP	62	36	69.4	26	65.4	67.7
XBV	61	35	77.1	26	76.9	77.0
XDSF	60	36	77.8	24	79.2	78.3
XBFs	57	34	73.5	23	73.9	73.7
XDFc	60	35	65.7	25	80.0	71.7
XBP	60	35	57.1	25	56.0	56.7
XBVBs	57	33	72.7	24	79.2	75.4
XBVBi	62	36	77.8	26	88.5	82.3

Figure 18 shows the calculated posterior probabilities for the stepwise discriminant scores. The posterior probabilities for XBVBi are available in Appendix C.

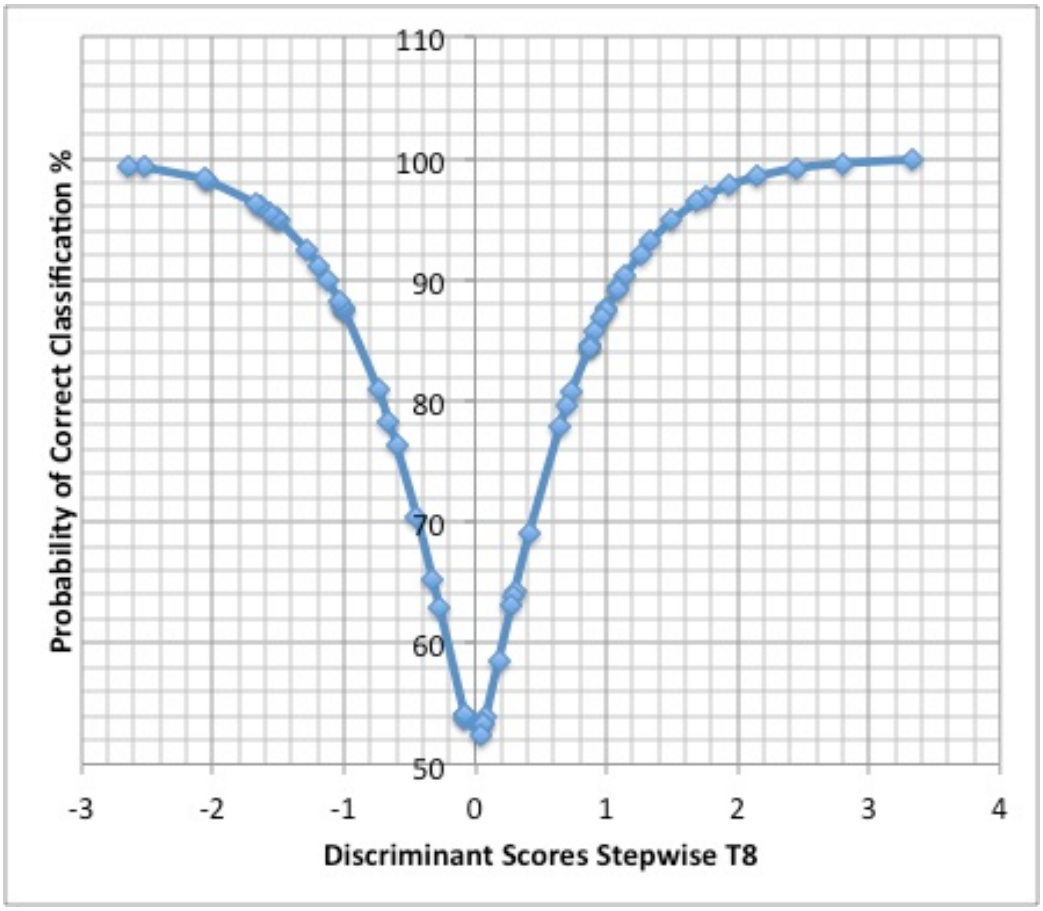

Figure 18: Posterior probabilities for T8 stepwise function

5.9 Ninth thoracic vertebra (T9)

As in T8, all dimensions but XHFs showed to be significant, eleven variables showed significance at level <0.01, four at level <0.05 see Table 35).

Table 35: Descriptive statistics, F-ratios and p-values for the variables measured on T9

	Males (n=37)		Females (n=25)			
Variable	**Mean**	**SD**	**Mean**	**SD**	**F-ratio**	**p-value**
XLV	77.42	3.94	70.57	4.44	36.82	0.00
XLS	41.60	3.47	38.45	4.88	7.96	0.01
XLVBs	28.48	2.39	25.06	2.07	31.98	0.00
XLVBi	28.71	2.51	25.48	1.95	28.10	0.00
XDFs	15.50	1.33	14.43	0.83	12.15	0.00
XHBp	22.16	1.39	20.05	1.60	28.59	0.00
XHBa	20.14	1.29	18.99	1.84	8.22	0.01
XHFs	11.21	1.49	10.81	1.06	1.23	0.27
XHTP	13.83	1.21	12.78	1.37	10.02	0.00
XBV	63.50	4.26	58.34	4.01	22.84	0.00
XDSF	34.62	3.01	31.41	2.66	18.10	0.00
XBFs	11.50	1.63	10.32	1.25	8.72	0.01
XDFc	17.10	1.56	15.57	1.38	15.48	0.00
XBP	6.22	1.27	5.41	0.95	7.32	0.01
XBVBs	31.93	2.64	28.73	2.15	24.02	0.00
XBVBi	40.47	3.05	35.23	2.62	48.30	0.00

XBVBi scored the highest F-ratio with a value of 48.30, followed by XLV with a value of 36.82, and XLVBs with a value of 31.98. The compiled descriptive statistics are presented in Table 35. Direct analyses provided the demarking points for the single variables, and are shown in Table 36.

Table 36: Discriminant function equations and demarking points for T9 using one measurement

Variable	F-ratio	Unstandardized Coefficient	Constant	Demarking Point		
XLV	36.818	0.241	-17.973	Female<	73.97	>Male
XLS	7.960	0.244	-9.821	Female<	39.97	>Male
XLVBs	31.976	0.441	-11.941	Female<	26.78	>Male
XLVBi	28.103	0.435	-11.924	Female<	27.11	>Male
XDFs	12.150	0.864	-13.016	Female<	14.97	>Male
XHBp	28.592	0.676	-14.386	Female<	21.10	>Male
XHBa	8.217	0.653	-12.848	Female<	19.56	>Male
XHTP	10.017	0.784	-10.507	Female<	13.30	>Male
XBV	22.844	0.240	-14.751	Female<	60.96	>Male
XDSF	18.100	0.347	-11.578	Female<	33.02	>Male
XBFs	8.719	0.672	-7.410	Female<	10.91	>Male
XDFc	15.481	0.672	-11.055	Female<	16.32	>Male
XBP	7.320	0.870	-5.120	Female<	5.82	>Male
XBVBs	24.024	0.408	-12.500	Female<	30.36	>Male
XBVBi	48.296	0.347	-13.278	Female<	37.83	>Male

Two variables were selected for the stepwise analysis: XBVBi and XHBp. The associated coefficients, centroids and the constant are presented in Table 37, the sectioning point is set to zero.

Table 37: Stepwise discriminant function statistics for T9, sectioning point set to zero, results are cross-validated

Step	Variable		Exact F	df	Unstandardized Coefficient	Group Centroids
1	XBVBi	Max. Breadth of Body Inf.	39.010	1.52	0.24	M=0.786
2	XHBp	Max. Height of Body Post.	23.818	2.51	0.318	F=-1.144
	(Constant)					-14.862
	Accuracy male					81.8%
	Accuracy female					83.3%
	Accuracy total					82.5%

Only eight variables reached accuracies above 70% (see Table 38). XBVBi proved to be the best indicator when predicting sex, reaching an accuracy rate of 83.3% when used alone, followed by XLV with an accuracy rate of 80.4%. A stepwise approach did not increase the value. Using the selected variables XBVBi and XHBp combined, sex was predicted correctly in 82.5% of the cases.

Table 38: Cross-validated classification accuracies for T9

Function		Male		Female		Average
	N	Count	%	Count	%	Accuracy
Stepwise (XBVBi, XHBp)	57	33	81.8	24	83.3	82.5
XLV	56	33	78.8	23	82.6	80.4
XLS	56	33	66.7	23	65.2	66.1
XLVBs	58	34	76.5	24	70.8	74.1
XLVBi	59	35	62.9	24	75.0	67.8
XDFs	59	35	60.0	24	75.0	66.1
XHBp	58	34	73.5	24	75.0	74.1
XHBa	60	36	58.3	24	62.5	60.0
XHTP	62	37	54.1	25	68.0	59.7
XBV	62	37	73.0	25	72.0	72.6
XDSF	61	37	73.0	24	66.7	70.5
XBFs	57	34	58.8	23	69.6	63.2
XDFc	60	35	68.6	25	88.0	76.7
XBP	60	35	62.9	25	64.0	63.3
XBVBs	58	34	76.5	24	75.0	75.9
XBVBi	60	35	82.9	25	84.0	83.3

The posterior probabilities for the discriminant scores of the stepwise selection are calculated and shown in Figure 19. Posterior probabilities were also calculated for XBVBi and XLV, as both variables reached single accuracies above 80%, and are presented in the Appendix C.

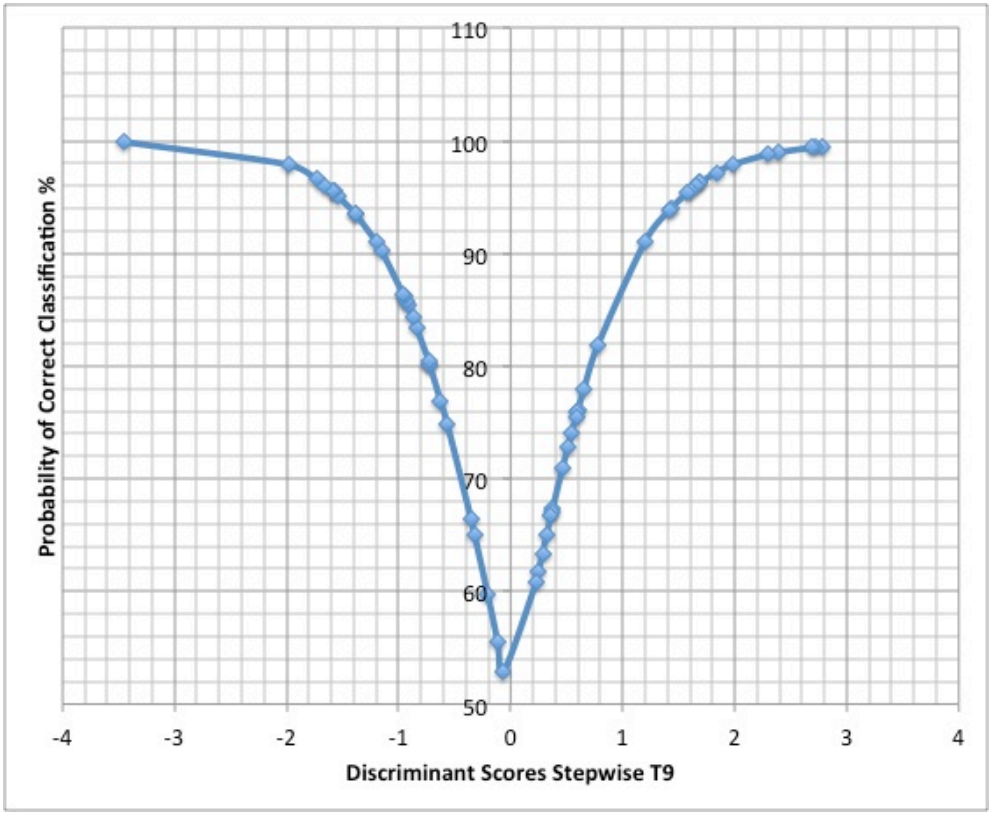

Figure 19: Posterior probabilities for T9 stepwise function

5.10 Tenth thoracic vertebra (T10)

ANOVA was carried out on the variables of T10 and provided descriptive statistics, presented here in Table 39.

Table 39: Descriptive statistics, F-ratios and p-values for the variables measured on T10

	Males (n=36)		**Females** (n=26)			
Variable	**Mean**	**SD**	**Mean**	**SD**	**F-ratio**	**p-value**
XLV	75.87	4.06	69.47	4.62	28.79	0.00
XLS	37.25	3.61	34.89	4.94	4.16	0.05
XLVBs	29.04	2.48	25.28	1.78	41.18	0.00
XLVBi	29.43	2.73	25.63	2.19	32.70	0.00
XDFs	15.43	1.34	14.23	0.99	14.87	0.00
XHBp	23.54	1.75	21.12	1.49	30.60	0.00
XHBa	21.29	1.87	19.65	1.66	12.35	0.00
XHFs	11.75	1.56	11.26	0.89	1.92	0.17
XHTP	13.92	1.33	12.57	1.55	13.68	0.00
XBV	58.63	5.01	53.74	4.45	15.78	0.00
XDSF	35.99	2.61	33.08	2.42	19.94	0.00
XBFs	12.01	1.48	11.47	1.37	2.10	0.15
XDFc	17.22	1.74	15.89	1.49	9.77	0.00
XBP	7.38	1.35	6.20	1.45	10.77	0.00
XBVBs	34.21	2.72	30.63	2.19	30.07	0.00
XBVBi	41.83	2.51	36.86	3.02	47.71	0.00

Three dimensions (XLS, XHFs and XBFs) proved not to be significant in predicting sex. The remaining thirteen variables showed significance in predicting sex at level <0.01 (Table 39). The subsequent direct analysis of the thirteen significant variables provided the demarking points and is presented in Table 40.

Table 40: Discriminant function equations and demarking points for T10 using one measurement

Variable	F-ratio	Unstandardized Coefficient	Constant	Demarking Point		
XLV	28.794	0.231	-16.876	Female<	72.76	>Male
XLS	4.159	0.235	-8.490	Female<	36.02	>Male
XLVBs	41.182	0.452	-12.407	Female<	27.19	>Male
XLVBi	32.699	0.400	-11.077	Female<	27.53	>Male
XDFs	14.872	0.829	-12.376	Female<	14.84	>Male
XHBp	30.595	0.611	-13.687	Female<	22.31	>Male
XHBa	12.353	0.562	-11.555	Female<	20.46	>Male
XHTP	13.684	0.701	-9.363	Female<	13.25	>Male
XBV	15.783	0.209	-11.820	Female<	56.16	>Male
XDSF	19.936	0.395	-13.717	Female<	34.49	>Male
XDFc	9.770	0.609	-10.142	Female<	16.56	>Male
XBP	10.767	0.717	-4.931	Female<	6.79	>Male
XBVBs	30.071	0.399	-13.026	Female<	32.41	>Male
XBVBi	47.710	0.364	-14.445	Female<	39.39	>Male

Only XBVBi was selected for the stepwise analysis. A table is therefore not presented here.

Table 41: Cross-validated classification accuracies for T10

Function		Male		Female		Average
	N	Count	%	Count	%	Accuracy
XLV	53	29	79.3	24	79.2	79.2
XLS	55	30	56.7	25	56.0	56.4
XLVBs	58	33	78.8	25	84.0	81.0
XLVBi	57	31	71.0	26	73.1	71.9
XDFs	61	35	65.7	26	76.9	70.5
XHBp	56	30	73.3	26	84.6	78.6
XHBa	59	33	78.8	26	61.5	71.2
XHTP	62	36	72.2	26	65.4	69.4
XBV	62	36	58.3	26	80.8	67.7
XDSF	62	36	72.2	26	69.2	71.0
XDFc	61	35	74.3	26	88.5	80.3
XBP	61	35	62.9	26	61.5	62.3
XBVBs	60	34	73.5	26	80.8	76.7
XBVBi	59	33	81.8	26	73.1	78.0

The accuracies for the single variables of T10 are presented in Table 41. XLVBs reached the highest single accuracy rate (cross-validated) with a value of 81.0%, closely followed by XDFc with a value of 80.3%. Variables reaching accuracies below 70% when predicting sex

are not presented here, as they are not considered reliable. A complete table with original and cross-validated performances are available in Appendix B.

The posterior probabilities for XLVBs, which scored the highest accuracy rate, are presented in Figure 20.

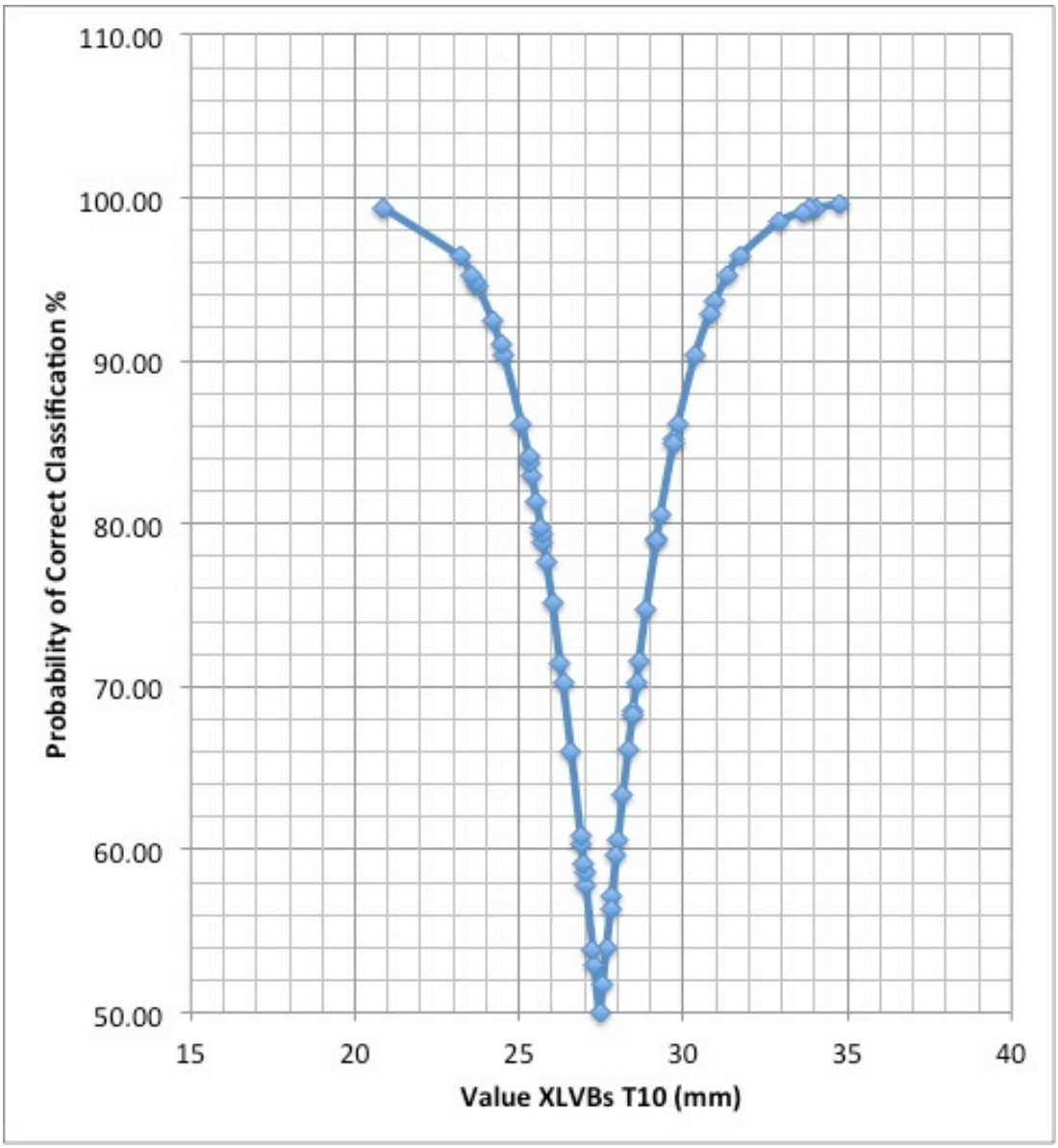

Figure 20: Posterior probabilities for value XLVBs in T10

5.11 Eleventh thoracic vertebra (T11)

ANOVA provided descriptive statistics for T11, including means, standard deviations, F-ratios, and levels of significance in predicting sex. The compiled statistics are presented in Table 42.

Table 42: Descriptive statistics, F-ratios and p-values for the variables measured on T11

	Males (n=37)		Females (n=27)			
Variable	**Mean**	**SD**	**Mean**	**SD**	**F-ratio**	**p-value**
XLV	74.41	3.91	68.56	4.00	28.31	0.00
XLS	31.97	3.06	31.36	4.10	0.38	0.54
XLVBs	29.60	2.52	25.72	2.23	37.60	0.00
XLVBi	30.16	3.40	26.23	2.26	26.81	0.00
XDFs	15.70	1.44	14.73	1.23	7.80	0.01
XHBp	25.27	1.62	23.03	1.65	27.49	0.00
XHBa	21.57	2.01	20.42	1.65	5.69	0.02
XHFs	11.76	1.04	10.90	1.16	8.82	0.00
XHTP	13.51	1.67	12.33	1.94	6.74	0.01
XBV	53.72	4.21	48.70	5.04	18.77	0.00
XDSF	36.00	2.78	32.40	2.59	26.91	0.00
XBFs	11.71	1.40	11.02	1.09	4.23	0.04
XDFc	18.78	2.06	17.20	1.35	11.84	0.00
XBP	8.56	1.84	7.20	1.33	10.41	0.00
XBVBs	37.92	2.68	33.38	2.39	46.33	0.00
XBVBi	45.18	3.01	39.57	2.81	56.08	0.00

The only variable not showing any significance in predicting sex was XLS. Out of the remaining variables, eleven showed to be highly dimorphic at level <0.01. XBVBi scored the highest F-ratio with a value of 56.08, followed by XBVBs with value 46.33, and XLVBs with value 37.60 (see Table 42). The direct analysis of the fifteen significant variables, including the demarking points, is presented in Table 43.

Table 43: Discriminant function equations and demarking points for T11 using one measurement

Variable	F-ratio	Unstandardized Coefficient	Constant	Demarking Point		
XLV	28.306	0.253	-18.153	Female<	71.53	>Male
XLVBs	37.599	0.417	-11.625	Female<	27.68	>Male
XLVBi	26.805	0.338	-9.610	Female<	28.18	>Male
XDFs	7.798	0.739	-11.293	Female<	15.22	>Male
XHBp	27.491	0.613	-14.872	Female<	24.17	>Male
XHBa	5.692	0.536	-11.301	Female<	21.00	>Male
XHFs	8.816	0.913	-10.379	Female<	11.33	>Male
XHTP	6.744	0.559	-7.273	Female<	12.92	>Male
XBV	18.768	0.218	-11.274	Female<	51.32	>Male
XDSF	26.912	0.370	-12.775	Female<	34.24	>Male
XBFs	4.234	0.788	-8.980	Female<	11.36	>Male
XDFc	11.843	0.562	-10.158	Female<	17.98	>Male
XBP	10.405	0.613	-4.879	Female<	7.88	>Male
XBVBs	46.328	0.392	-14.038	Female<	35.62	>Male
XBVBi	56.084	0.341	-14.625	Female<	42.40	>Male

As in T10, the stepwise analysis selected only one variable, XBVBi, which previously scored the highest F-ratio. Accuracies for the single variables are presented in Table 44. XBVBi showed to be the most accurate single variable predicting sex correctly in 81.0% of the cases when used alone, and was the only variable to reach a score above 80%

Table 44: Cross-validated classification accuracies for T11

Function		Male		Female		Average
	N	Count	%	Count	%	Accuracy
XLV	52	28	75.0	24	79.2	76.9
XLVBs	58	32	75.0	26	76.9	75.9
XLVBi	62	35	65.7	27	81.5	72.6
XDFs	62	35	57.1	27	66.7	61.3
XHBp	59	32	78.1	27	77.8	78.0
XHBa	61	35	51.4	26	65.4	57.4
XHFs	57	31	64.5	26	69.2	66.7
XHTP	64	37	59.5	27	70.4	64.1
XBV	64	37	67.6	27	85.2	75.0
XDSF	62	36	77.8	26	80.8	79.0
XBFs	58	32	56.3	26	69.2	62.1
XDFc	61	34	61.8	27	85.2	72.1
XBP	61	34	67.6	27	74.1	70.5
XBVBs	59	32	75.0	27	77.8	76.3
XBVBi	63	37	81.1	26	80.8	81.0

Posterior probabilities are for the dimension of single variable XBVBi are presented in Figure 21.

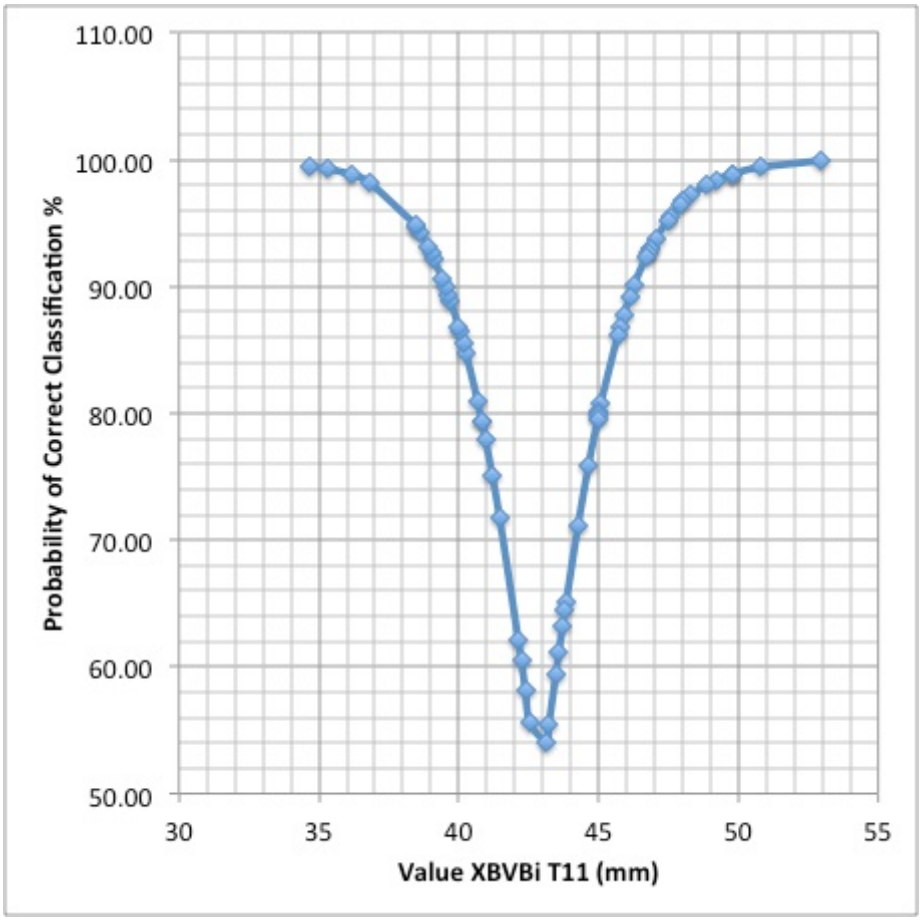

Figure 21: Posterior probabilities for value XBVBi in T11

5.12 Twelfth thoracic vertebra (T12)

The descriptive statistics show that thirteen dimensions are significant in determining sex in T12. XLS, XHFs and XBP all reached levels above 0.05, and are therefore not regarded as significant (see Table 45).

Table 45: Descriptive statistics, F-ratios and p-values for the variables measured on T12

	Males (n=38)		Females (n=28)			
Variable	**Mean**	**SD**	**Mean**	**SD**	**F-ratio**	**p-value**
XLV	77.79	4.18	71.17	3.15	39.63	0.00
XLS	31.64	2.72	29.98	3.26	4.16	0.05
XLVBs	30.77	3.13	26.67	2.25	33.89	0.00
XLVBi	30.61	3.20	26.97	2.68	23.28	0.00
XDFs	16.64	1.39	15.72	1.14	8.09	0.01
XHBp	26.35	1.76	23.99	1.85	26.55	0.00
XHBa	23.13	2.07	21.82	1.91	6.74	0.01
XHFs	11.57	1.52	11.11	1.26	1.63	0.21
XHTP	16.11	2.61	14.71	1.95	5.45	0.02
XBV	49.17	4.73	44.30	4.69	15.99	0.00
XDSF	35.74	2.66	32.41	2.94	22.44	0.00
XBFs	10.85	1.34	9.71	1.20	12.17	0.00
XDFc	21.75	2.11	20.27	1.30	10.66	0.00
XBP	8.18	2.12	7.61	1.17	1.64	0.21
XBVBs	41.19	3.02	36.52	2.54	43.28	0.00
XBVBi	46.91	3.39	41.08	2.95	53.16	0.00

Out of the remaining thirteen variables, XBVBi reached the highest F-ratio value with 53.16. XBVBs and XLV reached values of 43.28, and 39.63, respectively (Table 45). Direct analyses of the thirteen significant variables produced the demarking points for the single dimensions and are presented in Table 46.

Table 46: Discriminant function equations and demarking points for T12 using one measurement

Variable	F-ratio	Unstandardized Coefficient	Constant	Demarking Point		
XLV	39.628	0.263	-19.784	Female<	74.61	>Male
XLS	4.157	0.339	-10.496	Female<	30.81	>Male
XLVBs	33.890	0.360	-10.416	Female<	28.71	>Male
XLVBi	23.275	0.335	-9.727	Female<	28.83	>Male
XDFs	8.085	0.776	-12.612	Female<	16.19	>Male
XHBp	26.551	0.556	-14.056	Female<	25.15	>Male
XHBa	6.744	0.499	-11.262	Female<	22.49	>Male
XHTP	5.451	0.426	-6.603	Female<	15.41	>Male
XBV	15.992	0.212	-9.997	Female<	46.79	>Male
XDSF	22.439	0.359	-12.302	Female<	34.06	>Male
XBFs	12.174	0.779	-8.059	Female<	10.28	>Male
XDFc	10.661	0.553	-11.683	Female<	21.02	>Male
XBVBs	43.282	0.355	-13.882	Female<	38.81	>Male
XBVBi	53.164	0.312	-13.842	Female<	43.92	>Male

XBVBs and XDSF were selected for the stepwise analysis, results are presented in Table 47. The sectioning points are set to zero.

Table 47: Stepwise discriminant function statistics for T12, sectioning point set to zero, results are cross-validated

Step	Variable		Exact F	df	Unstandardized Coefficient	Group Centroids
1	XBVBs	Max. Breadth of Body Sup.	43.007	1.45	0.319	M=0.898
2	XDSF	Max. Dist. of Facets Sup.	25.035	2.44	0.129	F=-1.213
	(Constant)					-16.811
	Accuracy male					76.5%
	Accuracy female					82.1%
	Accuracy total					79.0%

XBVBi scored the highest accuracy rate in determining sex with value of 83.3%. The only other single variable predicting sex correctly with an accuracy rate above 80% was XLV with 81.5%. The stepwise approach did not increase these accuracy rates. The combination of XBVBs and XDSF determined sex correctly in 79.0% of all cases, cross-validated. The results of variables scoring above 70% in accuracy when predicting sex are presented in Table 48.

Table 48: Cross-validated classification accuracies for T12

Function		Male		Female		Average
	N	Count	%	Count	%	Accuracy
Stepwise (XBVBs, XDSF)	62	34	76.5	28	82.1	79.0
XLV	54	32	75.0	22	90.9	81.5
XLS	54	32	62.5	22	54.5	59.3
XLVBs	63	35	62.9	28	82.1	71.4
XLVBi	63	35	62.9	28	82.1	71.4
XDFs	65	37	62.2	28	67.9	64.6
XHBp	63	35	80.0	28	71.4	76.2
XHBa	64	36	58.3	28	57.1	57.8
XHTP	62	35	48.6	27	70.4	58.1
XBV	61	35	68.6	26	69.2	68.9
XDSF	64	36	72.2	28	78.6	75.0
XBFs	63	35	62.9	28	71.4	66.7
XDFc	65	37	70.3	28	85.7	76.9
XBVBs	64	36	72.2	28	82.1	76.6
XBVBi	66	38	81.6	28	85.7	83.3

Figure 22 shows the calculated posterior probabilities for the stepwise discriminant scores of T12. Posterior probabilities were also calculated for single variables XBVBi and XLV, and are available in the Appendix C.

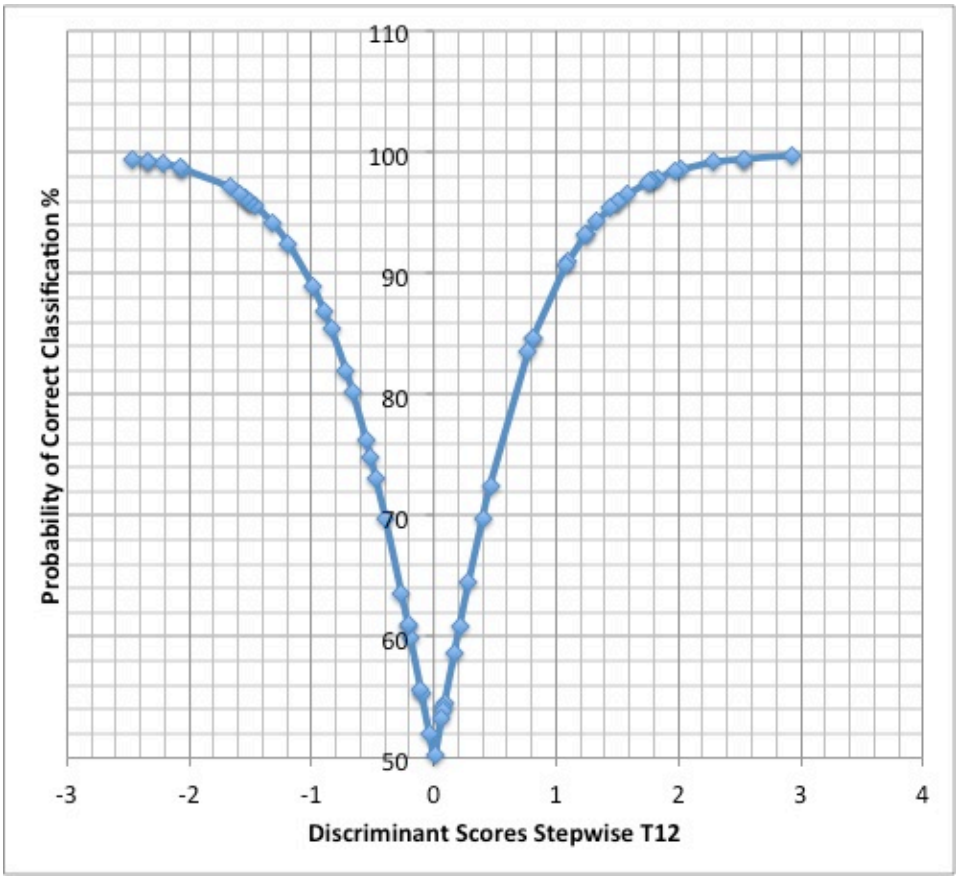

Figure 22: Posterior probabilities for T12 stepwise function

5.13 Fixed-Model Approach

In order to test for an increase of accuracies derived from stepwise method, a fixed-model method was tested on all vertebrae using the overall best performing variables. To determine the best-performing variables, all single accuracies were gathered and the average accuracy was calculated. The results show that only variables XLV and XBVBi had an average accuracy rate of above 80%. However, in order to get a more dependable result in the fixed-model approach XBV was also included, as the overall accuracy rate was very close to 80% (see Table 49).

Table 49: Overview of single accuracies of the Fixed-Model approach

	T1	T2	T3	T4	T5	T6	T7	T8	T9	T10	T11	T12	Total
XLV	87.5	79.7	78.7	85.0	86.8	82.2	78.0	78.6	80.4	79.2	76.9	81.5	**81.2**
XLS	73.4	65.0	65.6	68.3	60.0	74.2	64.4	73.2	66.1	56.4		59.3	66.0
XLVBs	80.0	77.8	75.4	80.6	75.9	73.0	76.7	75.9	74.1	81.0	75.9	71.4	76.5
XLVBi	81.3	74.6	77.3	80.4	75.4	78.7	75.0	70.7	67.8	71.9	72.6	71.4	74.8
XDFs	66.2	63.1	62.7	62.9	62.9	59.4	54.0	66.7	66.1	70.5	61.3	64.6	63.4
XHBp	79.7	77.4	71.9	66.7	77.6	79.7	73.7	69.6	74.1	78.6	78.0	76.2	75.3
XHBa	69.2	66.7	60.3	62.7	70.7	74.6	75.0	69.5	60.0	71.2	57.4	57.8	66.3
XHFs		65.1	60.3		59.6	62.9	47.5				66.7		60.4
XHTP	76.9	73.8	82.1	76.2	75.4	78.5	76.9	67.7	59.7	69.4	64.1	58.1	71.6
XBV	87.7	83.1	89.4	82.5	80.0	84.8	87.5	77.0	72.6	67.7	75.0	68.9	**79.7**
XDSF	71.4	82.5	83.1	70.5	76.3	73.4	80.6	78.3	70.5	71.0	79.0	75.0	76.0
XBFs		68.3	71.9	61.3	59.6	67.7	61.0	73.7	63.2		62.1	66.7	65.6
XDFc	72.3	75.4	77.6	73.0	77.4	70.8	73.0	71.7	76.7	80.3	72.1	76.9	74.8
XBP	75.0	64.6	66.7	61.9	65.1	53.8	64.1	56.7	63.3	62.3	70.5		64.0
XBVBs	70.3	73.0	78.5	75.8	77.6	79.4	78.3	75.4	75.9	76.7	76.3	76.6	76.2
XBVBi	75.0	81.3	86.6	83.3	81.3	84.4	83.1	82.3	83.3	78.0	81.0	83.3	**81.9**

Variables XLV, XBV and XBVBi combined were then tested in a direct approach on every vertebra.

5.13.1 Fixed-Model Approach for T1

Table 50 shows the result of the fixed-model approach for T1. In comparison to the stepwise approach, the accuracies slightly decreased. The posterior probabilities chart is presented in Figure 23.

Table 50: Fixed-Model statistics for T1, results are cross-validated

Variable		F	Unstandardized Coefficient	Group Centroids
XLV	Max. Length	65.631	0.144	M=1.165
XBV	Max. Breadth	90.640	0.186	F=-1.457
XBVBi	Max. Breadth of Body Inf.	31.815	0.003	
(Constant)				-22.884
Accuracy male				91.4%
Accuracy female				85.7%
Accuracy total				88.9%

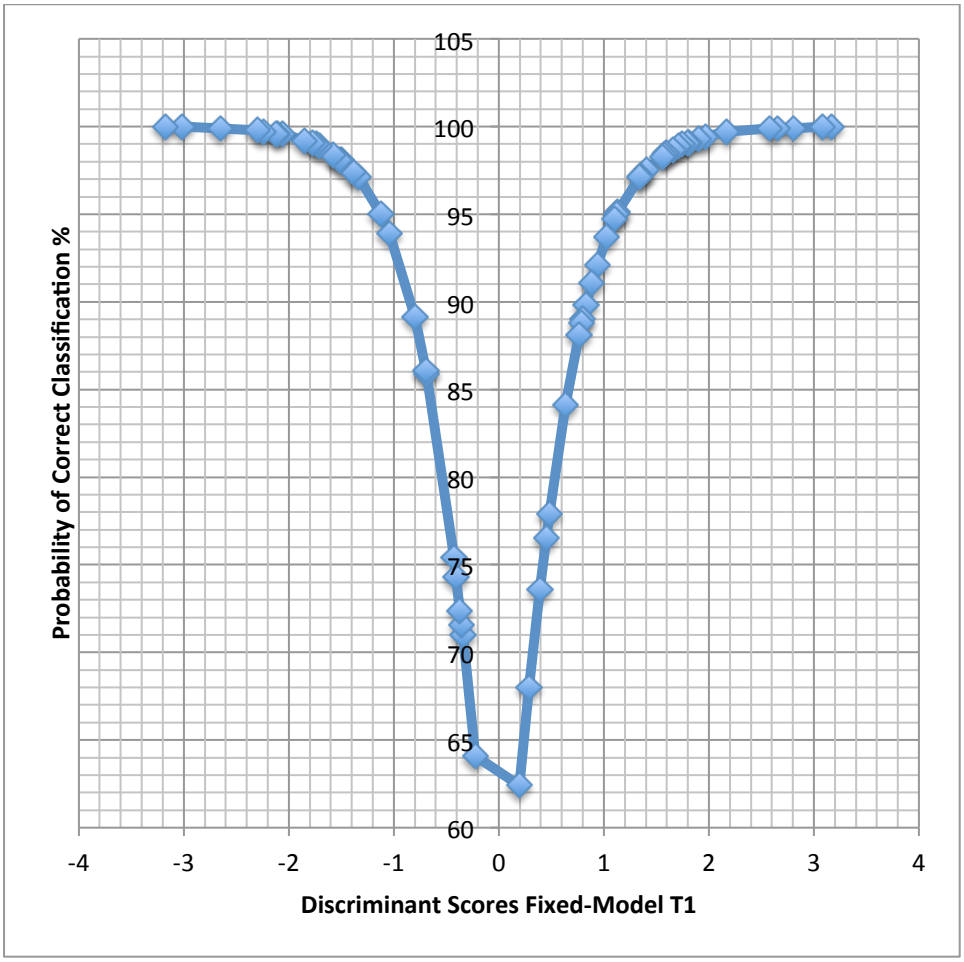

Figure 23: Posterior probabilities for T1 Fixed-Model

5.13.2 Fixed-Model Approach for T2

The results of the T2 fixed-model approach did also not increase the overall accuracies, although the male accuracies showed slightly higher figures (see Table 51) when compared to the stepwise method. See Figure 24 for the posterior probabilities for the fixed-model approach in T2.

Table 51: Fixed-Model statistics for T2, results are cross-validated

Variables		**F**	**Unstandardized Coefficient**	**Group Centroids**
XLV	Max. Length	44.205	0.118	M=1.193
XBV	Max. Breadth	62.765	0.098	F=-1.370
XBVBi	Max. Breadth of Body Inf.	59.094	0.195	
(Constant)				-21.094
Accuracy male				90.3%
Accuracy female				85.2%
Accuracy total				87.9%

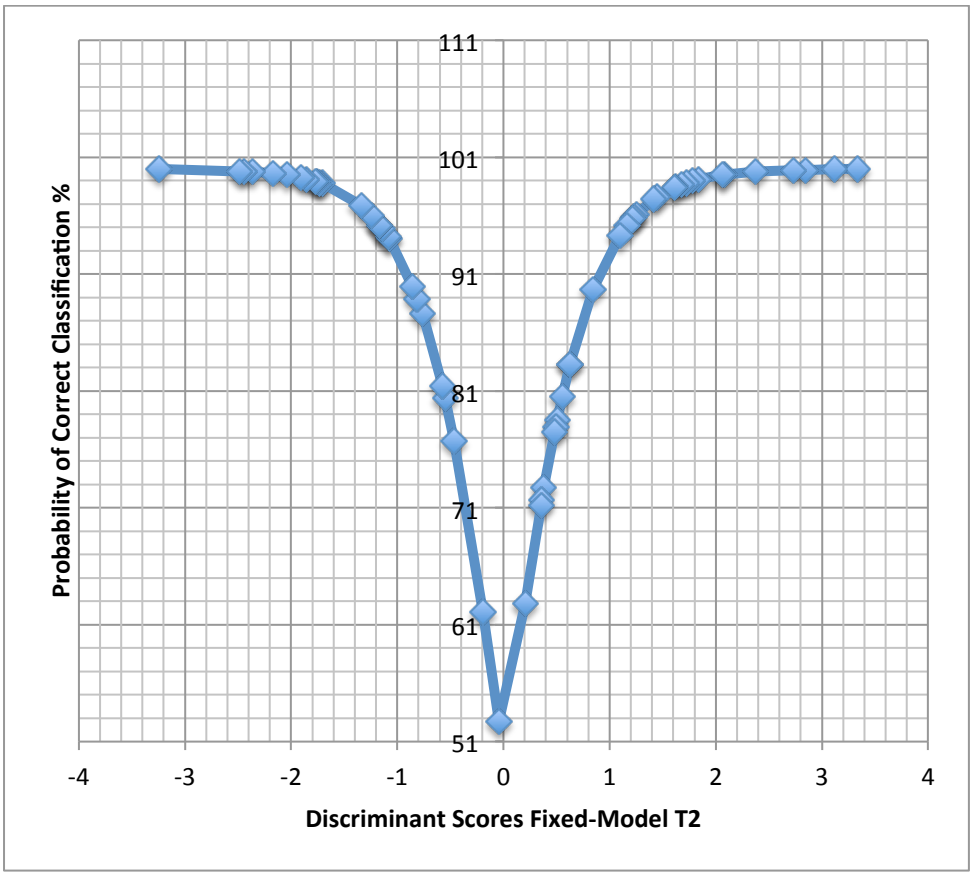

Figure 24: Posterior probabilities for T2 Fixed-Model

5.13.3 Fixed-Model Approach for T3

T3 showed only a minimal increase in the overall accuracy rate with females predicting sex correctly in 90% of the cases (see Table 52). The posterior probabilities for T2 are presented in Figure 25.

Table 52: Fixed-Model statistics for T3, results are cross-validated

Variables		**F**	**Unstandardized Coefficient**	**Group Centroids**
XLV	Max. Length	38.517	0.062	M=1.101
XBV	Max. Breadth	62.591	0.113	F=-1.346
XBVBi	Max. Breadth of Body Inf.	65.179	0.251	
(Constant)				-19.582
Accuracy male				81.8%
Accuracy female				92.6%
Accuracy total				86.7%

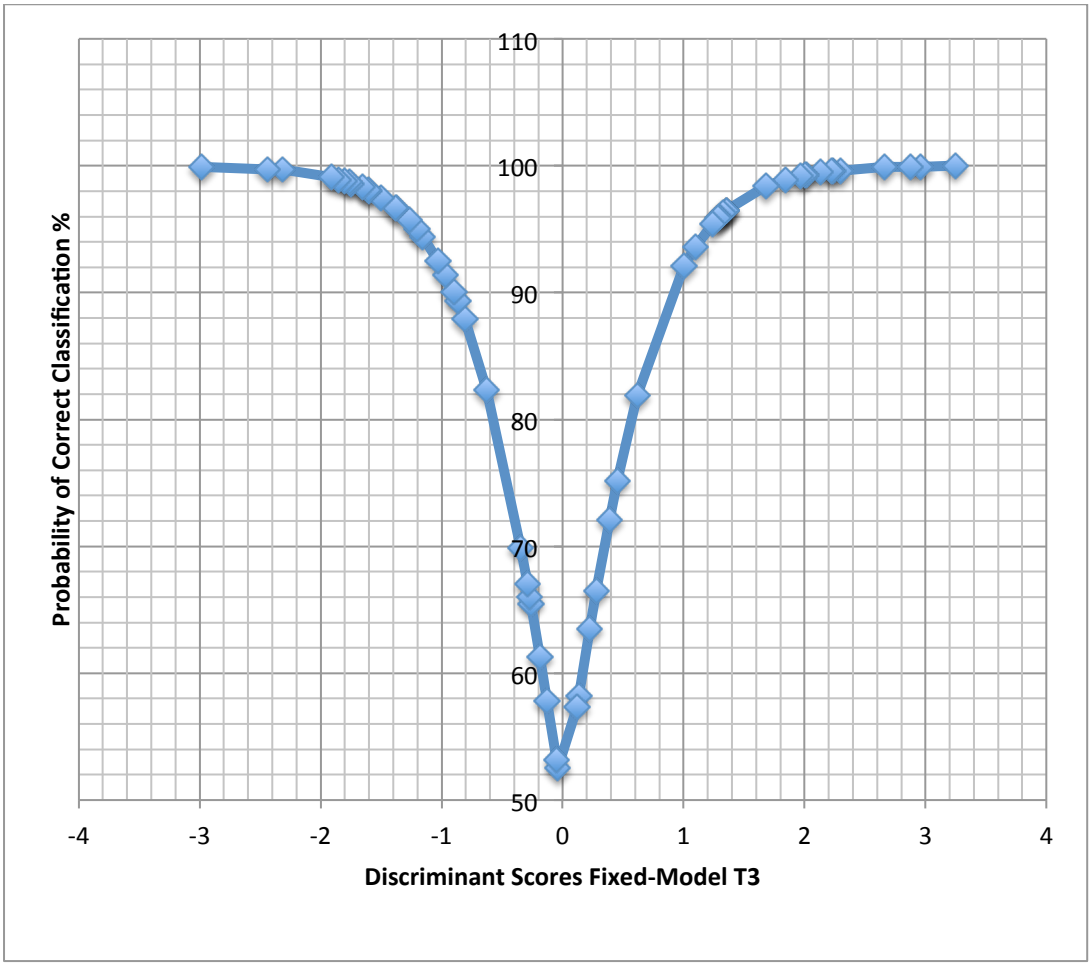

Figure 25: Posterior probabilities for T3 Fixed-Model

5.13.4 Fixed-Model Approach for T4

Table 53 shows the slightly decreased accuracy rates for the fixed-model in T4, the posterior probabilities for T4 are presented in Figure 26.

Table 53: Fixed-Model statistics for T4, results are cross-validated

Variables		**F**	**Unstandardized Coefficient**	**Group Centroids**
XLV	Max. Length	44.943	0.114	M=1.094
XBV	Max. Breadth	33.509	0.035	F=-1.346
XBVBi	Max. Breadth of Body Inf.	64.414	0.339	
(Constant)				-21.206
Accuracy male				78.1%
Accuracy female				88.5%
Accuracy total				82.8%

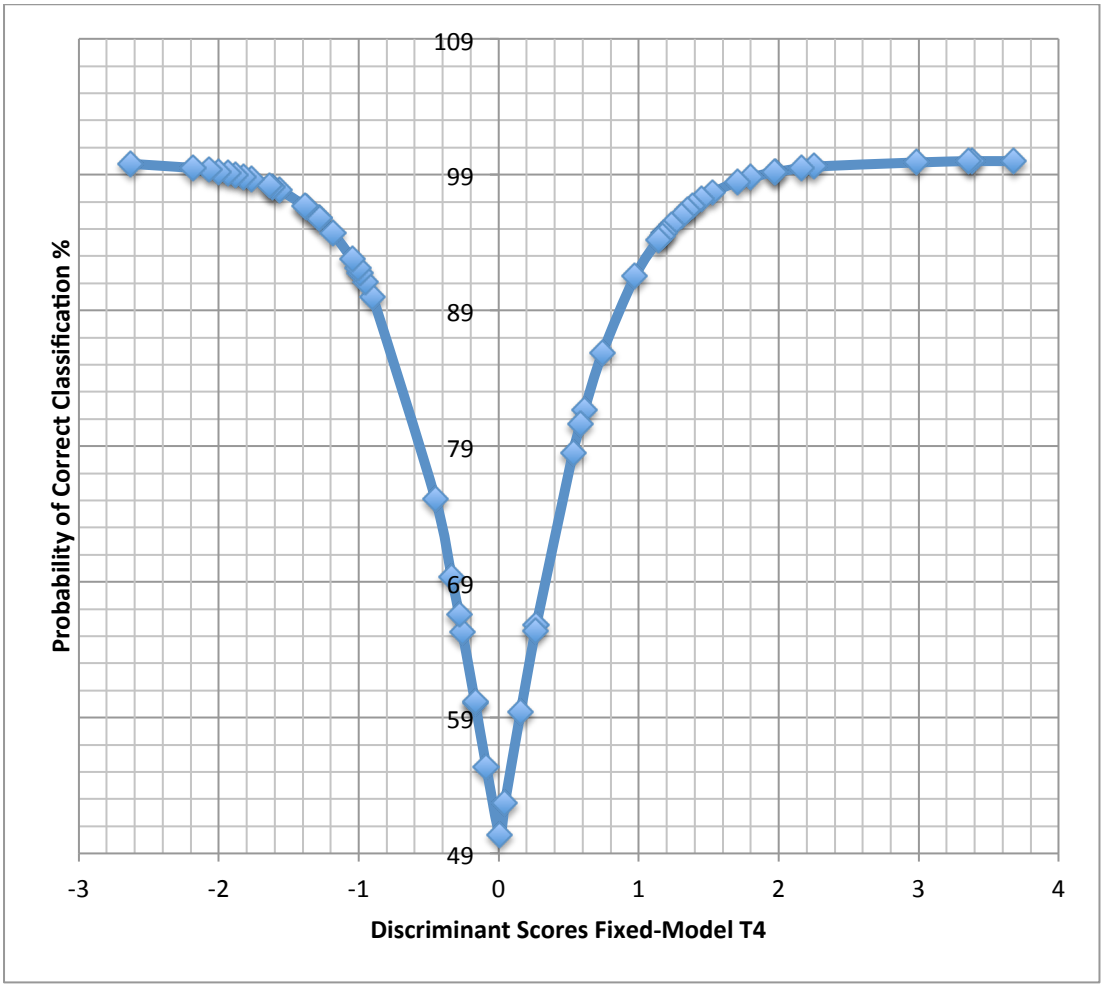

Figure 26: Posterior probabilities for T4 Fixed-Model

5.13.5 Fixed-Model Approach for T5

Also in T5 (see Table 54) the accuracy rates could not be improved by the fixed-model approach. Even though the females predicted sex correctly at a better rate, the overall accuracy slightly decreased in comparison to the stepwise method. Figure 27 shows the posterior probabilities for the fixed-model approach in T5.

Table 54: Fixed-Model statistics for T5, results are cross-validated

Variables		**F**	**Unstandardized Coefficient**	**Group Centroids**
XLV	Max. Length	47.622	0.179	M=1.007
XBV	Max. Breadth	27.179	-0.026	F=-1.373
XBVBi	Max. Breadth of Body Inf.	44.743	0.294	
(Constant)				-21.063
Accuracy male				80.0%
Accuracy female				90.9%
Accuracy total				84.6%

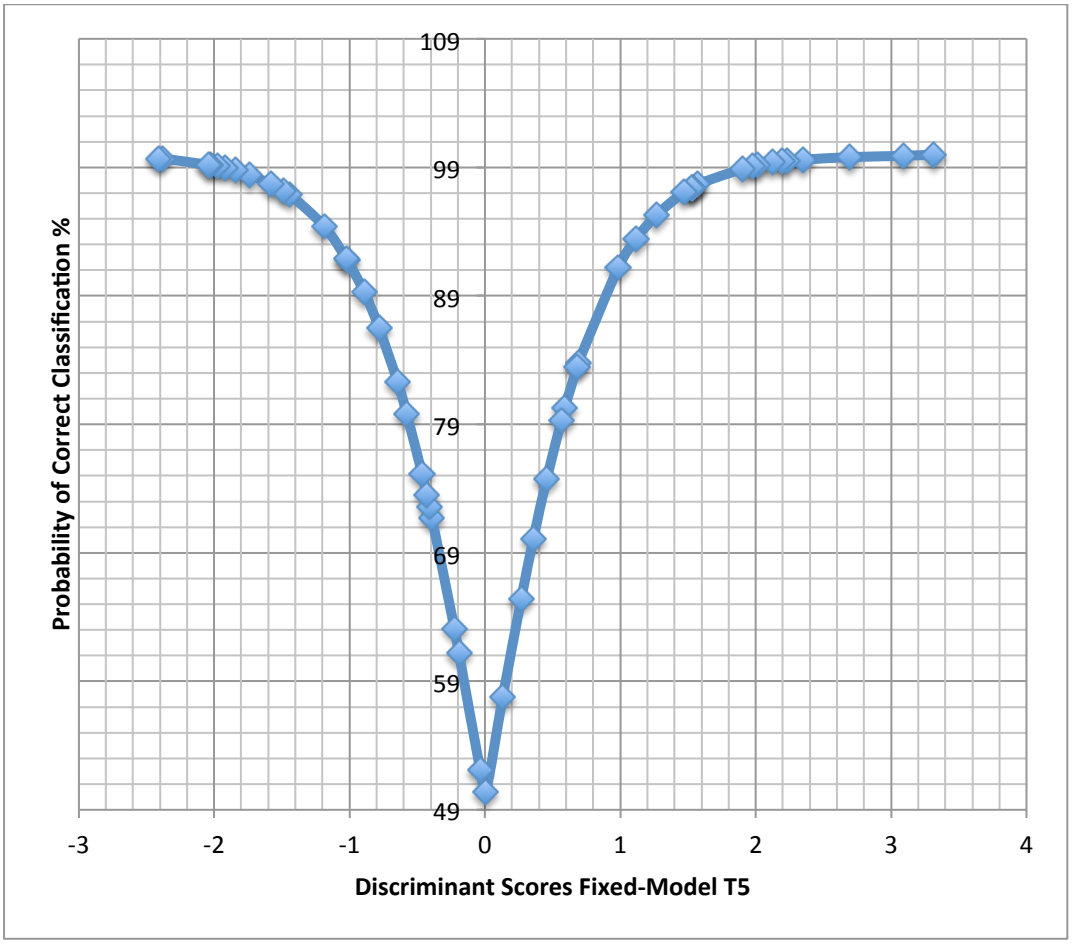

Figure 27: Posterior probabilities for T5 Fixed-Model

5.13.6 Fixed-Model Approach for T6

T6 improved the overall accuracy by 1.7% using the fixed-model (see Table 55). The posterior probabilities chart is presented in Figure 28.

Table 55: Fixed-Model statistics for T6, results are cross-validated

Variables		**F**	**Unstandardized Coefficient**	**Group Centroids**
XLV	Max. Length	65.323	0.146	M=1.135
XBV	Max. Breadth	53.434	0.052	F=-1.345
XBVBi	Max. Breadth of Body Inf.	58.195	0.191	
(Constant)				-20.525
Accuracy male				87.5%
Accuracy female				92.6%
Accuracy total				89.8%

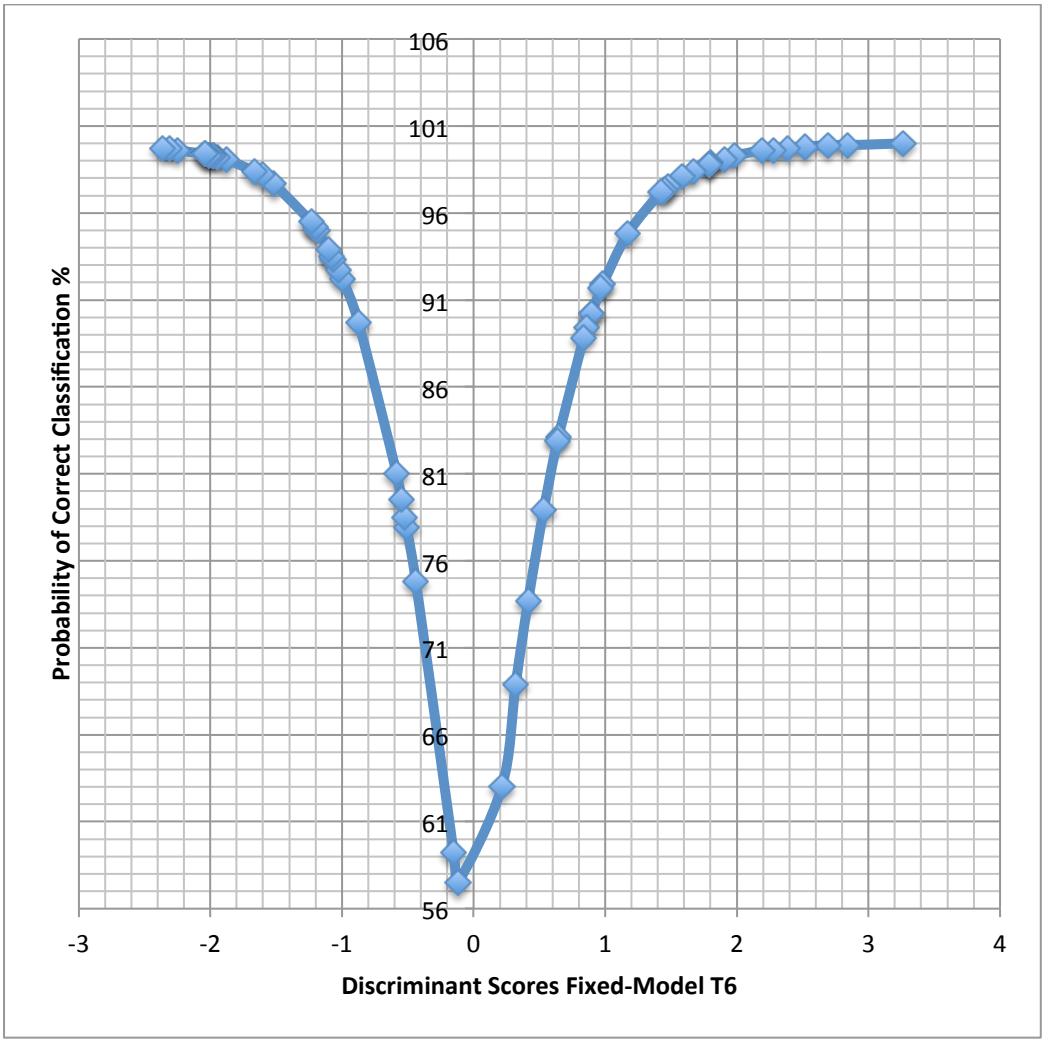

Figure 28: Posterior probabilities for T6 Fixed-Model

5.13.7 Fixed-Model Approach for T7

Also in T7, the fixed-model could slightly increase the overall prediction rate. In comparison to the stepwise approach, the males scored significantly higher (see Table 56). Posterior probabilities are presented in Figure 29.

Table 56: Fixed-Model statistics for T7, results are cross-validated

Variables		**F**	**Unstandardized Coefficient**	**Group Centroids**
XLV	Max. Length	43.526	0.079	M=0.907
XBV	Max. Breadth	54.294	0.128	F=-1.285
XBVBi	Max. Breadth of Body Inf.	46.352	0.135	
(Constant)				-18.718
Accuracy male				88.2%
Accuracy female				83.3%
Accuracy total				86.2%

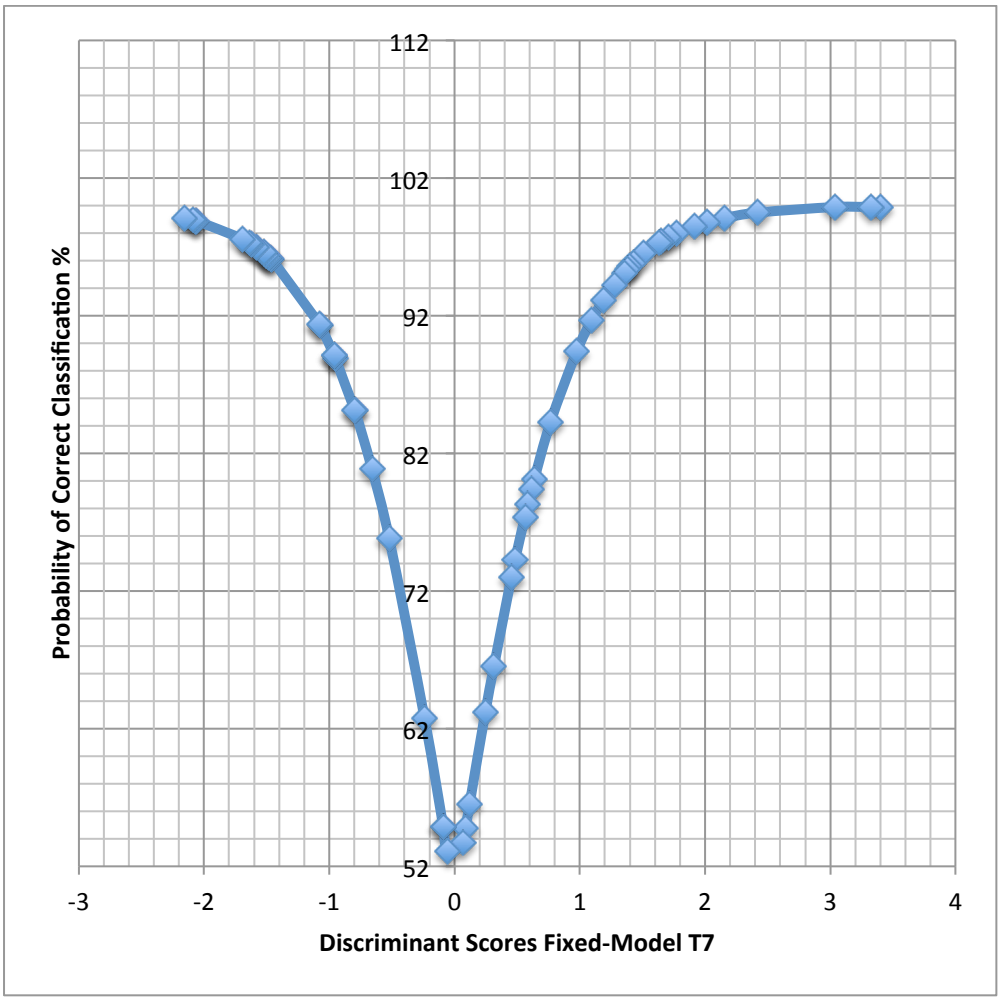

Figure 29: Posterior probabilities for T7 Fixed-Model

5.13.8 Fixed-Model Approach for T8

A noticeable increase in accuracy can be seen in T8. While the females performed at the same prediction rate, the males could increase the overall accuracy by 6.6% (see Table 57). Figure 30 shows the posterior probabilities for the fixed-model approach in T8.

Table 57: Fixed-Model statistics for T8, results are cross-validated

Variables		**F**	**Unstandardized Coefficient**	**Group Centroids**
XLV	Max. Length	38.764	0.119	M=0.872
XBV	Max. Breadth	37.734	0.107	F=-1.126
XBVBi	Max. Breadth of Body Inf.	33.862	0.094	
(Constant)				-18.959
Accuracy male				90.3%
Accuracy female				79.2%
Accuracy total				85.5%

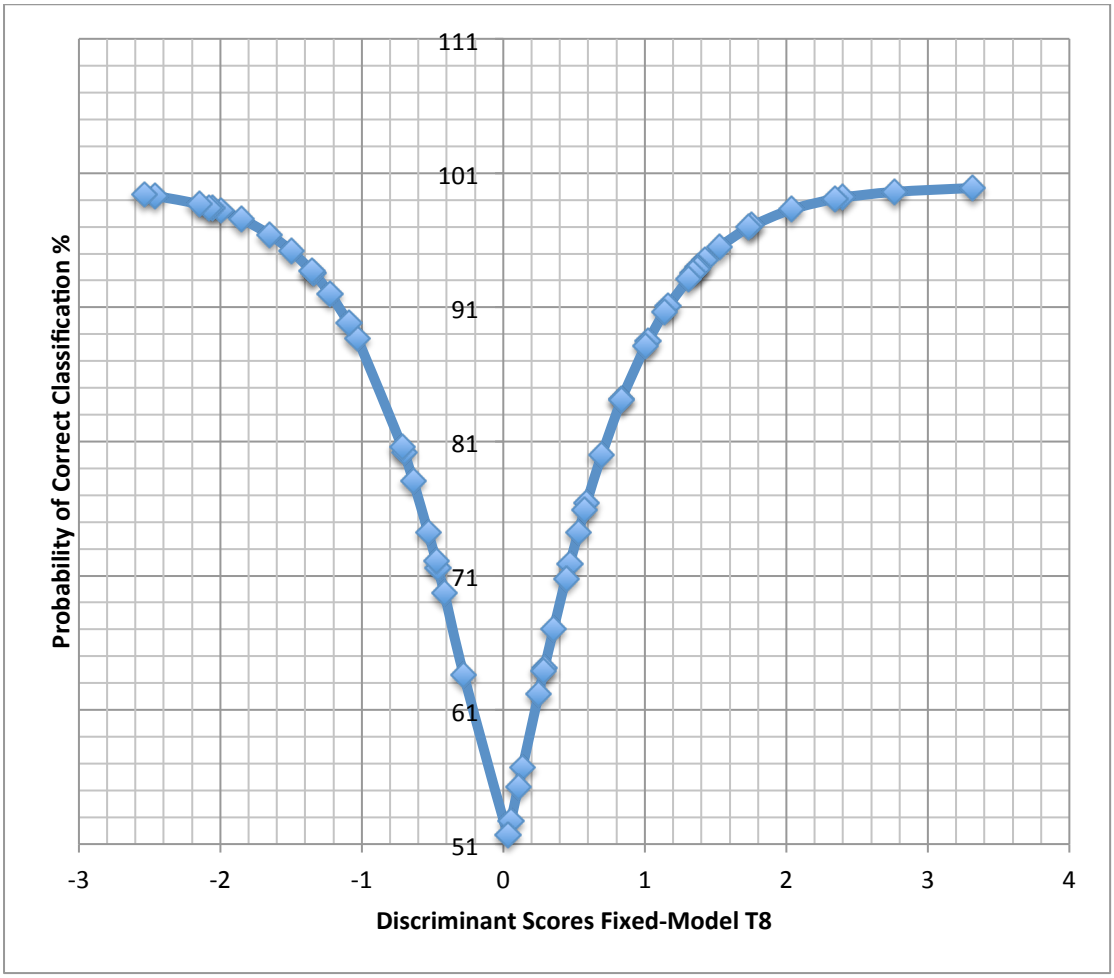

Figure 30: Posterior probabilities for T8 Fixed-Model

5.13.9 Fixed-Model Approach for T9

Table 58 shows the results of the fixed-model approach in T9. All accuracies show lower values when compared to the stepwise approach. Posterior probabilities for T9 are presented in Figure 31.

Table 58: Fixed-Model statistics for T9, results are cross-validated

Variables		**F**	**Unstandardized Coefficient**	**Group Centroids**
XLV	Max. Length	35.284	0.120	M=0.807
XBV	Max. Breadth	17.672	-0.011	F=-1.123
XBVBi	Max. Breadth of Body Inf.	41.921	0.225	
(Constant)				-16.741
Accuracy male				81.3%
Accuracy female				78.3%
Accuracy total				80.0%

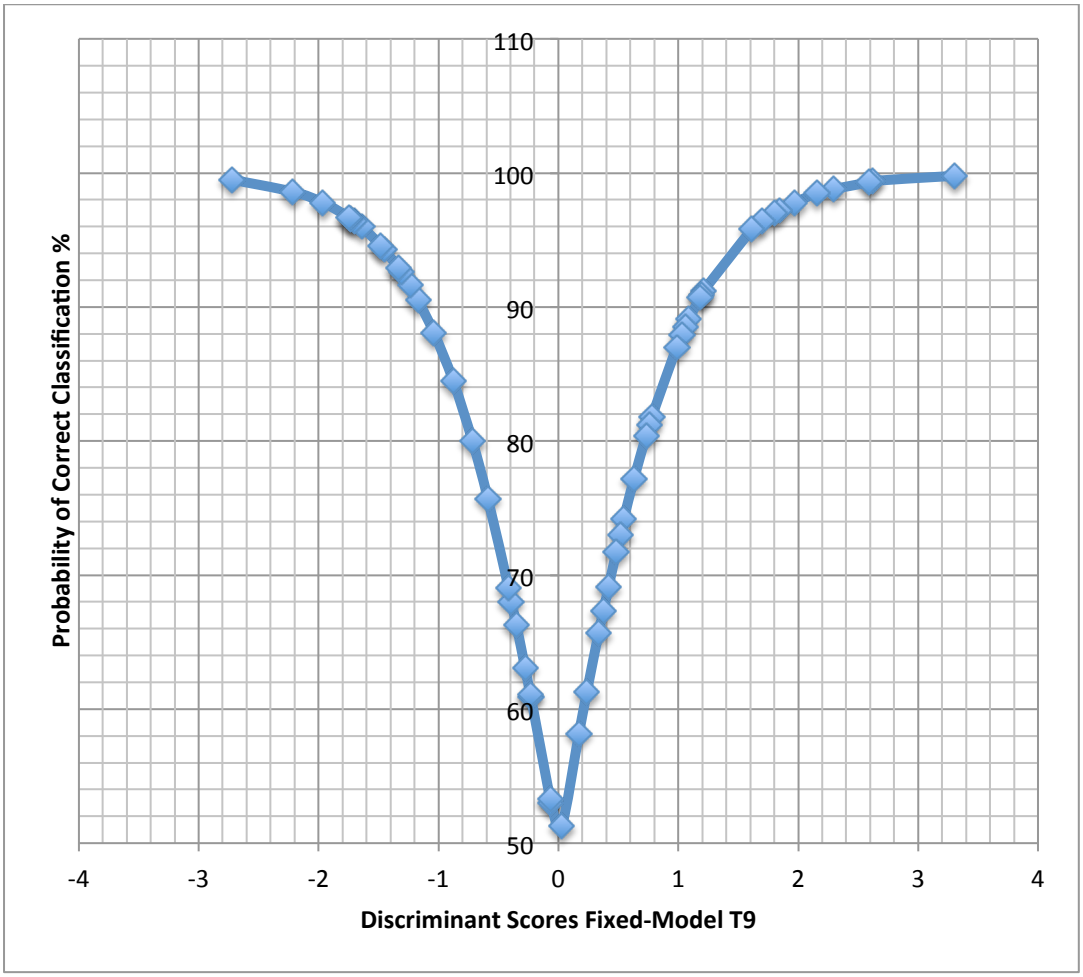

Figure 31: Posterior probabilities for T9 Fixed-Model

5.13.10 Fixed-Model Approach for T10

In comparison to the stepwise approach, all accuracies showed significantly higher figures in T10. The overall accuracy increased by 6% (see Table 59). Figure 32 shows the posterior probabilities for T10.

Table 59: Fixed-Model statistics for T10, results are cross-validated

Variables		**F**	**Unstandardized Coefficient**	**Group Centroids**
XLV	Max. Length	30.348	0.045	M=1.005
XBV	Max. Breadth	15.263	0.062	F=-1.088
XBVBi	Max. Breadth of Body Inf.	46.648	0.286	
(Constant)				-18.047
Accuracy male				84.6%
Accuracy female				83.3%
Accuracy total				84.0%

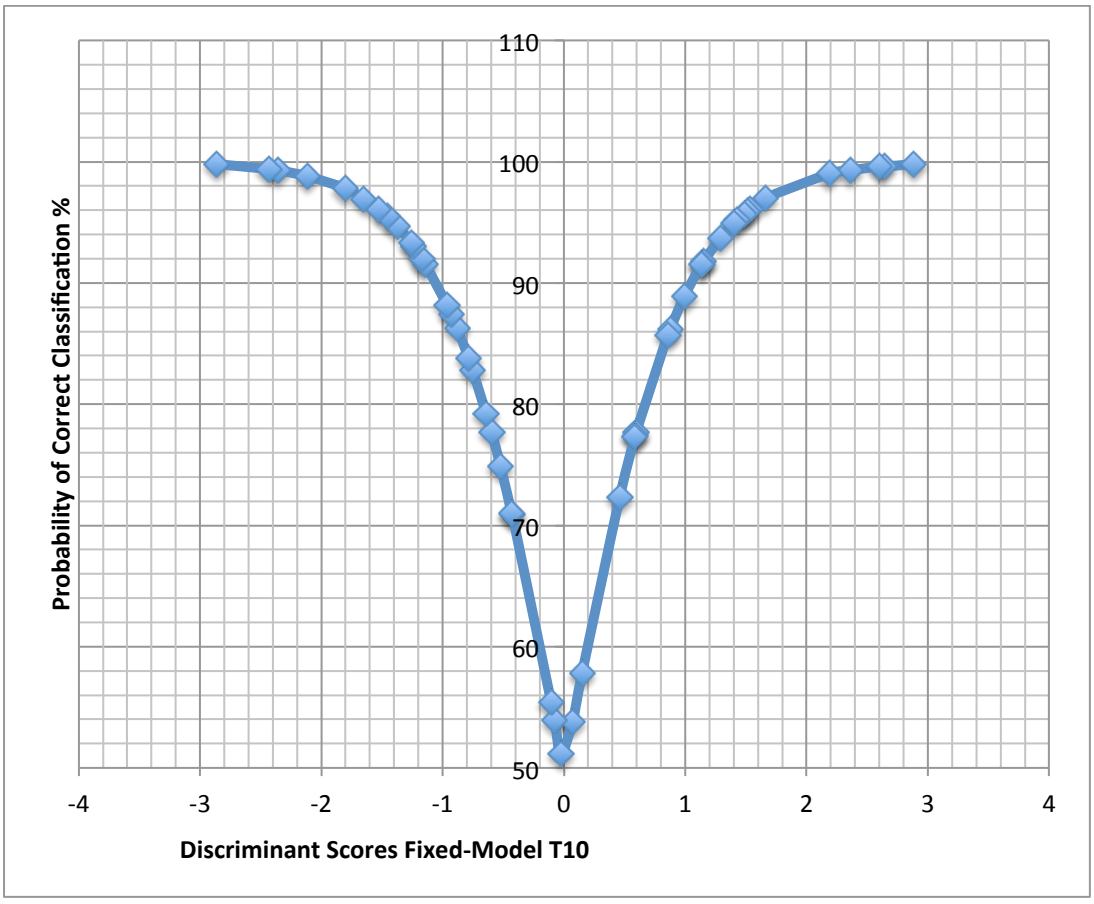

Figure 32: Posterior probabilities for T10 Fixed-Model

5.13.11 Fixed-Model Approach for T11

The most significant increase can bee seen in T11. All accuracies improved at least by 6% when compared to the stepwise approach (see Table 60). The overall accuracies improved by 6.9%. Posterior probabilities are presented in Figure 33.

Table 60: Fixed-Model statistics for T11, results are cross-validated

Variables		**F**	**Unstandardized Coefficient**	**Group Centroids**
XLV	Max. Length	27.286	0.014	M=1.037
XBV	Max. Breadth	17.690	0.039	F=-1.263
XBVBi	Max. Breadth of Body Inf.	64.239	0.316	
(Constant)				-16.490
Accuracy male				85.7%
Accuracy female				87.0%
Accuracy total				86.3%

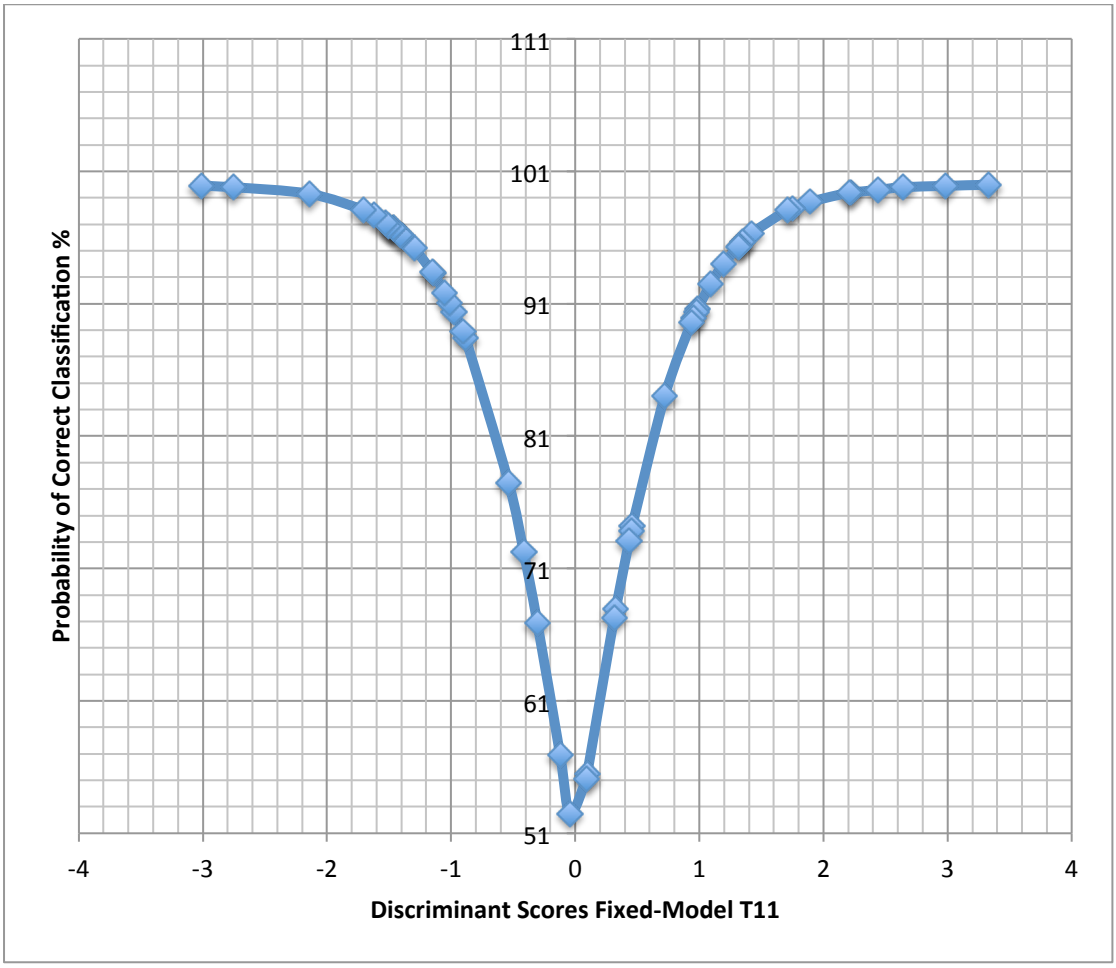

Figure 33: Posterior probabilities for T11 Fixed-Model

5.13.12 Fixed-Model Approach for T12

Even though the females performed slightly better, the fixed-model of T12 did not improve the overall accuracies (see Table. 61). Figure 34 provides the posterior probabilities for T12.

Table 61: Fixed-Model statistics for T12, results are cross-validated

Variables		**F**	**Unstandardized Coefficient**	**Group Centroids**
XLV	Max. Length	38.658	0.124	M=0.811
XBV	Max. Breadth	12.569	0.039	F=-1.216
XBVBi	Max. Breadth of Body Inf.	40.581	0.165	
(Constant)				-18.340
Accuracy male				70.0%
Accuracy female				85.0%
Accuracy total				76.0%

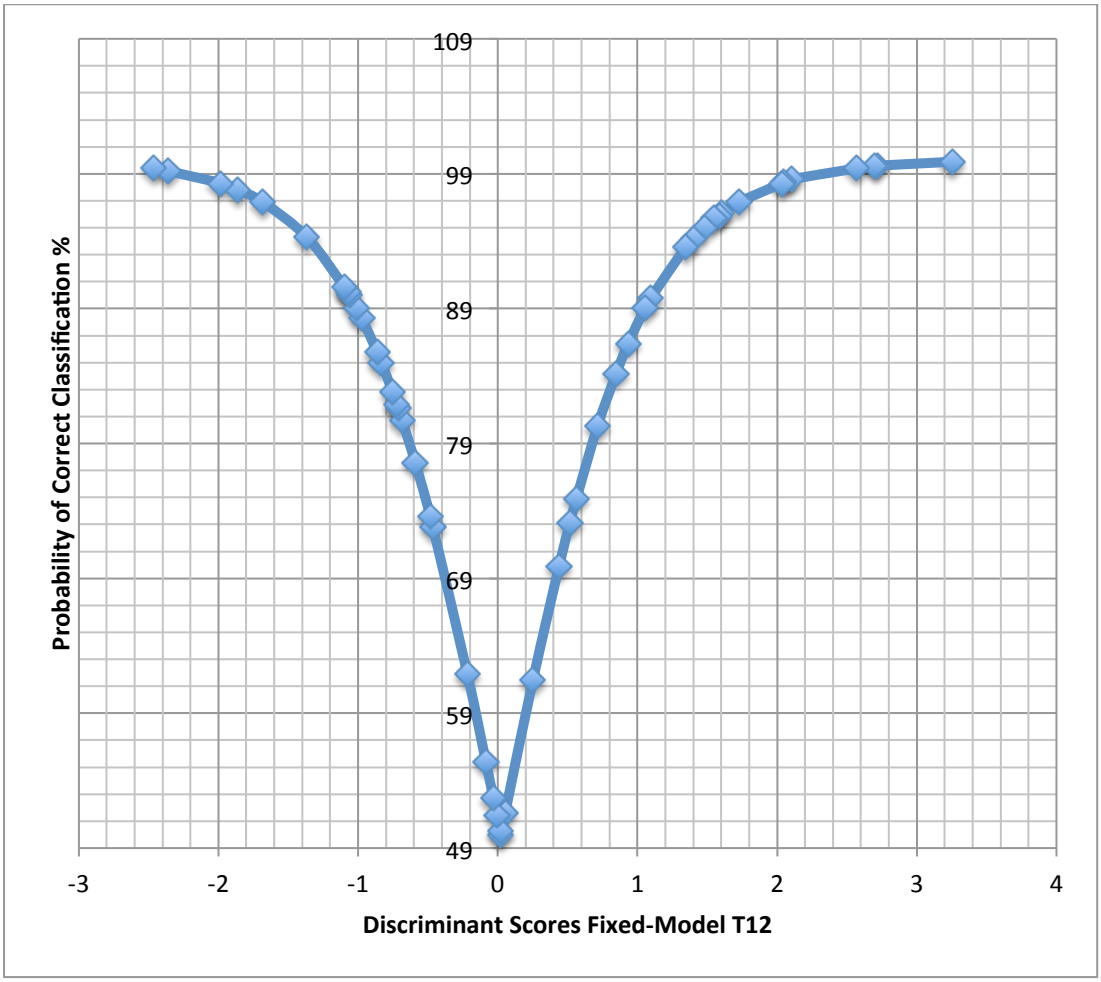

Figure 34: Posterior probabilities for T12 Fixed-Model

5.14 Summary Results

Most measurements in every vertebra had p-values smaller than the alpha level of 0.05. Out of the 16 measurements taken, the greatest number of measurements per vertebra not being significant at level <0.05 was three (in T10 and T12). Some measurements had a higher frequency of not being significant. XHFs was not significant for determining sex in seven of the twelve vertebrae, having a p-value greater than 0.05. XLS was not significant in three vertebrae, XBFs in two, and XDFs and XBP were each not significant in 1 vertebra.

Certain variables also proved to be better discriminators than others. XLVBi was selected eight times in the stepwise procedure, and XLV five times. Both measurements also showed the highest overall F-values when compared to other variables. The levels of classification accuracy varied greatly among the vertebrae. The lowest classification rate in a grouping was scored in T12, reaching 70.0% accuracy for the males using the fixed-model. The highest rate of classification was reached for males in the T2 grouping with 93.5% accuracy. The lowest accuracy level for females in a grouping reached 73.1% in T10, while the highest rate of classification (92.9%) was reached in T7 using variables XBV and XHTP combined. Looking at the prediction accuracies of the single variables, XBV reached the highest score in T3 with 89.4%, while XHFs scored the lowest in T7 with 47.5%. The stepwise analysis of T1 reached the overall highest total accuracy with 90.6%, with 38/64 cases predicting above the confidence level of 95% (see Appendix D). The fixed-model approach showed mixed results. T8, T10 and T11 showed significant improvement of more than 6% in accuracy when compared to the stepwise approach. Nevertheless, only six out of the 12 vertebrae showed higher results.

6 Discussion

Various researchers have conducted studies on vertebrae, establishing standards in the estimation of sex for several different populations (MacLaughlin & Oldale 1992, Liguoro 1994, Marino 1995, Wescott 2000, Pastor 2005, Tague 2007, Yu et al. 2008, Kibii et al. 2010, Marlow & Pastor 2011, Hou et al. 2012, Zheng et al. 2012), yet only few have been specifically concerned with the thoracic vertebrae even though past results showed high accuracies in determining sex (MacLaughlin and Oldale 1992; Pastor 2005; Yu et al. 2008; Zheng et al. 2012).

The present study demonstrated the presence of sexual dimorphism in the thoracic vertebrae. Analysis of variance (ANOVA) was carried out on 70 individuals of Cretan origin in order to test for the significance of sex, and discriminant function analyses were used in order to provide equations for future use in estimating sex from the thoracic vertebrae. The findings of this study show that in all thoracic vertebrae at least several metric dimensions demonstrate significant differences between males and females.

A direct comparison can only be made with T11 and T12, as they are the only thoracic vertebrae subject to previous studies. The findings for T12 are similar to the ones of Yu's study (Yu et al. 2008) in regards to the high degree of sexual dimorphism for the maximum inferior breadth of the vertebral body (XBVBi). This variable showed to be the trait with the highest single accuracy in the current study with 83.3% and yielded a similar, although not the highest, result in Yu's study, where its equivalent variable (iBDcm) reached an accuracy rate of 80.4%, using 102 three-dimensional vertebral models of Korean individuals. Hou et al. (2012), who studied a collection of 141 three-dimensional vertebral models of northeast Chinese origin, reached an accuracy of 83.0% with their equivalent variable iBDc. A similar result was reached in Pastor's study (Pastor 2005). His variable CENLAT (medio-lateral diameter of the centrum) yielded the highest single accuracy with 76.9%, which derived from 53 individuals of the Spitalfields collection. In comparison to the remaining thoracic vertebrae of this study, XBVBi reached the highest single accuracies in four of the twelve bones.

Zheng's (2012) study for the first lumbar vertebra determined EPWu (the upper end-plate width of the vertebral body) as the variable with the highest overall accuracy with 86.6%. It is interesting to see, that this variable is directly attached to XBVBi of T12 in the present study. The corresponding variable to XBVBi in Zheng's (2012) study was EPWl, which predicted sex correctly in 85.2% of the cases when used alone.

The maximum length of vertebra (XLV) was the only other variable in T12 scoring above 80%, and also the highest scoring variable in Hou's study. Comparing the results, XLV reached an accuracy rate of 81.5%, while the equivalent measurement (iVL) in Hou's research reached 90.1% (Hou et al. 2012). The maximum length of vertebra was also the variable with the highest single accuracy (81.7%) in Wescott's study of the second cervical vertebra, but not in Marlow's who adapted Wescott's method on the same bone (Wescott 2000, Marlow & Pastor 2011). A direct comparison to MacLaughlin and Oldales's (1992) variables for T11 cannot be made as they differ significantly.

The stepwise approach in T12 selected the maximum superior breadth of the vertebra (XBVBs) and the maximum distance of the superior facets (XDSF), reaching an overall accuracy of 79.0%. Hou and Yu reached far higher scores in their analyses, 94.2% and 90.0%, respectively. A direct comparison is not possible, as several of the measurements/ratios in both of the studies do not exist in the current one.

Overall, the maximum breadth of vertebra (XBV) proved to be the highest scoring single dimension in five out of twelve vertebrae, but with poor results in T12. Its accuracy of 68.9% is comparable to previous studies by Yu and Hou (Yu et al. 2008, Hou et al. 2012) who have reached similar results with their equivalent variable TDm, scoring 62.7% and 67.4%, respectively. Comparison to the C1 and C2 studies is not made due to the strong morphological differences between the bones.

A combination of measurements only reached higher results in T1 (90.6%), T2 (89.5%) and T6 (88.1%). XBVBi and XLV were the two dimensions that were selected most in the stepwise approach.

The highest result using a single variable was reached in T3 with variable XBV (maximum breadth of vertebra), reaching a cross-validated classification accuracy of 89.4%, with 28/66 cases predicting correctly above the confidence level of 95%.

Multi-variate function in T1 used two variables (XBV and XLV) and reached the highest cross-validated accuracy rate with 90.6%, and 38/64 cases predicting correctly at a confidence level >95% (see APPENDIX D).

Overall, the current study agrees with previous ones that the means of metric measurements are generally larger in males than in females (Zhang, Yu, Hou, Wescott, Kibii). In addition, females were assigned more frequently to the correct sex than males, in single variate- as

well as in multi-variate analyses. This finding concurs with the study of MacLaughlin and Oldale (1992).

In regards to population specific differences, Wescott (2000) noted that the discriminating ability is reduced when different populations are pooled. Human proportions vary between populations, therefore affecting accurate metric determinations of sex. The most reliable results are therefore made if the population investigated is as similar as possible (Marlow & Pastor 2011).

The applicability of this method to other Greek collections cannot be drawn, as no similar studies exist. Even though a comparison to the previously mentioned studies for other populations yielded similar results, in terms of the significance of variables, comparative data are only available for T11 and T12.

Overall, the present results demonstrate that the vertebrae are not only effective when determining sex, but are also of equal value when compared to other bones of the Greek population (see Table 49).

Table 62: Overview of accuracies from the Cretan collection

Bone	Author	Year	Accuracy
Crania	Kranioti et al.	2008	88.2%
Femur	Kranioti, Vorniotakis et al.	2009	92.9%
Humerus	Kranioti, Bastir et al.	2009	89.7%
Clavicle	Papaioannou et al.	2012	89.8%
Scapula	Papaioannou et al.	2012	95.9%
Thoracic Vertebrae	Gambaro	2013	90.6%

Ancestry remains an important factor when determining sex from a thoracic vertebra, and needs to be taken into consideration. The method used in this study should be applied to other populations in order to test its applicability.

7 Conclusion

While previous studies are based on archaeological material (see Marlow & Pastor 2011), the present study is based on a contemporary and documented collection, making it immediately applicable to forensic investigation. Establishing methods from modern reference data has been stressed repeatedly and is an important aspect (Ubelaker 2008, Dirkmaat et al. 2008), not least to comply with the implications of the Daubert criteria (Klepinger 2006). This study shows that the thoracic vertebrae of the Greek population are sexually dimorphic, reaching single accuracy rates up to 89.4%. Multi-variate analysis yielded results as high as 90.6% accuracy with 38 out of 64 cases predicting correctly above the confidence level of 95%. These results clearly show the value of the vertebrae in regards to determining sex in the Greek population. But although the calculated posterior probabilities may provide an additional asset to the application of this method, the actual number/position of the vertebra to be investigated needs to be known. Even though it is unlikely that a thoracic vertebra is used solely for sex estimation when a complete skeleton is present, it is useful in cases where skeletons are fragmentary or incomplete. Further research with larger sample sizes of other populations is necessary in order to assess the extent of sexual dimorphism between the ethnical groups.

8 References

Aitken C., Roberts P., Jackson G., 2010. *Fundamentals of Probability and Statistical Evidence in Criminal Proceedings,* Practitioner Guide No 1, Royal Statistical Society's Working Group on Statistics and the Law

Barrier I.L., 2007. *Sex Determination from the Bones of the Forearm in a Modern South African Sample* [Dissertation]. Pretoria, University of Pretoria

Barrier I.L., L'Abbé E.N., 2008. Sex Determination from the Radius and Ulna in a Modern South African sample. *Forensic Science International,* 179:85.E81-85.e87

Barrio, P.A., Trancho, G.J., Sanchez, J.A., 2006. Metacarpal Sexual Determination in a Spanish Population. *Journal of Forensic Sciences*, 51(5):990-95

Bass, W. M., 1987 *Human Osteology: A Laboratory and Field Manual*, 3rd ed. Columbia, Missouri Archaeological Society

Berrizbeitia, E.L., 1989. Sex Determination with the Head of the Radius. *Journal of Forensic Sciences,* 34(5):1206-13

Brickley, M.B., Ferllini, R., 2007. *Forensic Anthropology: Case Studies from Europe*, Springfield, Charles C Thomas Publisher, Ltd.

Britz H.M., Thomas D.C., Clement J.G., Cooper D.M., 2009. The Relation of Femoral Osteon Geometry to Age, Sex, Height and Weight. *Bone*, 45:77-83

Brooks S.T., Suchey J.M., 1990. Skeletal Age Estimation Based on the Os Pubis: A Comparison of the Acsádi and Nemeskéri and Suchey-Brooks methods. *Human Evolution*, 5:227–38

Brown R.P., Ubelaker D.H., Shanfield M.S., 2007. Evaluation of Purkait's Triangle Method for Determining Sexual Dimorphism. *Journal of Forensic Sciences*, 52(3):553-56

Buckberry, J.L., Chamberlain, A.T., 2002. Age Estimation from the auricular surface of the Ilium: A Revised Method. *American Journal of Physical Anthropology*, 119(3):231-39

Buikstra J.E., Ubelaker D., 1994. Standards for Data Collection from Human Skeletal Remains: Proceedings of a Seminar at the Field Museum of Natural History. Fayetteville, Archaeological Survey Research Series No. 44.

Burns, R.B., Burns, R.A., 2008. *Business Research Methods and Statistics Using SPSS*, London, SAGE Publications, Ltd.

Bytheway J.A., Ross A.H., 2010. A Geometric Morphometric Approach to Sex Determination of the Human Adult Os Coxa. *Journal of Forensic Sciences*, 55(4):859-64

Case, T.D. and Ross, A.H., 2007. Sex Determination from Hand and Foot Bone Lengths. *Journal of Forensic Sciences*, 52(2):264-70

Deshmukh A.G., Devershi D.B., 2006. Comparison of Cranial Sex Determination by Univariate and Multivariate Analysis. *Journal of the Anatomical Society of India*, 55:48-51

DeVilliers H., 1968. The skull of the South African Negro. *South African Journal of Science*, (64):118-124

Dirkmaat, D.C., 2012. *A Companion to Forensic Anthropology*, Chichester, John Wiley & Sons, Ltd.

Dirkmaat, D.C., Cabo L.L., Ousley S.D., Symes S.A., 2008. New Perspectives in Forensic Anthropology. *Yearbook of Physical Anthropology,* 51:33-52

Dittrick J., Myers Suchey J., 1986. Sex Determination of Prehistoric Central California Skeletal Remains Using Discriminant Analysis of the Femur and Humerus. *American Journal of Physical Anthropology,* 70:3-9

Falsetti, A.B., 1995. Sex Assessment from Metacarpals of the Human Hand. *Journal of Forensic Sciences*, 40(5):774-76

Falys, C.G., Schutkowski, H., Weston, D.A., 2005. The Distal Humerus - A Blind Test of Rogers' Sexing Technique Using a Documented Skeletal Collection. *Journal of Forensic Sciences*, 50(6):1289-93

Franklin D., 2010. Forensic Age Estimation in Human Skeletal Remains: Current Concepts and Future Directions. *Legal Medicine*, 12:1-7

Fully G., 1956. Une Nouvelle Méthode de Détermination de la Taille. *Annales de médecine légale*, 35:266-273

Gilsanz V., Boechat I.M., Roe T.F., Loro L.M., Sayre J.W., Goodman W.G., 1994. Gender Differences in Vertebral Body Sizes in Children and Adolescents. *Radiology*, 190:673-77

Gualdi-Russo, E., 2007. Sex Determination from the Talus and Calcaneus measurements. *Forensic Science International*, 171(2-3):151-56

Holland T.D., 1991. Sex Assessment Using the Proximal Tibia. *American Journal of Physical Anthropology*, 85:221-27

Holman D.J., Bennett K.A., 1991. Determination of Sex from Arm Bone Measurements. *American Journal of Physical Anthropology,* 84:421-426

Hou W.B, Cheng K.L., Tian S.Y., Lu Y.Q., Han Y.Y., Lai Y., Li Y.Q., 2012. Metric Method for Sex Determination Based on the 12th Thoracic Vertebra in Contemporary North-Easterners in China. *Journal of Forensic and Legal Medicine*, 19:137-43

Ingle S., 1991. Bones of Contention: Witnesses From the Grave: The Stories Bones Tell *By Christopher Joyce and Eric Stover,* Los Angeles Times, Los Angeles

İşcan M.Y., 1988. Rise of Forensic Anthropology. *Yearbook of Physical Anthropology,* 31:203-30

İşcan M.Y., Loth S.R., 1997. The Scope of Forensic Anthropology. In: Eckert W.G., editor. *Introduction to Forensic Sciences*. Boca Raton, CRC Press, p 343-369.

İşcan M.Y., Loth S.R., Wright R.K., 1984. Metamorphosis at the Sternal Rib End: A New Method to Estimate Age at Death in White Males. American Journal of Physical Anthropology, 65(2):147-56).

İşcan M.Y., Miller-Shaivitz, P., 1984. Determination of Sex from The Tibia. *American Journal of Physical Anthropology*, 64(1):53-57

Kerley E.R., Ubelaker D.H., 1978. Revisions in the Microscopic Method of Estimating Age at Death in Human Cortical Bone. *American Journal of Physical Anthropology,* 49:545-46

Kibii J.M., Pan R., Tobias P.V., 2010. Morphometric Variations of the 7th Cervical Vertebrae of Zulu, White, and Colored South Africans. *Clinical Anatomy,* 23:399-406

Kieser J.A, Moggi-Cechi J., Groenenveld H.T., 1992. Sex Allocation of Skeletal Material by Analysis of the Proximal Tibia, *Forensic Science International*, 56:29-36

King C.A., İşcan Y.M., Loth S.R., 1998. Metric and Comparative Analysis of Sexual Dimorphism in the Thai Femur. *Journal of Forensic Sciences,* 43(5):954-58

Klepinger L., 2006. *Fundamentals of Forensic Anthropology*, Hoboken, John Wiley & Sons, Inc.

Kocak A., Aktas E.Ö., Ertürk S., Yemiscigil A., 2003. Sex Determination from the Sternal End of the Rib by Osteometric Analysis. *Legal Medicine*, 5(2):100-04

Kranioti E.F., 2009. *Identification of Sex Based on Digital Radiographs of the Skeleton* (Dissertation). Heraklion, University of Crete

Kranioti E.F., Bastir M., Sànchez-Meseguer A., Rosas A., 2009. A Geometric-Morphometric Study of the Cretan Humerus for Sex Identification. *Forensic Science International*, 189:111.e1-11.e8

Kranioti E.F., İşcan M.Y., Michalodimitrakis M., 2008. Craniometric Analysis of the Modern Cretan Population. *Forensic Science International*, 180(2e3):110.e1e5

Kranioti E.F., Michalodimitrakis, M., 2009. Sexual Dimorphism of the Humerus in Contemporary Cretans. *Journal of Forensic Sciences,* 54(5):996-1000

Kranioti E.F., Nathena D., Michalodimitrakis M., 2011. Sex Estimation of the Cretan Humerus: A Digital Radiometric Study. *International Journal of Legal Medicine*, 125(5):659-67

Kranioti E.F., Paine R.R., 2011. Forensic Anthropology in Europe: An Assessment of Current Status and Application. *Journal of Anthropological Sciences*, 89:71-91

Kranioti E.F., Vorniotakis N., Galiatsou C., İşcan M., Michalodimitrakis M., 2009. Sex Identification and Software Development Using Digital Femoral Head Radiographs. *Forensic Science International*, 189(1-3):113.e1-113.e7

Krogman W.M. and İşcan M.Y., 1986. *The Human Skeleton in Forensic Medicine*, 2nd ed. Springfield, Charles C. Thomas

Krogman, W.M., 1955. The Human Skeleton in Forensic Medicine. *Postgrad. Med*, 17A:48-72

Larsen P.K., Simonsen E.B., Lynnerup N., 2008. Gait Analysis in Forensic Medicine. *Journal of Forensic Sciences*, 53(5):1149-53

Lee, J.C., 2012. A novel Biometric System Based on Palm Vein Image. *Pattern Recognition Letters*, 33:1520-28

Liguoro D., Vandermeersch B., Guérin J., 1994. Dimensions of Cervical Vertebral Bodies According to Age and Sex, *Surgical and Radiologic Anatomy,* 16:149-55

Lovejoy, O.C.; Meindl, R.S.; Pryzbeck, T.R.; Mensforth, R.P., 1985. Chronological Metamorphosis of the Auricular Surface of the Ilium: A New Method for the Determination of Adult Skeletal Age at Death. *American Journal of Physical Anthropology,* 68:15-28

Lynnerup N., Vedel j., 2005. Person Identification by Gait Analysis and Photogrammetry. *Journal of Forensic Sciences*, 50(1):112-18

MacLaughlin S.M., Oldale K.N.M., 1992. Vertebral Body Diameters and Sex Prediction. *Annals of Human Biology*, 19(3):285-92

Mall G., Hubig M., Büttner A., Kuznik J., Penning R., Graw M., 2001. Sex Determination and Estimation of Stature from the Long Bones of the Arm. *Forensic Science International*, 117:23-70

Manolis S.K., Eliopoulos C., Koilias C.G., Fox S.C., 2009. Sex Determination Using Metacarpal Biometric Data from the Athens Collection. *Forensic Science International*, 193(1-3):130.e1-130.e6

Marino, E.A., 1995. Sex Estimation Using the First Cervical Vertebra. *American Journal of Physical Anthropology*, 97:127-33

Marlow E.J., Pastor R.F., 2011. Sex Determination Using the Second Cervical Vertebra - A Test of the Method. *Journal of Forensic Sciences*, 56(1):165-69

Mountrakis C., Eliopoulos C., Koilias, C.G., Manolis S.K., 2010. Sex Determination Using Metatarsal Osteometrics from the Athens Collection. *Forensic Science International*, 200:178.e1-178.e7

Musgrave J.H., Harneja N.K., 1978. The Estimation of Adult Stature from Metacarpal Bone Length. *American Journal of Physical Anthropology*, 48:113-20

Navsa N., 2010. *Skeletal Morphology of the Human Hand as Applied in Forensic Anthropology* (Dissertation). Pretoria, University of Pretoria

Osipov B., Harvati K., Nathena D., Spanakis K., Karantanas A. and Kranioti E.F., 2013. Sexual Dimorphism of the Bony Labyrinth: A New Age-Independent Method. *American Journal of Physical Anthropology*, doi:10.1002/ajpa.22279

Papaioannou V.A., Kranioti E.F., Joveneaux P., Nathena D., Michalodimitrakis M., 2012. Sexual Dimorphism of the Scapula and the Clavicle in a Contemporary Greek Population: Applications in Forensic Identification. *Forensic Science International*, 10;217(1-3):231.e1-7

Pastor F., 2005. Sexual Dimorphism in Vertebral Dimensions at the T12/L1 Junction: *Proceedings of the American Academy of Forensic Sciences,* 11: 302-03

Patriquin M.L., Steyn M., Loth, S.R., 2005. Metric Analysis of Sex Differences in South African Black and White Pelves. *Forensic Science International* 147:119-27

Perini T.A., de Oliveira G.L., dos Santos Ornellas J, Palha de Oliveira F., 2005. Technical Error of Measurement in Anthropometry. *Revista Brasileira de Medicina do Esporte,* 11(1):81-90

Phenice T.W., 1969. A Newly Developed Visual Method of Sexing the Os Pubis. *American Journal of Physical Anthropology*, 30:297-302

Pickering R., Bachman D., 2009. *The Use of Forensic Anthropology,* 2nd ed. Boca Raton, Taylor & Francis Group

Pons J., 1955. The Sexual Diagnosis of Isolated Bones of the Skeleton. *Human Biology*, 27(1):12-21

Purkait R., 2001. Measurements of Ulna - A New Method for Determination of Sex. *Journal of Forensic Sciences,* 46(4):924-27

Purkait R., 2003. Sex Determination from Femoral Head Measurements: A New Approach. *Legal Medicine,* 5(1):347-50

Purkait R., 2005.Triangle Identified at the Proximal End of the Femur: A New Sex Determinant. *Forensic Science International*, 147(2-3):135-39

Purkait R., Chandra H., 2004. A Study of Sexual Variation in Indian Femur. *Forensic Science International*, 146:25-33

Quintyn C.B., 2010. *The Existence or Non-existence of Race?: Forensic Anthropology, Population Admixture and the Future of Racial Classification in the U.S.* Youngstown, Teneo Press

Robling A.G., Ubelaker D.H., 1997. Sex Estimation from the Metatarsals. *Journal of Forensic Sciences*, 42(6):1062-69

Rogers T., 1999. A Visual Method of Determining the Sex of Skeletal Remains Using the Distal Humerus. *Journal of Forensic Sciences*, 44(1):57-60

Sacragi A., Ikeda T., 1995. Sex Identification from the Distal Fibula. *International Journal of Osteoarchaeology*, 5:139-143.

Sauer N.J., 1992. Forensic Anthropology and the Concept of Race: If Races Don't Exist, Why are Forensic Anthropologists so Good at Identifying them? *Social Science & Medicine*, 34(2):107-11

Scheuer J.L. and Elkington N.M., 1993. Sex Determination from Metacarpals and the First Proximal Phalanx. *Journal of Forensic Sciences*, 38(4):769-78

Schulter-Ellis F.P., Hayek L.C., Schmidt D.J., 1985. Determination of Sex with a Discriminant Analysis of New Pelvic Bone Measurements: Part II. *Journal of Forensic Sciences*, 30(1):178-85

Singh G., Singh S., Sing SP., 1973. Identification of Sex from the Radius. *Journal of the Indian Academy of Sciences*, 13(1):10-16

Smith S.L., 1996. Attribution of Hand Bones to Sex and Population Groups. *Journal of Forensic Sciences*, 41(3):469-77

Spencer F., 1981. The Rise of Academic Physical Anthropology in the United States (1880-1980): A Historical Overview. *American Journal of Physical Anthropology,* 56:353-64

Spradley K.M., Jantz R.L., 2011. Sex Estimation in Forensic Anthropology: Skull Versus Postcranial Elements. *Journal of Forensic Sciences*, 56(2):289-96

Standring S., Gray H., 2005. *Gray's anatomy: The Anatomical Basis of Clinical Practice*, 39th ed. Edinburgh, Churchill Livingstone, Elsevier

Stephan C.N., Henneberg M., 2006. Recognition by Forensic Facial Approximation: Case Specific Examples and Empirical Tests. *Forensic Science International*, 156(2-3):182-91

Stewart T.D., 1982. Pioneer Contributions of Harris Hawthorne Wilder, Ph.D., to Forensic Sciences. *Journal of Forensic Sciences*, 27(4):754-62

Steyn M., İşcan M.Y., de Kock M., Kranioti E.F., Michalodimitrakis M., L'Abbé, E.N., 2009. Analysis of Ante Mortem Trauma in Three Modern Skeletal Populations. *International Journal of Osteoarchaeology*, 20(5):561-71

Stout S.D, Dietze H.D., İşcan M.Y., Loth S.R., 1994. Estimation of Age at Death Using Cortical Histomorphometry of the Sternal End of the 4th rib. *Journal of Forensic Sciences,* 39(3):778-84

Tague R.G., 2007. Costal Process of the First Sacral Vertebra: Sexual Dimorphism and Obstetrical Adaptation. *American Journal of Physical Anthropology*, 132(3):395-405

Taylor J.R., Twomey L.T., 1984. Sexual Dimorphism in Human Vertebral Body Shape. *Journal of Anatomy*, 138(2):281-86

Tersigni-Tarrant M.A., Shirley N.R., 2013. *Forensic Anthropology: An Introduction*. Boca Raton, Taylor & Francis Group, LLC

Thieme FP., Schull WJ., 1957. Sex Determination from the Skeleton. *Human Biology,* 29(3):242-273

Thomas P., 2003. *Forensic Anthropology: The Growing Science of Talking Bones*. New York, Facts On File

Tome P., Fierrez J., Vera-Rodriguez R., Ramos D., 2013. Identification Using Face Regions: Application and Assessment in Forensic Scenarios. *Forensic Science International*, http://dx.doi.org/10.1016/j.forsciint.2013.08.020

Ubelaker, D.H., 2006. Introduction to Forensic Anthropology. In: Schmitt A., Cunha E., Pinheiro J. (editors) *Forensic Anthropology and Medicine: Complementary Sciences From Recovery to Cause of Death*. Totowa, Humana Press

Ubelaker, D.H., 2008. Forensic Anthropology: Methodology and Diversity of Applications. In: Katzenberg A.M., Saunders S.R. (editors) *Biological Anthropology of the Human Skeleton* (2nd ed.). Hoboken, John Wiley and Sons

Voisin M.D., 2009. *Sexual Dimorphism in the 12th Thoracic Vertebra and its Potential for Sex Estimation of Human Skeletal Remains* (Dissertation). Wichita, Wichita State University

Washburn S.L., 1948. Sex Differences in the Pubic Bone. *American Journal of Physical Anthropology*, 6(2):199-208

Wescott D.J., 2000. Sex Variation in the Second Cervical Vertebra. *Journal of Forensic Sciences*, 45(2):462-66

White T.D., Folkens P.A., 2005. *The Human Bone Manual*, London, Elsevier Academic Press

Yu S.B., Lee U.Y., Kwak D.S., Ahn Y.W., Jin C.Z, Zhao J., Sui H.J., Han S.H., 2008. Determination of Sex for the 12th Thoracic Vertebra by Morphometry of Three-Dimensional Reconstructed Vertebral Models. *Journal of Forensic Sciences*, 53(3):620-25

Zheng W.X., Cheng F.B., Cheng K.L., Tian Y., Lai Y., Zhang W.S., Zheng Y.J., Li Y.Q., 2012. Sex Assessment Using Measurements of the First Lumbar Vertebra. *Forensic Science International,* 219(1):285.e1-285.e5

9 Appendices

Appendix A: TEM

Technical Error of Measurement (TEM): Results for T1

Variable	N	Absolute mean (mm)	Absolute TEM (mm)	Relative TEM (%)
XLV	20	41.55099984	1.03877500	4.0
XLS	20	15.03444253	0.37586106	2.6
XLVBs	20	3.09595446	0.07739886	1.1
XLVBi	19	2.65470615	0.06986069	1.1
XDFs	20	3.34968802	0.08374220	1.1
XHBp	19	3.35466720	0.08828072	1.2
XHBa	20	2.74040000	0.06851000	1.1
XHFs	20	2.09362054	0.05234051	0.9
XHTP	20	2.45512849	0.06137821	1.0
XBV	20	54.44528978	1.36113224	4.7
XDSF	19	13.88421732	0.36537414	2.7
XBFs	20	3.00015153	0.07500379	1.1
XDFc	20	7.53941150	0.18848529	1.7
XBP	20	0.74879353	0.01871984	0.5
XBVBs	19	8.22255515	0.21638303	1.9
XBVBi	19	11.24462595	0.29591121	2.4

Technical Error of Measurement (TEM): Results for T2

Variable	N	Absolute mean (mm)	Absolute TEM (mm)	Relative TEM (%)
XLV	17	28.13130591	0.82739135	4.6
XLS	18	16.57700206	0.46047228	3.0
XLVBs	18	2.02205879	0.05616830	1.2
XLVBi	19	3.88393145	0.10220872	1.4
XDFs	20	2.69310026	0.06732751	1.0
XHBp	18	3.97514114	0.11042059	1.5
XHBa	18	3.96196819	0.11005467	1.4
XHFs	19	0.86482728	0.02275861	0.7
XHTP	20	2.78986138	0.06974653	1.1
XBV	20	61.13213304	1.52830333	4.9
XDSF	19	15.57494796	0.40986705	2.8
XBFs	19	1.81815909	0.04784629	1.0
XDFc	20	3.56859053	0.08921476	1.3
XBP	20	0.57699001	0.01442475	0.5
XBVBs	18	8.44497736	0.23458270	2.2
XBVBi	19	10.88281683	0.28638992	2.2

Technical Error of Measurement (TEM): Results for T3

Variable	N	Absolute mean (mm)	Absolute TEM (mm)	Relative TEM (%)
XLV	18	43.74035345	1.21500982	4.9
XLS	18	16.79985020	0.46666251	3.2
XLVBs	19	3.07345715	0.08088045	1.3
XLVBi	19	3.95176977	0.10399394	1.5
XDFs	20	1.61341107	0.04033528	0.9
XHBp	18	3.96687082	0.11019086	1.5
XHBa	18	3.31564883	0.09210136	1.5
XHFs	19	0.97834444	0.02574591	0.7
XHTP	20	3.02904400	0.07572610	1.1
XBV	20	50.10618498	1.25265462	4.6
XDSF	20	15.95683457	0.39892086	2.5
XBFs	20	1.70884065	0.04272102	0.8
XDFc	20	2.84522735	0.07113068	1.1
XBP	19	0.31170394	0.00820274	0.4
XBVBs	19	8.30430347	0.21853430	2.0
XBVBi	20	10.62160298	0.26554007	2.0

Technical Error of Measurement (TEM): Results for T4

Variable	N	Absolute mean (mm)	Absolute TEM (mm)	Relative TEM (%)
XLV	16	23.51811103	0.73494097	4.8
XLS	16	12.90506135	0.40328317	3.4
XLVBs	17	3.88307636	0.10786323	1.6
XLVBi	15	4.64917244	0.15497241	2.2
XDFs	18	2.61363927	0.07260109	1.2
XHBp	15	2.41083873	0.08036129	1.5
XHBa	16	2.98523574	0.09328862	1.5
XHFs	17	1.10303847	0.03244231	0.9
XHTP	18	2.68727326	0.07464648	1.2
XBV	18	40.89384567	1.13594016	4.8
XDSF	18	18.13594757	0.50377632	3.1
XBFs	17	1.10305018	0.03244265	0.9
XDFc	18	3.93358846	0.10926635	1.5
XBP	18	0.26401285	0.00733369	0.4
XBVBs	17	7.15760287	0.21051773	2.1
XBVBi	17	13.57936458	0.39939308	2.9

Technical Error of Measurement (TEM): Results for T5

Variable	N	Absolute mean (mm)	Absolute TEM (mm)	Relative TEM (%)
XLV	17	28.85087219	0.84855506	4.9
XLS	17	21.03671916	0.58435331	3.8
XLVBs	18	5.45332979	0.15148138	1.7
XLVBi	17	4.87682454	0.14343602	1.8
XDFs	20	3.55116841	0.08877921	1.2
XHBp	16	4.53238950	0.13330557	1.7
XHBa	16	4.46487330	0.13952729	1.8
XHFs	18	1.38099457	0.03836096	0.9
XHTP	20	3.34848870	0.08371222	1.1
XBV	20	45.56578609	1.13914465	4.4
XDSF	18	7.70298906	0.21397192	2.2
XBFs	18	1.32329776	0.03675827	0.9
XDFc	20	2.34784919	0.05869623	1.0
XBP	20	0.28710227	0.00717756	0.3
XBVBs	17	8.65061356	0.25442981	2.2
XBVBi	19	15.78105138	0.41529083	2.8

Technical Error of Measurement (TEM): Results for T6

Variable	N	Absolute mean (mm)	Absolute TEM (mm)	Relative TEM (%)
XLV	16	29.99707772	0.93740868	5.0
XLS	16	16.54810878	0.51712840	4.0
XLVBs	17	5.07612482	0.14929779	1.9
XLVBi	16	6.87764829	0.21492651	2.4
XDFs	17	1.26345355	0.03716040	1.0
XHBp	15	4.27377206	0.12210777	1.7
XHBa	17	2.99793336	0.08817451	1.5
XHFs	17	1.03572879	0.03046261	0.9
XHTP	19	2.00825025	0.05284869	1.0
XBV	19	44.24341549	1.16430041	4.8
XDSF	19	9.23721924	0.24308472	2.1
XBFs	17	1.15996485	0.03411661	0.9
XDFc	18	2.94392870	0.08177580	1.4
XBP	18	0.26967275	0.00749091	0.4
XBVBs	17	9.17581502	0.26987691	2.7
XBVBi	18	14.77904438	0.41052901	2.8

Technical Error of Measurement (TEM): Results for T7

Variable	N	Absolute mean (mm)	Absolute TEM (mm)	Relative TEM (%)
XLV	15	17.68286673	0.58942889	4.7
XLS	15	20.42985829	0.68099528	4.8
XLVBs	15	8.99819140	0.29993971	2.8
XLVBi	16	4.85443439	0.15170107	2.0
XDFs	17	1.97000650	0.05794137	1.2
XHBp	15	4.58320228	0.15277341	2.0
XHBa	15	3.05018634	0.10167288	1.6
XHFs	15	0.75335408	0.02511180	0.9
XHTP	18	1.49424431	0.04150679	1.0
XBV	17	27.90017645	0.82059342	4.9
XDSF	17	9.89534624	0.29103960	2.5
XBFs	15	0.76380947	0.02546032	0.9
XDFc	17	2.55723836	0.07521289	1.3
XBP	17	0.38464742	0.01131316	0.5
XBVBs	15	6.98243250	0.23274775	2.7
XBVBi	18	16.92973502	0.47027042	3.0

Technical Error of Measurement (TEM): Results for T8

Variable	N	Absolute mean (mm)	Absolute TEM (mm)	Relative TEM (%)
XLV	17	33.68019591	0.99059400	4.8
XLS	17	22.22296448	0.65361660	3.9
XLVBs	17	6.65511843	0.19573878	2.1
XLVBi	17	7.33356178	0.21569299	2.5
XDFs	17	2.02909885	0.05967938	1.2
XHBp	17	4.33244480	0.12742485	1.7
XHBa	16	3.13338113	0.09215827	1.4
XHFs	16	0.75896656	0.02371771	0.9
XHTP	18	2.06012476	0.05421381	1.0
XBV	17	28.10192745	0.82652728	4.5
XDSF	18	10.14691567	0.26702410	2.4
XBFs	17	1.06641985	0.03136529	0.9
XDFc	17	3.26874393	0.09613953	1.5
XBP	17	0.27627505	0.00812574	0.4
XBVBs	16	8.23809401	0.25744044	2.6
XBVBi	18	16.17651479	0.44934763	2.8

Technical Error of Measurement (TEM): Results for T9

Variable	N	Absolute mean (mm)	Absolute TEM (mm)	Relative TEM (%)
XLV	15	17.29157776	0.54036181	4.6
XLS	15	9.14371711	0.30479057	3.0
XLVBs	16	5.23795689	0.16368615	2.1
XLVBi	16	7.10923664	0.22216364	2.3
XDFs	16	1.45521351	0.04547542	1.2
XHBp	16	3.53664432	0.11052014	1.9
XHBa	16	4.13086068	0.12908940	1.8
XHFs	15	1.18796317	0.03959877	1.1
XHTP	17	2.38305505	0.07008985	1.2
XBV	17	30.25467562	0.88984340	4.7
XDSF	17	10.89527460	0.32044925	2.6
XBFs	16	1.00623572	0.03144487	1.0
XDFc	17	2.69578435	0.07928778	1.4
XBP	17	0.20497281	0.00602861	0.4
XBVBs	16	9.46836239	0.29588632	2.7
XBVBi	16	11.48298330	0.35884323	3.1

Technical Error of Measurement (TEM): Results for T10

Variable	N	Absolute mean (mm)	Absolute TEM (mm)	Relative TEM (%)
XLV	14	21.20415297	0.75729118	4.9
XLS	15	8.42341628	0.28078054	2.9
XLVBs	16	5.42415314	0.16950479	2.2
XLVBi	17	8.59290806	0.25273259	2.3
XDFs	17	2.89926134	0.08527239	1.3
XHBp	17	5.47062763	0.16090081	1.9
XHBa	17	5.49409961	0.16159116	1.9
XHFs	17	1.36632675	0.04018608	0.9
XHTP	17	1.76411442	0.05188572	1.0
XBV	17	36.20045890	1.06471938	4.7
XDSF	17	12.20525319	0.35897803	3.0
XBFs	17	1.89396806	0.05570494	1.1
XDFc	17	2.38941085	0.07027679	1.3
XBP	17	0.41186360	0.01211364	0.5
XBVBs	17	11.16595900	0.32841056	2.7
XBVBi	17	17.28225654	0.50830166	3.5

Technical Error of Measurement (TEM): Results for T11

Variable	N	Absolute mean (mm)	Absolute TEM (mm)	Relative TEM (%)
XLV	14	11.45797882	0.40921353	3.9
XLS	14	9.08374166	0.32441934	3.3
XLVBs	17	7.82207472	0.23006102	2.4
XLVBi	17	5.38781658	0.15846519	1.9
XDFs	17	3.19874446	0.09408072	1.4
XHBp	17	5.13209695	0.15094403	1.9
XHBa	17	3.99019856	0.11735878	1.6
XHFs	17	1.02116854	0.03003437	0.8
XHTP	17	2.29825475	0.06759573	1.2
XBV	17	28.71452588	0.84454488	4.5
XDSF	17	13.26257982	0.39007588	2.8
XBFs	17	0.89628270	0.02636126	0.8
XDFc	17	3.06908487	0.09026720	1.5
XBP	17	0.86964546	0.02557781	0.8
XBVBs	17	8.27823988	0.24347764	2.4
XBVBi	16	10.70628062	0.33457127	3.4

Technical Error of Measurement (TEM): Results for T12

Variable	N	Absolute mean (mm)	Absolute TEM (mm)	Relative TEM (%)
XLV	13	11.77380991	0.45283884	4.3
XLS	13	6.91035453	0.26578287	3.2
XLVBs	16	9.10609277	0.28456540	2.6
XLVBi	16	5.27802422	0.16493826	2.1
XDFs	17	2.53207300	0.07447274	1.3
XHBp	16	6.39556080	0.19986128	2.1
XHBa	16	5.77184464	0.18037014	2.1
XHFs	17	1.37171877	0.04034467	1.0
XHTP	16	3.19942100	0.09998191	1.6
XBV	14	11.26390123	0.40228219	3.5
XDSF	17	12.11775345	0.35640451	2.7
XBFs	17	0.91697153	0.02696975	0.8
XDFc	17	3.49885420	0.10290748	1.6
XBP	17	0.56641285	0.01665920	0.6
XBVBs	17	14.32091609	0.42120341	3.0
XBVBi	17	24.58879317	0.72319980	4.0

Appendix B: Original and cross-validated accuracies

Original and cross-validated accuracies for T1

Function			Male		Female		Average
		N	Count	%	Count	%	Accuracy
Stepwise	Original	64	36	91.7	28	89.3	90.6
	Cross-validated	64	36	91.7	28	89.3	90.6
XLV	Original	64	36	88.9	28	85.7	87.5
	Cross-validated	64	36	88.9	28	85.7	87.5
XLS	Original	64	36	75.0	28	71.4	73.4
	Cross-validated	64	36	75.0	28	71.4	73.4
XLVBs	Original	65	36	77.8	29	86.2	81.5
	Cross-validated	65	36	77.8	29	82.8	80.0
XLVBi	Original	64	36	75.0	28	92.9	82.8
	Cross-validated	64	36	75.0	28	89.3	81.3
XDFs	Original	65	36	63.9	29	69.0	66.2
	Cross-validated	65	36	63.9	29	69.0	66.2
XHBp	Original	64	36	77.8	28	82.1	79.7
	Cross-validated	64	36	77.8	28	82.1	79.7
XHBa	Original	65	36	63.9	29	75.9	69.2
	Cross-validated	65	36	63.9	29	75.9	69.2
XHTP	Original	65	36	75.0	29	79.3	76.9
	Cross-validated	65	36	75.0	29	79.3	76.9
XBV	Original	65	36	91.7	29	86.2	89.2
	Cross-validated	65	36	88.9	29	86.2	87.7
XDSF	Original	63	34	61.8	29	82.8	71.4
	Cross-validated	63	34	61.8	29	82.8	71.4
XDFc	Original	65	36	69.4	29	75.9	72.3
	Cross-validated	65	36	69.4	29	75.9	72.3
XBP	Original	64	35	71.4	29	82.8	76.6
	Cross-validated	64	35	71.4	29	79.3	75.0
XBVBs	Original	64	35	71.4	29	69.0	70.3
	Cross-validated	64	35	71.4	29	69.0	70.3
XBVBi	Original	64	35	77.1	29	72.4	75.0
	Cross-validated	64	35	77.1	29	72.4	75.0

Original and cross-validated accuracies for T2

Function			Male		Female		Average
		N	Count	%	Count	%	Accuracy
Stepwise	Original	57	31	93.5	26	84.6	89.5
	Cross-validated	57	31	93.5	26	84.6	89.5
XLV	Original	59	32	84.4	27	77.8	81.4
	Cross-validated	59	32	84.4	27	74.1	79.7
XLS	Original	60	32	62.5	28	67.9	65.0
	Cross-validated	60	32	62.5	28	67.9	65.0
XLVBs	Original	63	35	71.4	28	85.7	77.8
	Cross-validated	63	35	71.4	28	85.7	77.8
XLVBi	Original	63	34	61.8	29	89.7	74.6
	Cross-validated	63	34	61.8	29	89.7	74.6
XDFs	Original	65	35	65.7	30	60.0	63.1
	Cross-validated	65	35	65.7	30	60.0	63.1
XHBp	Original	62	34	73.5	28	82.1	77.4
	Cross-validated	62	34	73.5	28	82.1	77.4
XHBa	Original	63	34	70.6	29	62.1	66.7
	Cross-validated	63	34	70.6	29	62.1	66.7
XHFs	Original	63	35	62.9	28	67.9	65.1
	Cross-validated	63	35	62.9	28	67.9	65.1
XHTP	Original	65	35	77.1	30	73.3	75.4
	Cross-validated	65	35	77.1	30	70.0	73.8
XBV	Original	65	35	82.9	30	83.3	83.1
	Cross-validated	65	35	82.9	30	83.3	83.1
XDSF	Original	63	35	85.7	28	78.6	82.5
	Cross-validated	63	35	85.7	28	78.6	82.5
XBFs	Original	63	35	68.6	28	67.9	68.3
	Cross-validated	63	35	68.6	28	67.9	68.3
XDFc	Original	65	35	74.3	30	76.7	75.4
	Cross-validated	65	35	74.3	30	76.7	75.4
XBP	Original	65	35	65.7	30	63.3	64.6
	Cross-validated	65	35	65.7	30	63.3	64.6
XBVBs	Original	63	34	73.5	29	72.4	73.0
	Cross-validated	63	34	73.5	29	72.4	73.0
XBVBi	Original	64	34	85.3	30	80.0	82.8
	Cross-validated	64	34	82.4	30	80.0	81.3

Original and cross-validated accuracies for T3

Function			Male		Female		Average
		N	Count	%	Count	%	Accuracy
Stepwise	Original	66	36	83.3	30	90.0	86.4
	Cross-validated	66	36	83.3	30	90.0	86.4
XLV	Original	61	33	81.8	28	75.0	78.7
	Cross-validated	61	33	81.8	28	75.0	78.7
XLS	Original	61	33	63.6	28	67.9	65.6
	Cross-validated	61	33	63.6	28	67.9	65.6
XLVBs	Original	65	35	71.4	30	83.3	76.9
	Cross-validated	65	35	71.4	30	80.0	75.4
XLVBi	Original	66	36	75.0	30	80.0	77.3
	Cross-validated	66	36	75.0	30	80.0	77.3
XDFs	Original	67	36	58.3	31	67.7	62.7
	Cross-validated	67	36	58.3	31	67.7	62.7
XHBp	Original	64	35	68.6	29	75.9	71.9
	Cross-validated	64	35	68.6	29	75.9	71.9
XHBa	Original	63	34	61.8	29	58.6	60.3
	Cross-validated	63	34	61.8	29	58.6	60.3
XHFs	Original	63	34	55.9	29	65.5	60.3
	Cross-validated	63	34	55.9	29	65.5	60.3
XHTP	Original	67	36	77.8	31	87.1	82.1
	Cross-validated	67	36	77.8	31	87.1	82.1
XBV	Original	66	36	88.9	30	90.0	89.4
	Cross-validated	66	36	88.9	30	90.0	89.4
XDSF	Original	65	35	80.0	30	86.7	83.1
	Cross-validated	65	35	80.0	30	86.7	83.1
XBFs	Original	64	35	71.4	29	72.4	71.9
	Cross-validated	64	35	71.4	29	72.4	71.9
XDFc	Original	67	36	72.2	31	83.9	77.6
	Cross-validated	67	36	72.2	31	83.9	77.6
XBP	Original	66	35	62.9	31	71.0	66.7
	Cross-validated	66	35	62.9	31	71.0	66.7
XBVBs	Original	65	35	77.1	30	80.0	78.5
	Cross-validated	65	35	77.1	30	80.0	78.5
XBVBi	Original	67	36	86.1	31	87.1	86.6
	Cross-validated	67	36	86.1	31	87.1	86.6

Original and cross-validated accuracies for T4

Function			Male		Female		Average
		N	Count	%	Count	%	Accuracy
Stepwise	Original	58	32	84.4	26	88.5	86.2
	Cross-validated	58	32	81.3	26	88.5	84.5
XLV	Original	60	33	87.9	27	81.5	85.0
	Cross-validated	60	33	87.9	27	81.5	85.0
XLS	Original	60	33	69.7	27	70.4	70.0
	Cross-validated	60	33	66.7	27	70.4	68.3
XLVBs	Original	62	34	73.5	28	89.3	80.6
	Cross-validated	62	34	73.5	28	89.3	80.6
XLVBi	Original	56	30	76.7	26	84.6	80.4
	Cross-validated	56	30	76.7	26	84.6	80.4
XDFs	Original	62	33	63.6	29	62.1	62.9
	Cross-validated	62	33	63.6	29	62.1	62.9
XHBp	Original	57	32	62.5	25	72.0	66.7
	Cross-validated	57	32	62.5	25	72.0	66.7
XHBa	Original	59	33	63.6	26	65.4	64.4
	Cross-validated	59	33	60.6	26	65.4	62.7
XHTP	Original	63	34	73.5	29	79.3	76.2
	Cross-validated	63	34	73.5	29	79.3	76.2
XBV	Original	63	34	82.4	29	82.8	82.5
	Cross-validated	63	34	82.4	29	82.8	82.5
XDSF	Original	61	33	57.6	28	85.7	70.5
	Cross-validated	61	33	57.6	28	85.7	70.5
XBFs	Original	62	34	58.8	28	67.9	62.9
	Cross-validated	62	34	55.9	28	67.9	61.3
XDFc	Original	63	34	67.6	29	82.8	74.6
	Cross-validated	63	34	67.6	29	79.3	73.0
XBP	Original	63	34	58.8	29	65.5	61.9
	Cross-validated	63	34	58.8	29	65.5	61.9
XBVBs	Original	62	34	73.5	28	78.6	75.8
	Cross-validated	62	34	73.5	28	78.6	75.8
XBVBi	Original	60	32	81.3	28	85.7	83.3
	Cross-validated	60	32	81.3	28	85.7	83.3

Original and cross-validated accuracies for T5

Function			Male		Female		Average
		N	Count	%	Count	%	Accuracy
Stepwise	Original	52	30	86.7	22	90.9	88.5
	Cross-validated	52	30	83.3	22	90.0	86.5
XLV	Original	53	30	86.7	23	87.0	86.8
	Cross-validated	53	30	86.7	23	87.0	86.8
XLS	Original	55	31	58.1	24	70.8	63.6
	Cross-validated	55	31	58.1	24	62.5	60.0
XLVBs	Original	58	33	72.7	25	80.0	75.9
	Cross-validated	58	33	72.7	25	80.0	75.9
XLVBi	Original	61	33	72.7	28	78.6	75.4
	Cross-validated	61	33	72.7	28	78.6	75.4
XDFs	Original	62	34	52.9	28	75.0	62.9
	Cross-validated	62	34	52.9	28	75.0	62.9
XHBp	Original	58	33	81.8	25	72.0	77.6
	Cross-validated	58	33	81.8	25	72.0	77.6
XHBa	Original	58	33	69.7	25	72.0	70.7
	Cross-validated	58	33	69.7	25	72.0	70.7
XHFs	Original	57	32	56.3	25	64.0	59.6
	Cross-validated	57	32	56.3	25	64.0	59.6
XHTP	Original	65	36	77.8	29	72.4	75.4
	Cross-validated	65	36	77.8	29	72.4	75.4
XBV	Original	65	36	83.3	29	75.9	80.0
	Cross-validated	65	36	83.3	29	75.9	80.0
XDSF	Original	59	34	73.5	25	84.0	78.0
	Cross-validated	59	34	70.6	25	84.0	76.3
XBFs	Original	57	32	59.4	25	60.0	59.6
	Cross-validated	57	32	59.4	25	60.0	59.6
XDFc	Original	62	34	73.5	28	82.1	77.4
	Cross-validated	62	34	73.5	28	82.1	77.4
XBP	Original	63	35	65.7	28	64.3	65.1
	Cross-validated	63	35	65.7	28	64.3	65.1
XBVBs	Original	58	32	75.0	26	80.8	77.6
	Cross-validated	58	32	75.0	26	80.8	77.6
XBVBi	Original	64	36	75.0	28	89.3	81.3
	Cross-validated	64	36	75.0	28	89.3	81.3

Original and cross-validated accuracies for T6

Function			Male		Female		Average
		N	Count	%	Count	%	Accuracy
Stepwise	Original	59	32	87.5	27	88.9	88.1
	Cross-validated	59	32	87.5	27	88.9	88.1
XLV	Original	61	34	94.1	27	81.5	88.5
	Cross-validated	61	34	88.2	27	81.5	82.2
XLS	Original	62	35	71.4	27	77.8	74.2
	Cross-validated	62	35	71.4	27	77.8	74.2
XLVBs	Original	63	35	74.3	28	71.4	73.0
	Cross-validated	63	35	74.3	28	71.4	73.0
XLVBi	Original	61	35	75.0	25	84.0	78.7
	Cross-validated	61	35	75.0	25	84.0	78.7
XDFs	Original	64	36	55.6	28	64.3	59.4
	Cross-validated	64	36	55.6	28	64.3	59.4
XHBp	Original	59	34	82.4	25	76.0	79.7
	Cross-validated	59	34	82.4	25	76.0	79.7
XHBa	Original	63	36	75.0	27	74.1	74.6
	Cross-validated	63	36	75.0	27	74.1	74.6
XHFs	Original	62	35	60.0	27	66.7	62.9
	Cross-validated	62	35	60.0	27	66.7	62.9
XHTP	Original	65	36	75.0	29	86.2	80.0
	Cross-validated	65	36	72.2	29	86.2	78.5
XBV	Original	66	37	86.5	29	86.2	86.4
	Cross-validated	66	37	83.8	29	86.2	84.8
XDSF	Original	64	36	75.0	28	75.0	75.0
	Cross-validated	64	36	72.2	28	75.0	73.4
XBFs	Original	62	35	65.7	27	70.4	67.7
	Cross-validated	62	35	65.7	27	70.4	67.7
XDFc	Original	65	37	64.9	28	78.6	70.8
	Cross-validated	65	37	64.9	28	78.6	70.8
XBP	Original	65	37	54.1	28	57.1	55.4
	Cross-validated	65	37	54.1	28	53.6	53.8
XBVBs	Original	63	35	77.1	28	82.1	79.4
	Cross-validated	63	35	77.1	28	82.1	79.4
XBVBi	Original	64	35	82.9	29	86.2	84.4
	Cross-validated	64	35	82.9	29	86.2	84.4

Original and cross-validated accuracies for T7

Function			Male		Female		Average
		N	Count	%	Count	%	Accuracy
Stepwise	Original	64	36	80.6	28	92.9	85.9
	Cross-validated	64	36	77.8	28	92.9	84.4
XLV	Original	59	35	80.0	24	75.0	78.0
	Cross-validated	59	35	80.0	24	75.0	78.0
XLS	Original	59	35	68.6	24	62.5	66.1
	Cross-validated	59	35	68.6	24	58.3	64.4
XLVBs	Original	60	36	77.8	24	75.0	76.7
	Cross-validated	60	36	77.8	24	75.0	76.7
XLVBi	Original	60	34	79.4	26	69.2	75.0
	Cross-validated	60	34	79.4	26	69.2	75.0
XDFs	Original	63	36	50.0	27	59.3	54.0
	Cross-validated	63	36	50.0	27	59.3	54.0
XHBp	Original	57	34	76.5	23	69.6	73.7
	Cross-validated	57	34	76.5	23	69.6	73.7
XHBa	Original	60	34	73.5	26	76.9	75.0
	Cross-validated	60	34	73.5	26	76.9	75.0
XHFs	Original	59	35	40.0	24	58.3	47.5
	Cross-validated	59	35	40.0	24	58.3	47.5
XHTP	Original	65	37	67.6	28	89.3	76.9
	Cross-validated	65	37	67.6	28	89.3	76.9
XBV	Original	64	36	83.3	28	92.9	87.5
	Cross-validated	64	36	83.3	28	92.9	87.5
XDSF	Original	62	35	77.1	27	85.2	80.6
	Cross-validated	62	35	77.1	27	85.2	80.6
XBFs	Original	59	35	57.1	24	66.7	61.0
	Cross-validated	59	35	57.1	24	66.7	61.0
XDFc	Original	63	36	66.7	27	81.5	73.0
	Cross-validated	63	36	66.7	27	81.5	73.0
XBP	Original	64	37	62.2	27	66.7	64.1
	Cross-validated	64	37	62.2	27	66.7	64.1
XBVBs	Original	60	36	72.2	24	87.5	78.3
	Cross-validated	60	36	72.2	24	87.5	78.3
XBVBi	Original	65	37	81.1	28	85.7	83.1
	Cross-validated	65	37	81.1	28	85.7	83.1

Original and cross-validated accuracies for T8

Function			Male		Female		Average
		N	Count	%	Count	%	Accuracy
Stepwise	Original	57	33	81.8	24	79.2	80.7
	Cross-validated	57	33	78.8	24	79.2	78.9
XLV	Original	56	32	81.3	24	79.2	80.4
	Cross-validated	56	32	81.3	24	75.0	78.6
XLS	Original	56	32	75.0	24	70.8	73.2
	Cross-validated	56	32	75.0	24	70.8	73.2
XLVBs	Original	58	34	76.5	24	75.0	75.9
	Cross-validated	58	34	76.5	24	75.0	75.9
XLVBi	Original	58	33	69.7	25	72.0	70.7
	Cross-validated	58	33	69.7	25	72.0	70.7
XDFs	Original	60	35	62.9	25	72.0	66.7
	Cross-validated	60	35	62.9	25	72.0	66.7
XHBp	Original	56	32	75.0	24	66.7	71.4
	Cross-validated	56	32	71.9	24	66.7	69.6
XHBa	Original	59	34	67.6	25	72.0	69.5
	Cross-validated	59	34	67.6	25	72.0	69.5
XHTP	Original	62	36	69.4	26	65.4	67.7
	Cross-validated	62	36	69.4	26	65.4	67.7
XBV	Original	61	35	77.1	26	76.9	77.0
	Cross-validated	61	35	77.1	26	76.9	77.0
XDSF	Original	60	36	77.8	24	79.2	78.3
	Cross-validated	60	36	77.8	24	79.2	78.3
XBFs	Original	57	34	73.5	23	73.9	73.7
	Cross-validated	57	34	73.5	23	73.9	73.7
XDFc	Original	60	35	65.7	25	80.0	71.7
	Cross-validated	60	35	65.7	25	80.0	71.7
XBP	Original	60	35	57.1	25	56.0	56.7
	Cross-validated	60	35	57.1	25	56.0	56.7
XBVBs	Original	57	33	72.7	24	79.2	75.4
	Cross-validated	57	33	72.7	24	79.2	75.4
XBVBi	Original	62	36	77.8	26	88.5	82.3
	Cross-validated	62	36	77.8	26	88.5	82.3

Original and cross-validated accuracies for T9

Function			Male		Female		Average
		N	Count	%	Count	%	Accuracy
Stepwise	Original	57	33	81.8	24	87.5	84.2
	Cross-validated	57	33	81.8	24	83.3	82.5
XLV	Original	56	33	78.8	23	82.6	80.4
	Cross-validated	56	33	78.8	23	82.6	80.4
XLS	Original	56	33	66.7	23	65.2	66.1
	Cross-validated	56	33	66.7	23	65.2	66.1
XLVBs	Original	58	34	76.5	24	70.8	74.1
	Cross-validated	58	34	76.5	24	70.8	74.1
XLVBi	Original	59	35	62.9	24	75.0	67.8
	Cross-validated	59	35	62.9	24	75.0	67.8
XDFs	Original	59	35	60.0	24	75.0	66.1
	Cross-validated	59	35	60.0	24	75.0	66.1
XHBp	Original	58	34	76.5	24	75.0	75.9
	Cross-validated	58	34	73.5	24	75.0	74.1
XHBa	Original	60	36	58.3	24	62.5	60.0
	Cross-validated	60	36	58.3	24	62.5	60.0
XHTP	Original	62	37	54.1	25	68.0	59.7
	Cross-validated	62	37	54.1	25	68.0	59.7
XBV	Original	62	37	73.0	25	76.0	74.2
	Cross-validated	62	37	73.0	25	72.0	72.6
XDSF	Original	61	37	73.0	24	66.7	70.5
	Cross-validated	61	37	73.0	24	66.7	70.5
XBFs	Original	57	34	58.8	23	69.6	63.2
	Cross-validated	57	34	58.8	23	69.6	63.2
XDFc	Original	60	35	68.6	25	88.0	76.7
	Cross-validated	60	35	68.6	25	88.0	76.7
XBP	Original	60	35	62.9	25	64.0	63.3
	Cross-validated	60	35	62.9	25	64.0	63.3
XBVBs	Original	58	34	76.5	24	75.0	75.9
	Cross-validated	58	34	76.5	24	75.0	75.9
XBVBi	Original	60	35	85.7	25	84.0	85.0
	Cross-validated	60	35	82.9	25	84.0	83.3

Original and cross-validated accuracies for T10

Function			Male		Female		Average
		N	Count	%	Count	%	Accuracy
Stepwise	Original	59	33	81.8	26	76.9	79.7
	Cross-validated	59	33	81.8	26	73.1	78.0
XLV	Original	53	29	82.8	24	79.2	81.1
	Cross-validated	53	29	79.3	24	79.2	79.2
XLS	Original	55	30	56.7	25	56.0	56.4
	Cross-validated	55	30	56.7	25	56.0	56.4
XLVBs	Original	58	33	78.8	25	88.0	82.8
	Cross-validated	58	33	78.8	25	84.0	81.0
XLVBi	Original	57	31	71.0	26	73.1	71.9
	Cross-validated	57	31	71.0	26	73.1	71.9
XDFs	Original	61	35	65.7	26	76.9	70.5
	Cross-validated	61	35	65.7	26	76.9	70.5
XHBp	Original	56	30	73.3	26	84.6	78.6
	Cross-validated	56	30	73.3	26	84.6	78.6
XHBa	Original	59	33	78.8	26	61.5	71.2
	Cross-validated	59	33	78.8	26	61.5	71.2
XHTP	Original	62	36	72.2	26	65.4	69.4
	Cross-validated	62	36	72.2	26	65.4	69.4
XBV	Original	62	36	58.3	26	80.8	67.7
	Cross-validated	62	36	58.3	26	80.8	67.7
XDSF	Original	62	36	72.2	26	73.1	72.6
	Cross-validated	62	36	72.2	26	69.2	71.0
XDFc	Original	61	35	74.3	26	88.5	80.3
	Cross-validated	61	35	74.3	26	88.5	80.3
XBP	Original	61	35	62.9	26	61.5	62.3
	Cross-validated	61	35	62.9	26	61.5	62.3
XBVBs	Original	60	34	73.5	26	80.8	76.7
	Cross-validated	60	34	73.5	26	80.8	76.7
XBVBi	Original	59	33	81.8	26	73.1	78.0
	Cross-validated	59	33	81.8	26	73.1	78.0

Original and cross-validated accuracies for T11

Function			Male		Female		Average
		N	Count	%	Count	%	Accuracy
Stepwise	Original	63	37	78.4	26	80.8	79.4
	Cross-validated	63	37	78.4	26	80.8	79.4
XLV	Original	52	28	75.0	24	79.2	76.9
	Cross-validated	52	28	75.0	24	79.2	76.9
XLVBs	Original	58	32	78.1	26	76.9	77.6
	Cross-validated	58	32	75.0	26	76.9	75.9
XLVBi	Original	62	35	65.7	27	81.5	72.6
	Cross-validated	62	35	65.7	27	81.5	72.6
XDFs	Original	62	35	57.1	27	66.7	61.3
	Cross-validated	62	35	57.1	27	66.7	61.3
XHBp	Original	59	32	78.1	27	77.8	78.0
	Cross-validated	59	32	78.1	27	77.8	78.0
XHBa	Original	61	35	51.4	26	65.4	57.4
	Cross-validated	61	35	51.4	26	65.4	57.4
XHFs	Original	57	31	64.5	26	69.2	66.7
	Cross-validated	57	31	64.5	26	69.2	66.7
XHTP	Original	64	37	59.5	27	70.4	64.1
	Cross-validated	64	37	59.5	27	70.4	64.1
XBV	Original	64	37	70.3	27	85.2	76.6
	Cross-validated	64	37	67.6	27	85.2	75.0
XDSF	Original	62	36	77.8	26	80.8	79.0
	Cross-validated	62	36	77.8	26	80.8	79.0
XBFs	Original	58	32	56.3	26	69.2	62.1
	Cross-validated	58	32	56.3	26	69.2	62.1
XDFc	Original	61	34	61.8	27	85.2	72.1
	Cross-validated	61	34	61.8	27	85.2	72.1
XBP	Original	61	34	67.6	27	74.1	70.5
	Cross-validated	61	34	67.6	27	74.1	70.5
XBVBs	Original	59	32	75.0	27	77.8	76.3
	Cross-validated	59	32	75.0	27	77.8	76.3
XBVBi	Original	63	37	81.1	26	80.8	81.0
	Cross-validated	63	37	81.1	26	80.8	81.0

Original and cross-validated accuracies for T12

Function			Male		Female		Average
		N	Count	%	Count	%	Accuracy
Stepwise	Original	62	34	79.4	28	82.1	80.6
	Cross-validated	62	34	76.5	28	82.1	79.0
XLV	Original	54	32	75.0	22	90.9	81.5
	Cross-validated	54	32	75.0	22	90.9	81.5
XLS	Original	54	32	62.5	22	54.5	59.3
	Cross-validated	54	32	62.5	22	54.5	59.3
XLVBs	Original	63	35	62.9	28	82.1	71.4
	Cross-validated	63	35	62.9	28	82.1	71.4
XLVBi	Original	63	35	65.7	28	82.1	73.0
	Cross-validated	63	35	62.9	28	82.1	71.4
XDFs	Original	65	37	62.2	28	67.9	64.6
	Cross-validated	65	37	62.2	28	67.9	64.6
XHBp	Original	63	35	80.0	28	75.0	77.8
	Cross-validated	63	35	80.0	28	71.4	76.2
XHBa	Original	64	36	58.3	28	60.7	59.4
	Cross-validated	64	36	58.3	28	57.1	57.8
XHTP	Original	62	35	48.6	27	70.4	58.1
	Cross-validated	62	35	48.6	27	70.4	58.1
XBV	Original	61	35	71.4	26	69.2	70.5
	Cross-validated	61	35	68.6	26	69.2	68.9
XDSF	Original	64	36	72.2	28	78.6	75.0
	Cross-validated	64	36	72.2	28	78.6	75.0
XBFs	Original	63	35	62.9	28	71.4	66.7
	Cross-validated	63	35	62.9	28	71.4	66.7
XDFc	Original	65	37	70.3	28	85.7	76.9
	Cross-validated	65	37	70.3	28	85.7	76.9
XBVBs	Original	64	36	75.0	28	82.1	78.1
	Cross-validated	64	36	72.2	28	82.1	76.6
XBVBi	Original	66	38	81.6	28	85.7	83.3
	Cross-validated	66	38	81.6	28	85.7	83.3

APPENDIX C: Posterior probabilities

Posterior Probabilities T1 XBV:

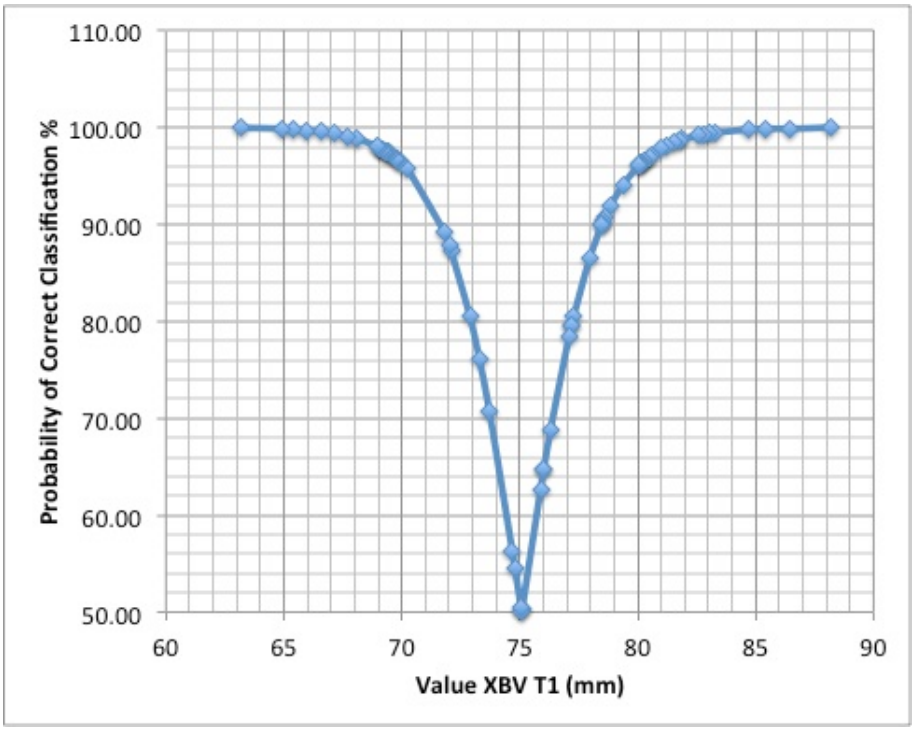

Posterior Probabilities T1 XLVBs:

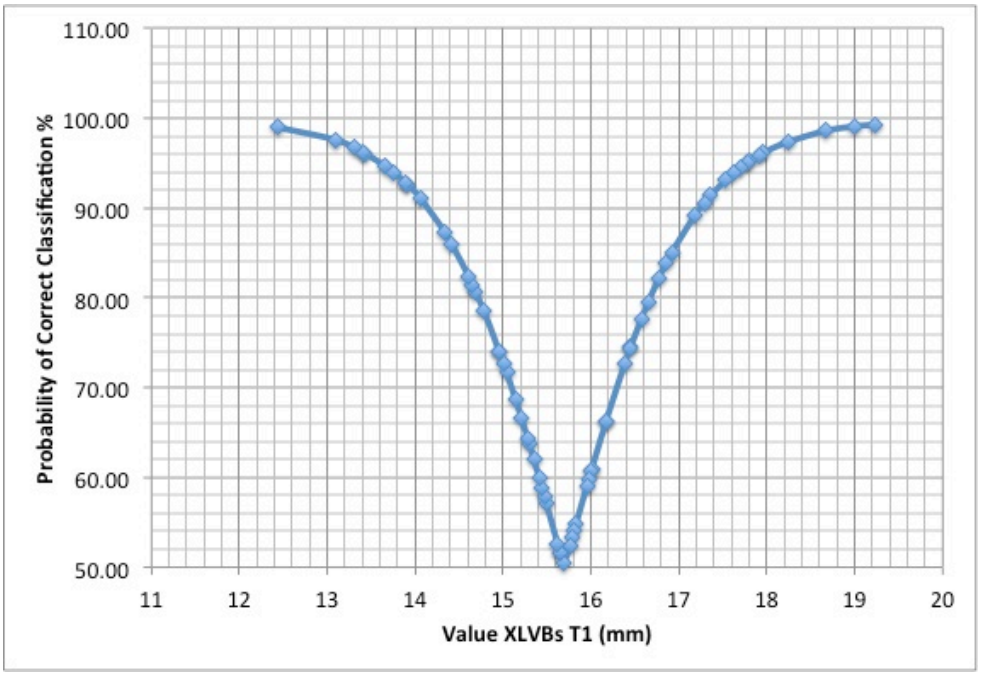

Posterior Probabilities T1 XLVBi:

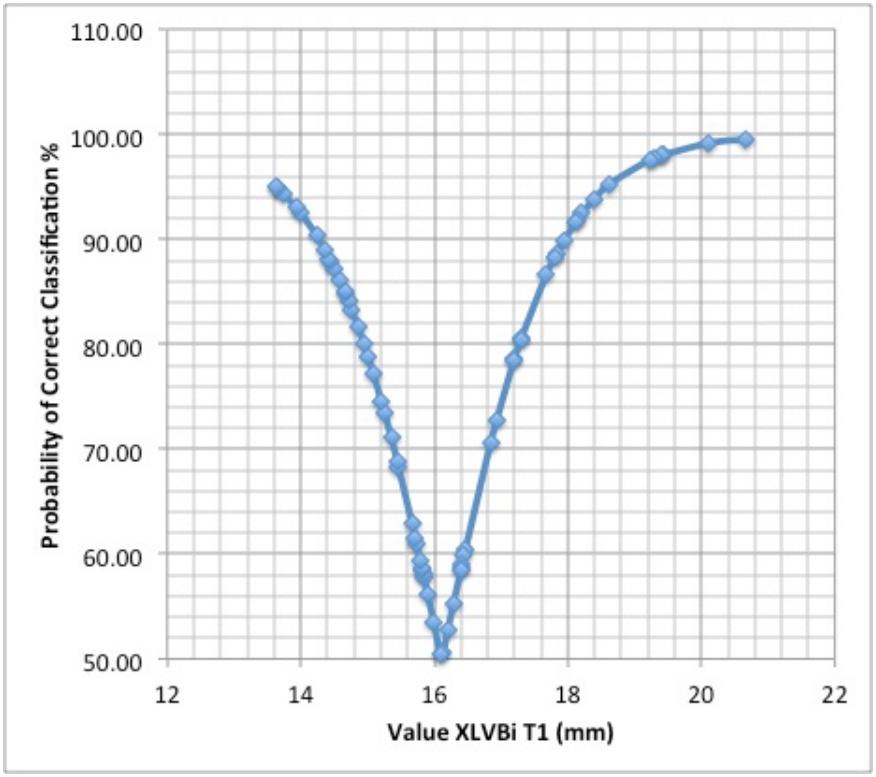

Posterior Probabilities T1 XLV:

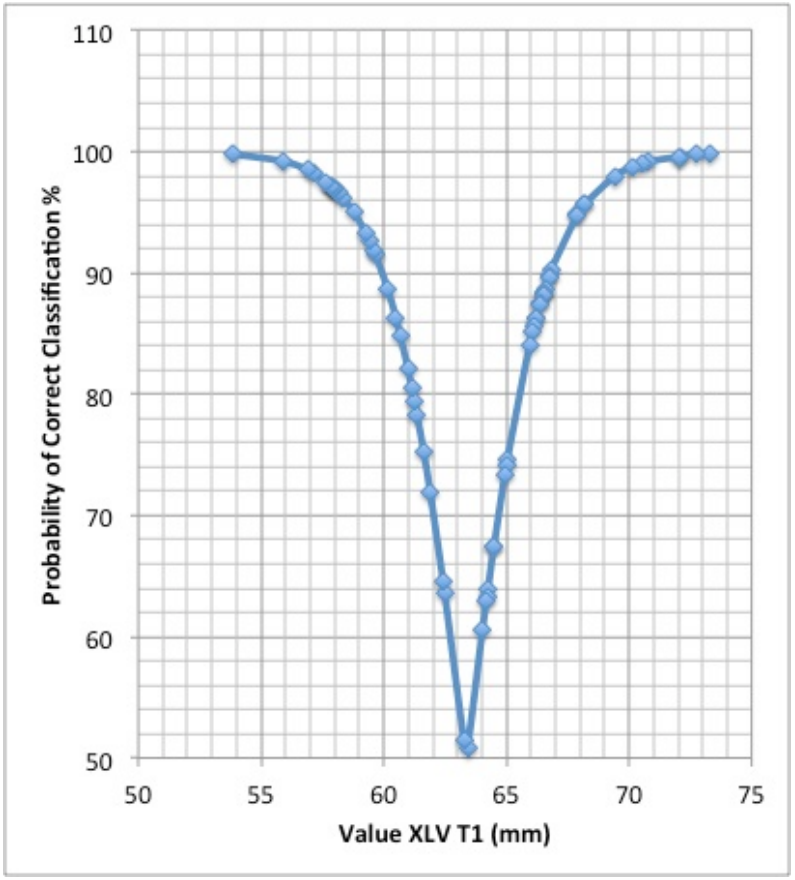

Posterior Probabilities T2 XBV:

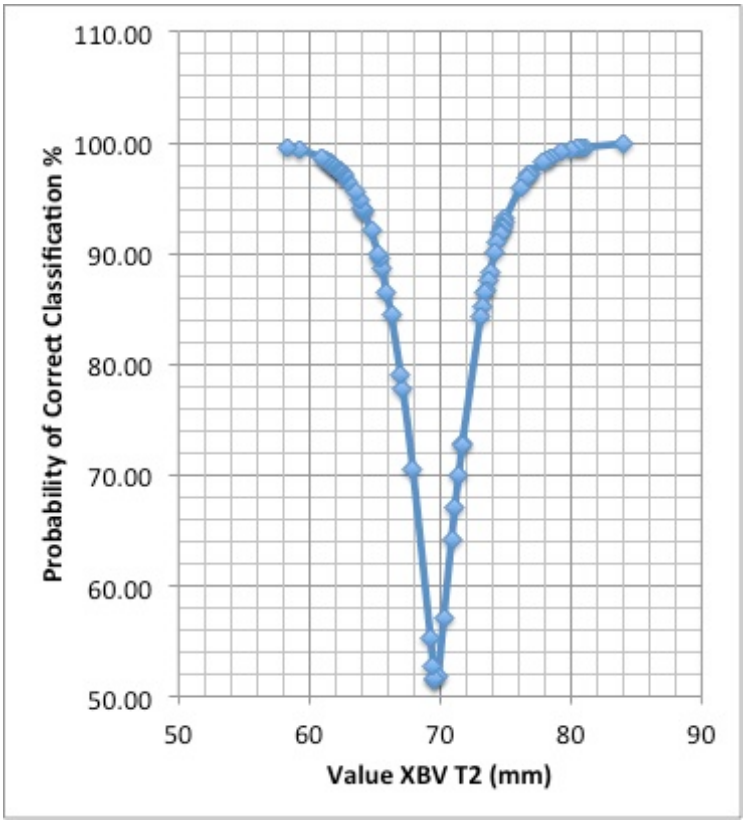

Posterior Probabilities T2 XBVBi:

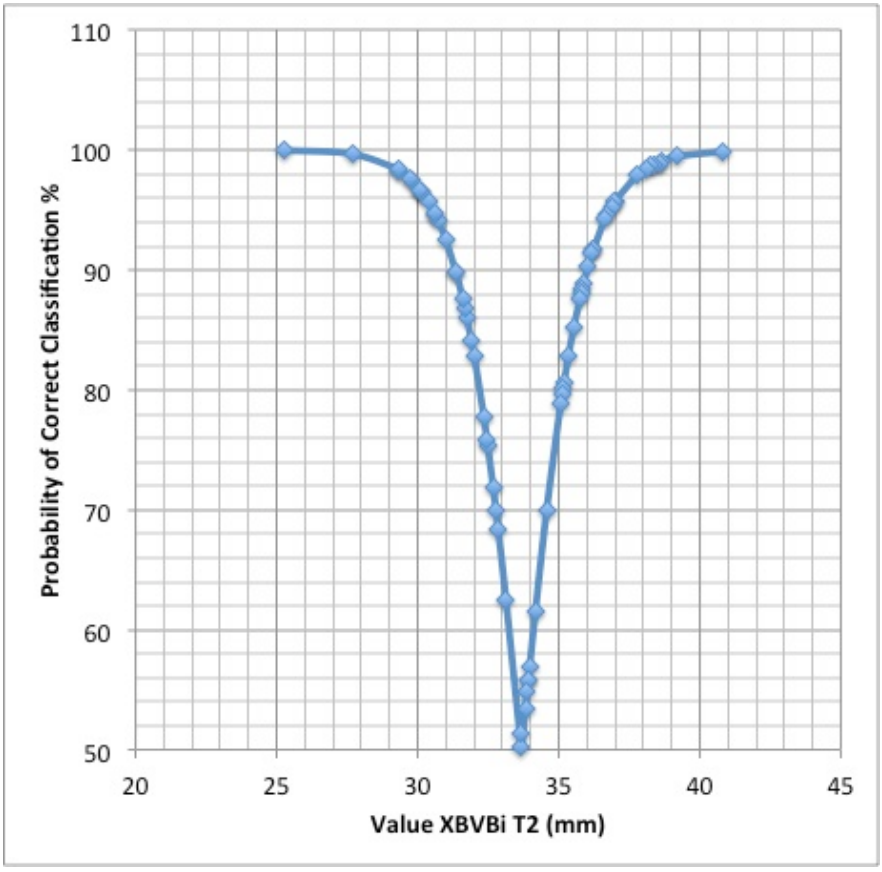

Posterior Probabilities T2 XDSF:

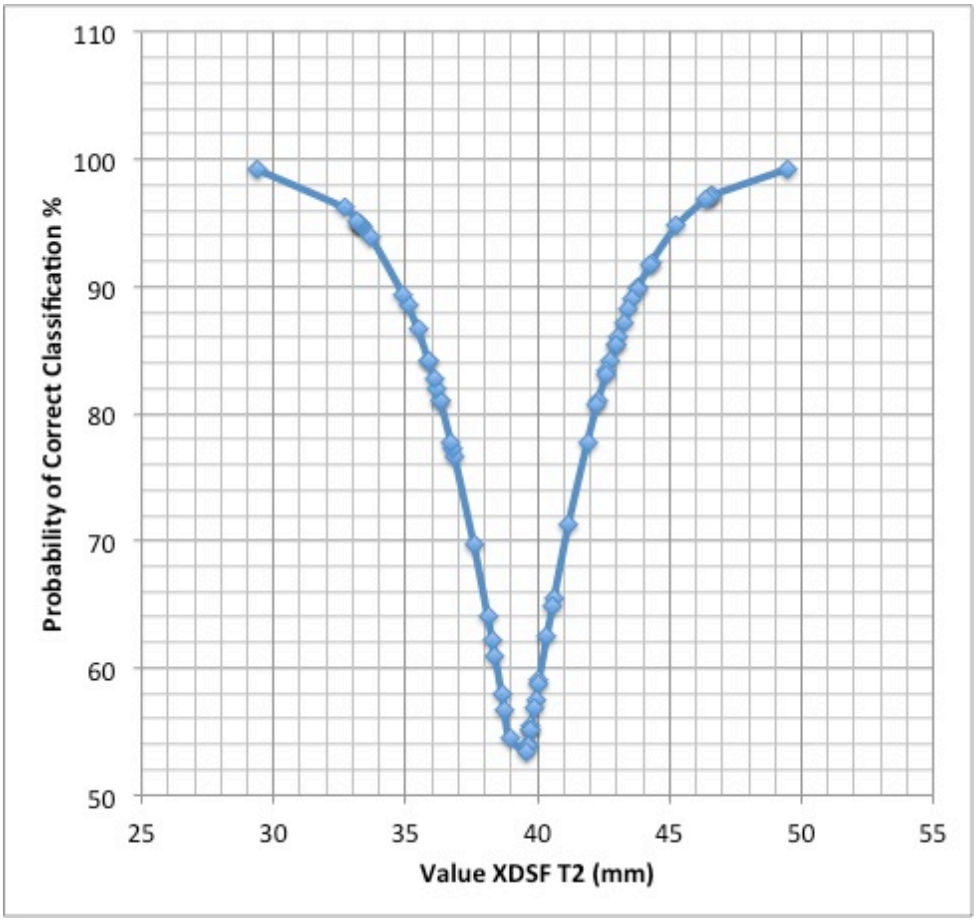

Posterior Probabilities T3 XBV:

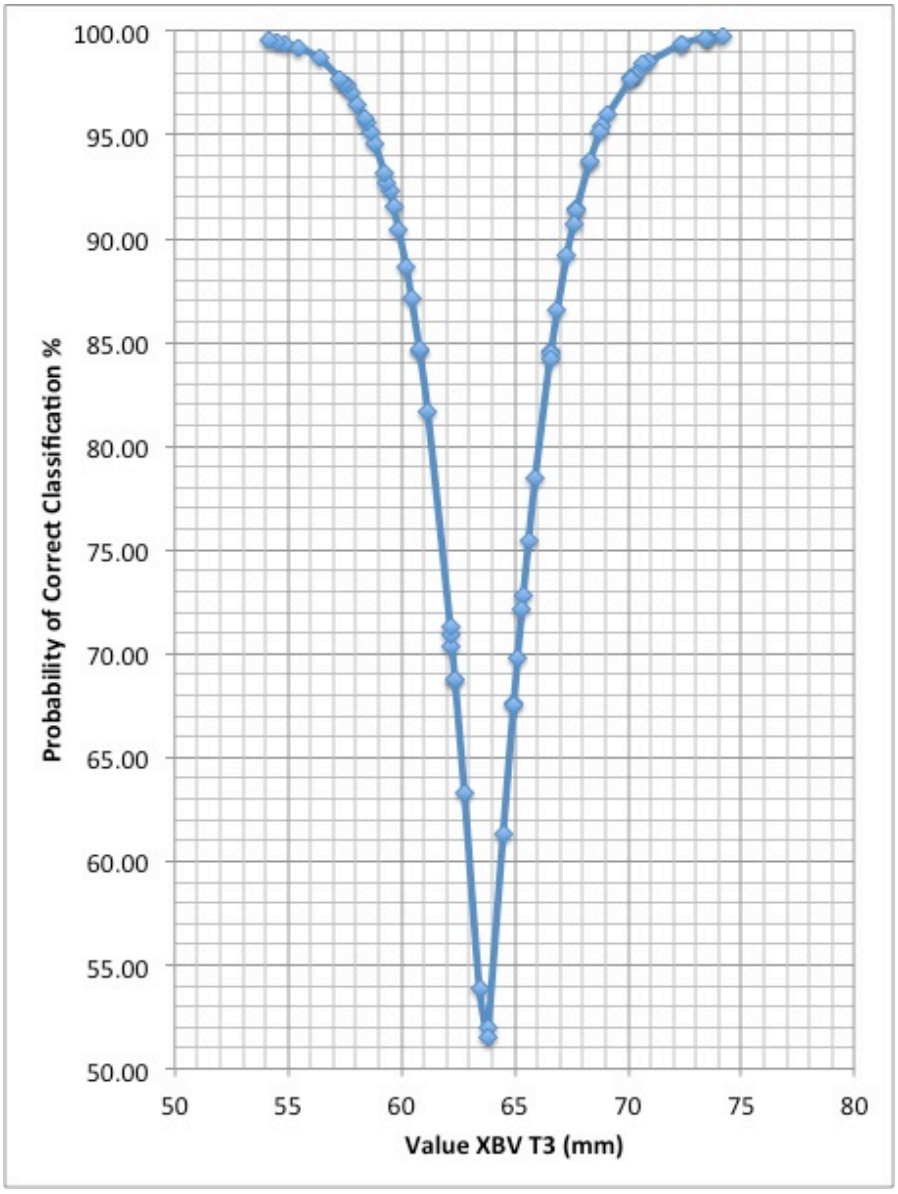

Posterior Probabilities T3 XBVBi:

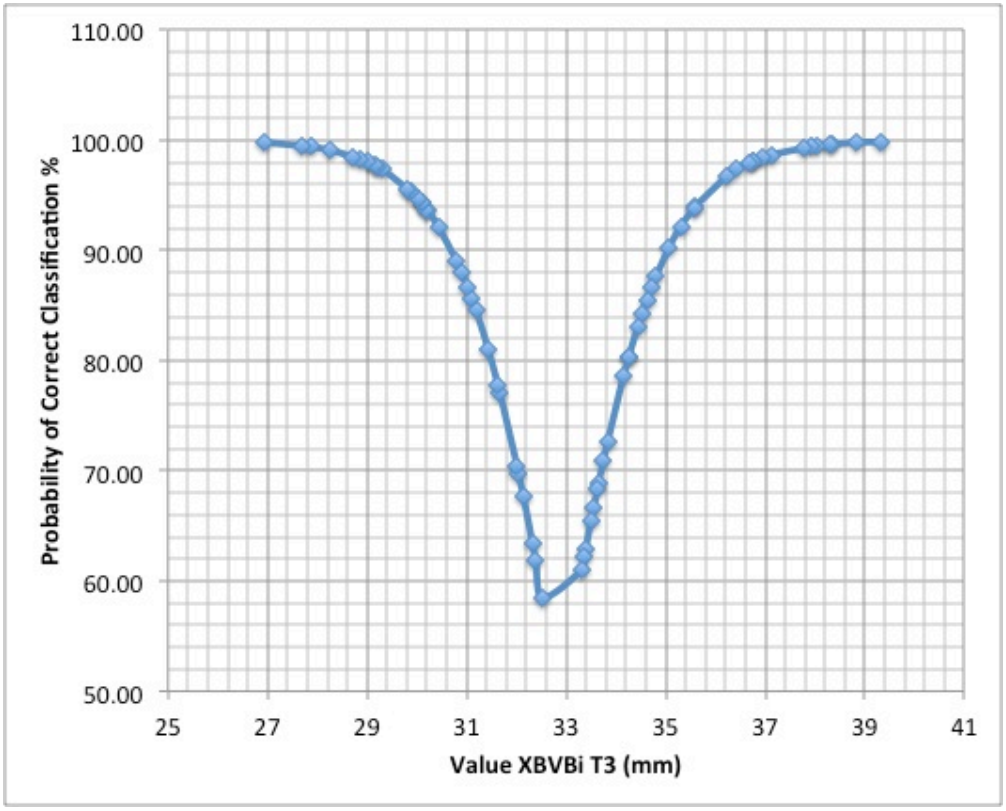

Posterior Probabilities T3 XHTP:

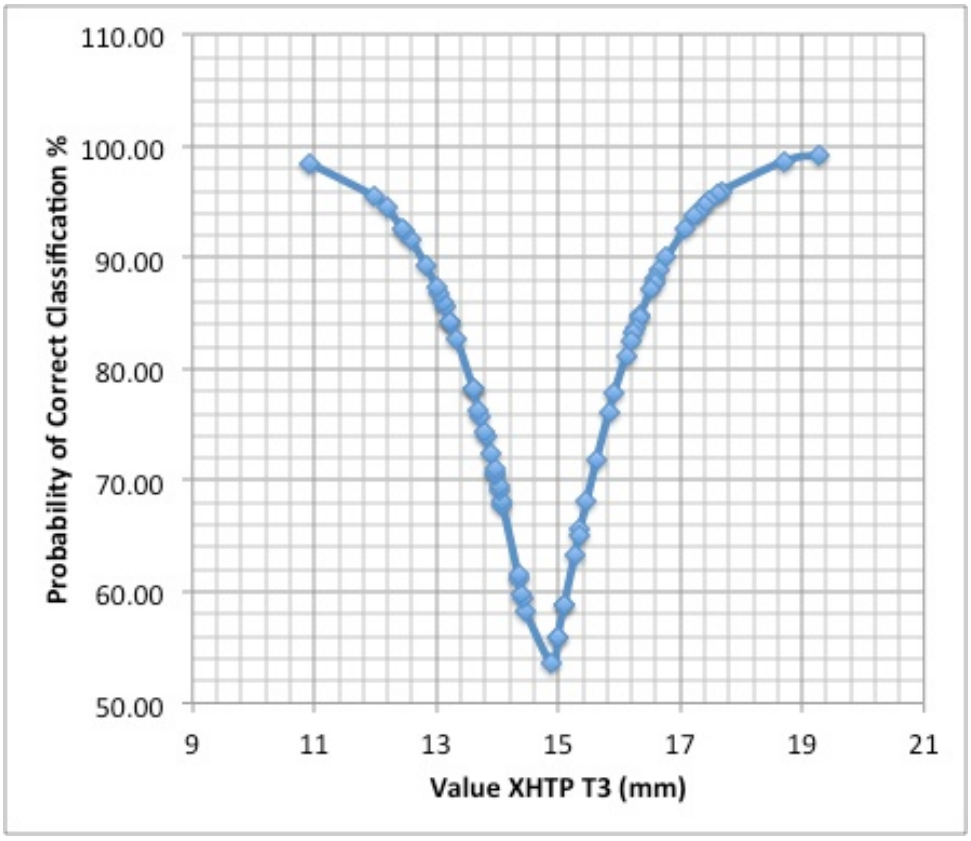

Posterior Probabilities T3 XDSF:

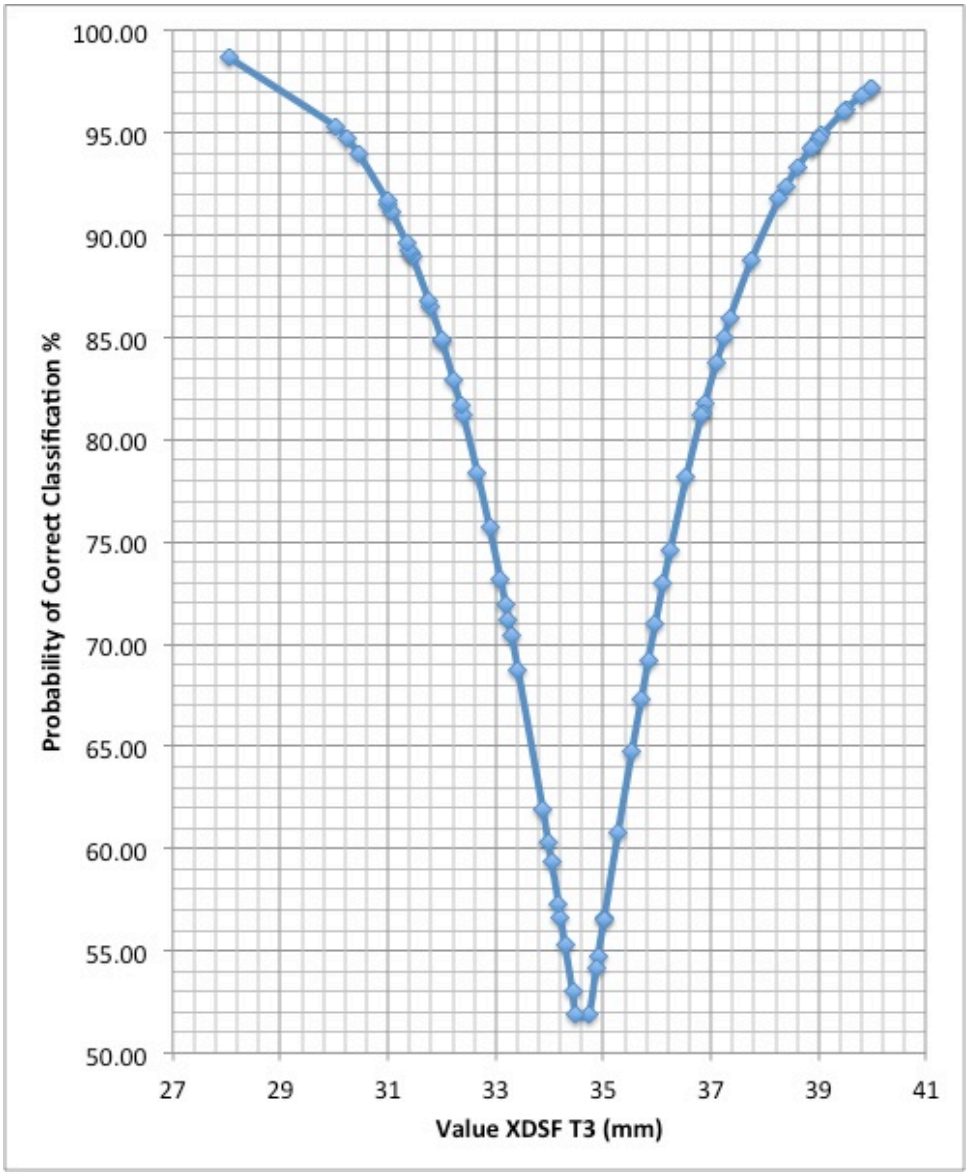

Posterior Probabilities T4 XBV:

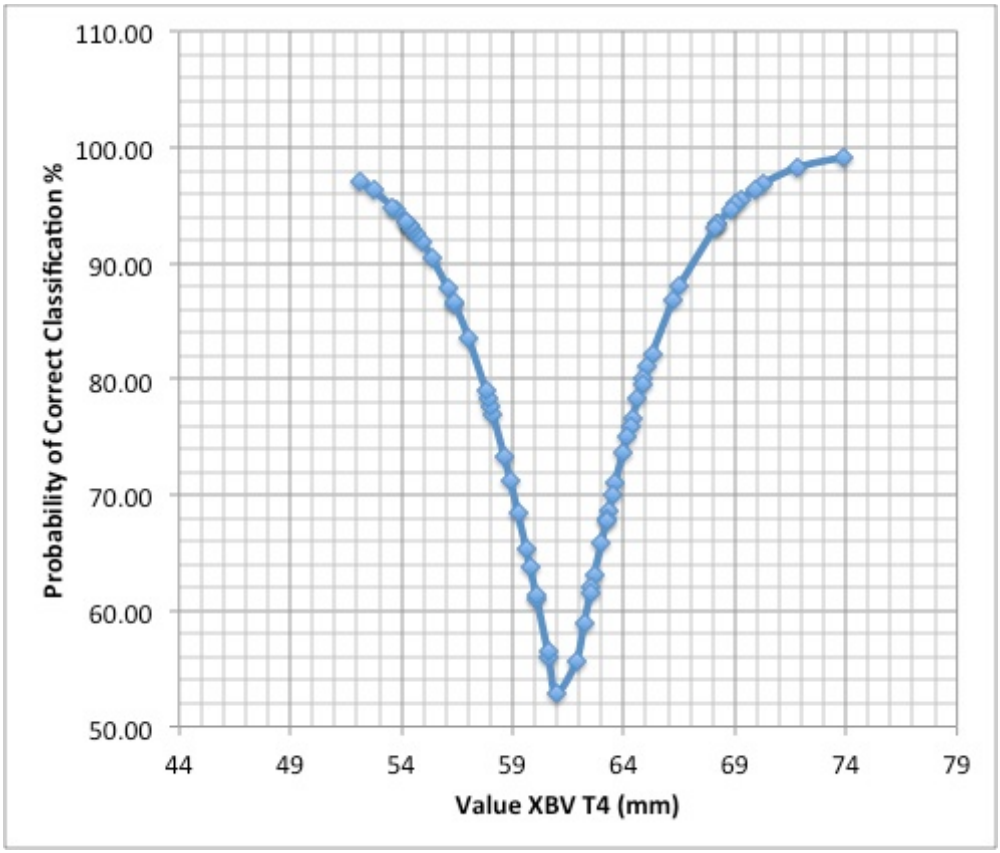

Posterior Probabilities T4 XBVBi:

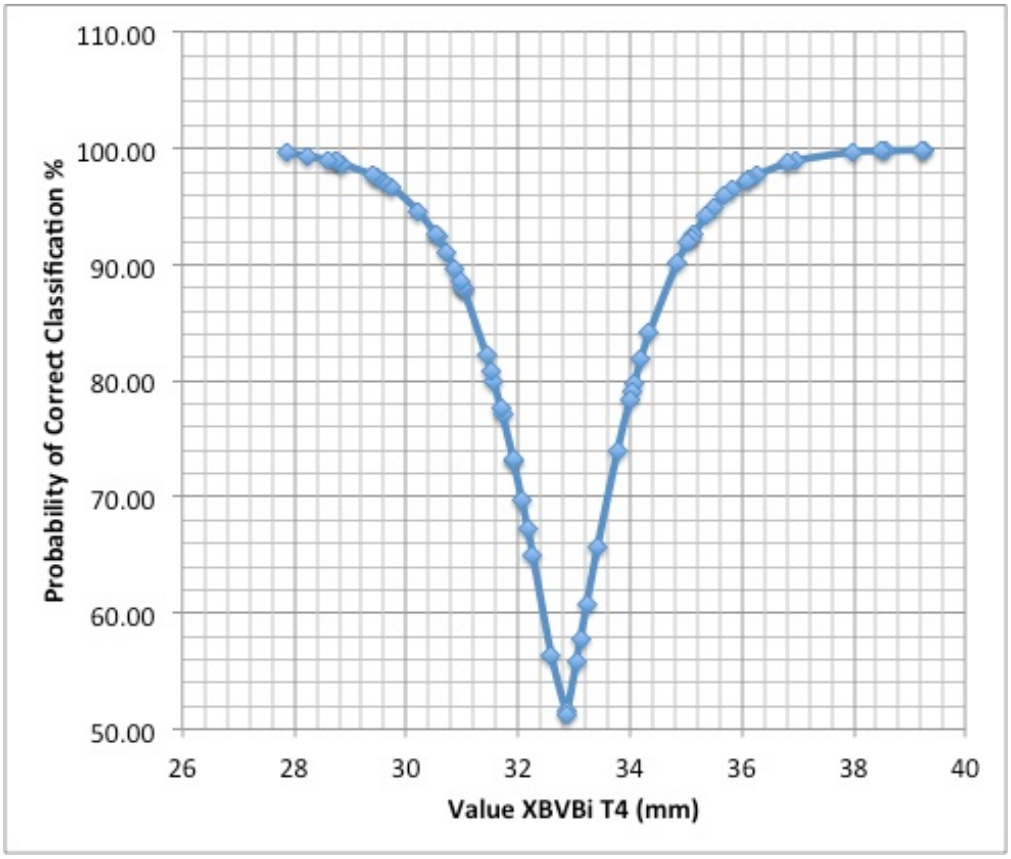

Posterior Probabilities T4 XLV:

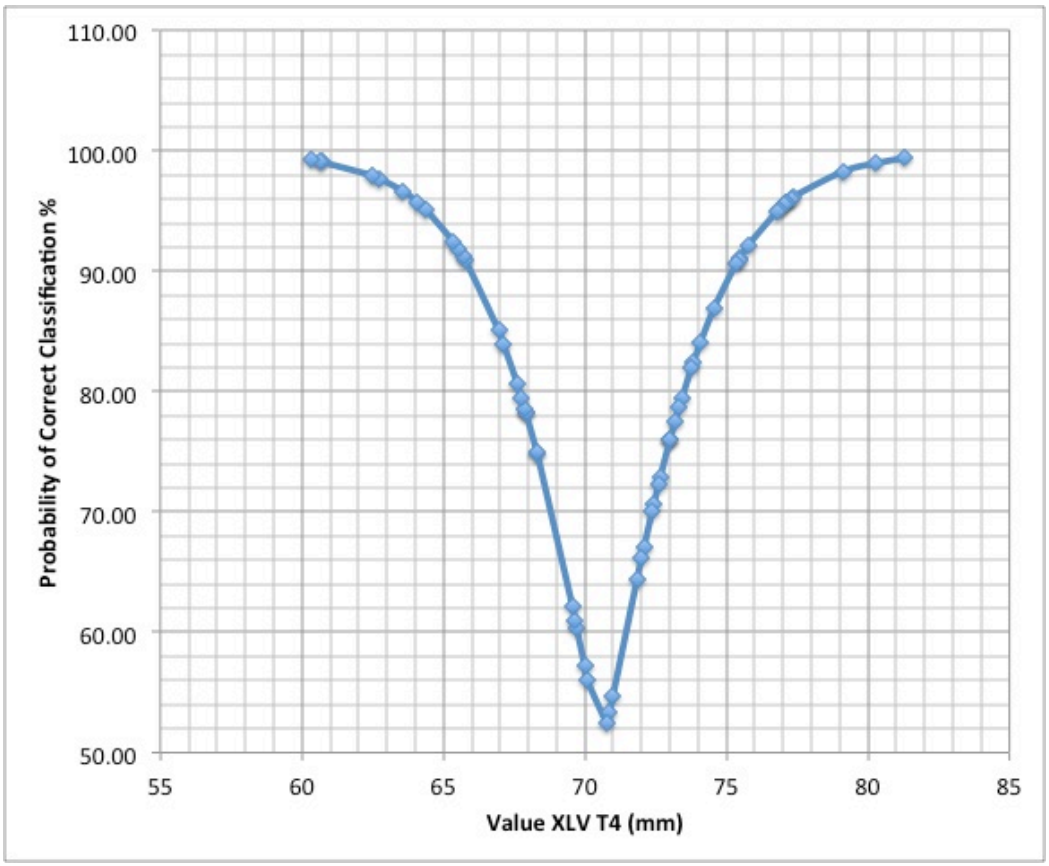

Posterior Probabilities T4 XLVBi:

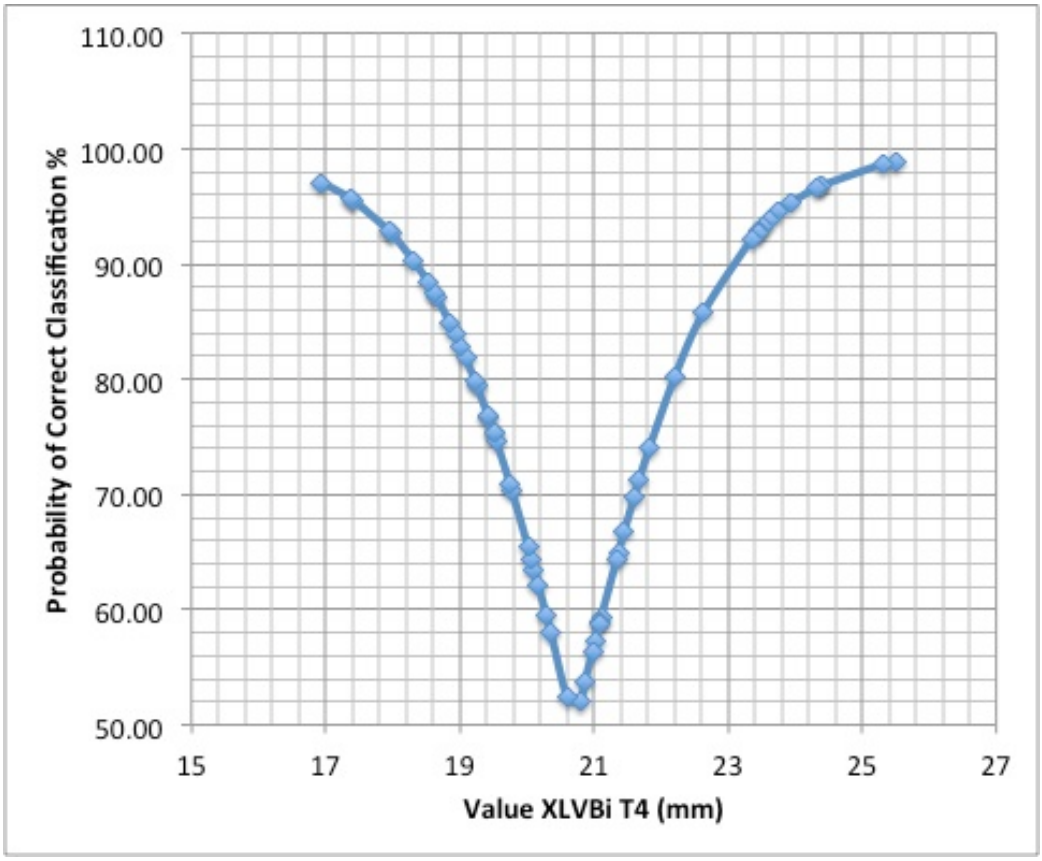

Posterior Probabilities T4 XLVBs:

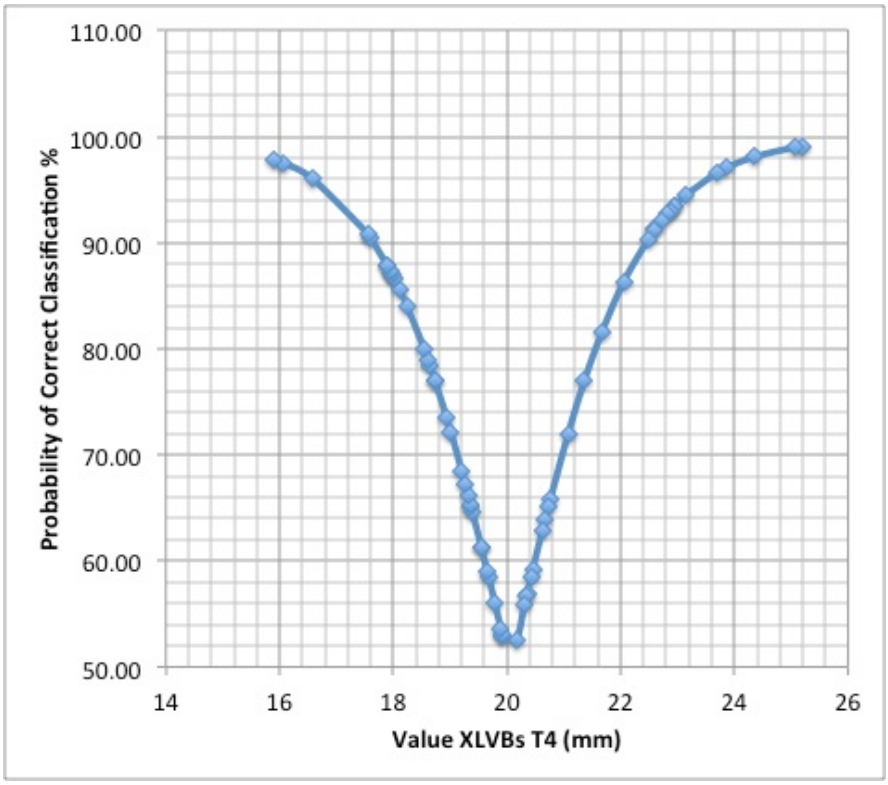

Posterior Probabilities T5 XBV:

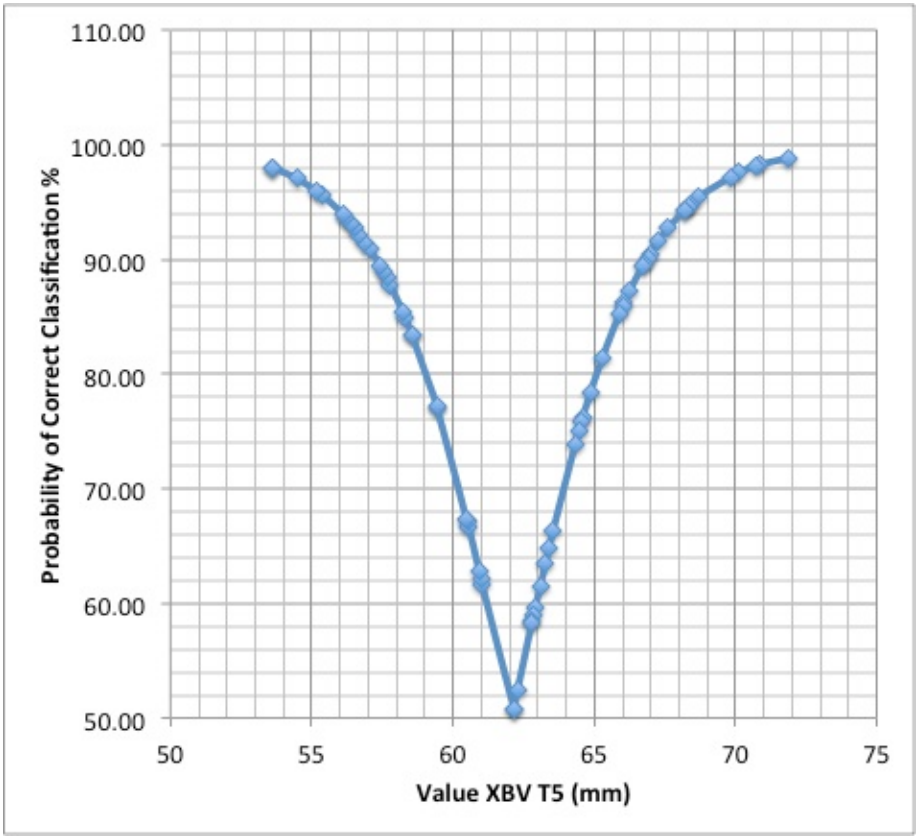

Posterior Probabilities T5 XBVBi:

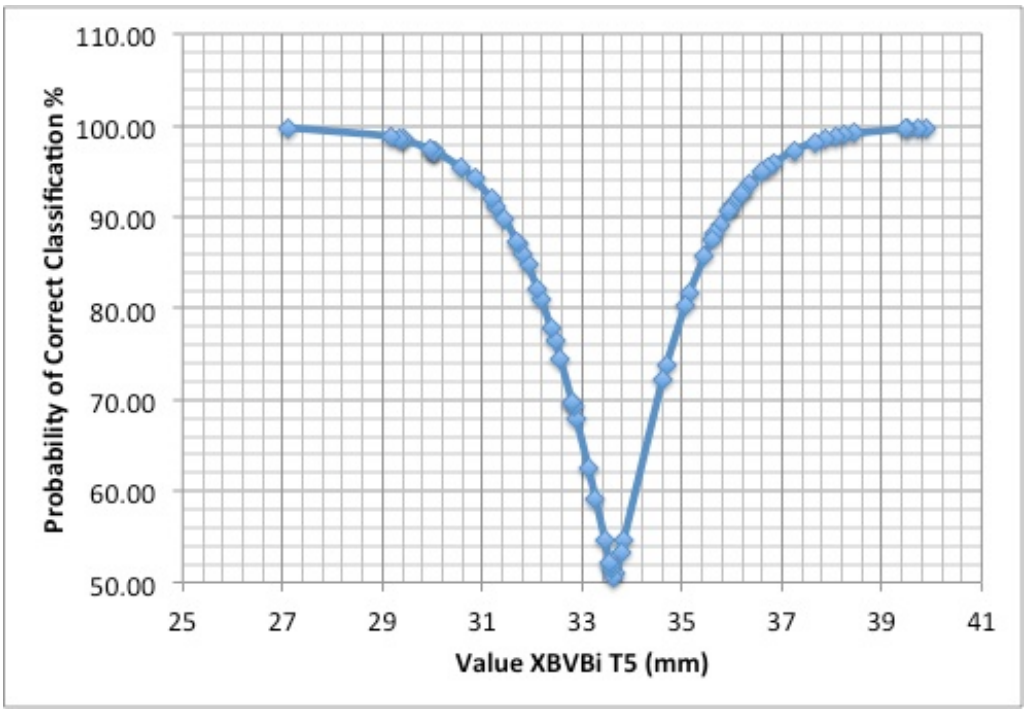

Posterior Probabilities T5 XLV

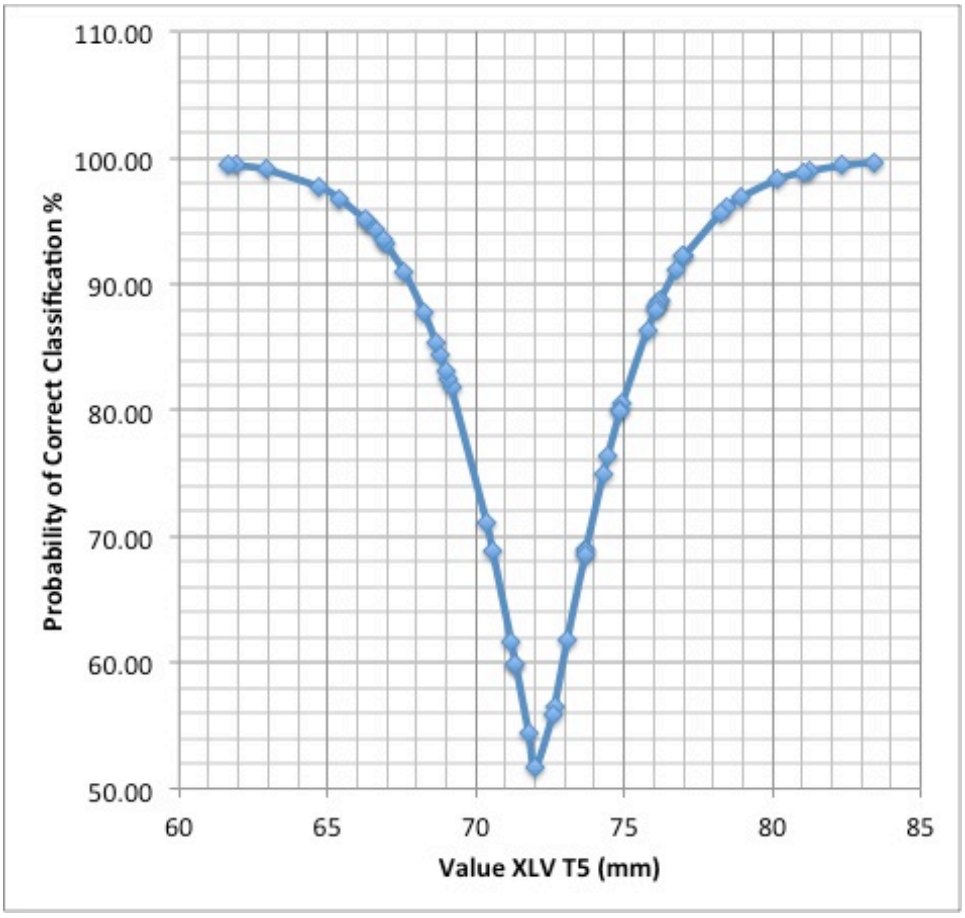

Posterior Probabilities T6 XBV:

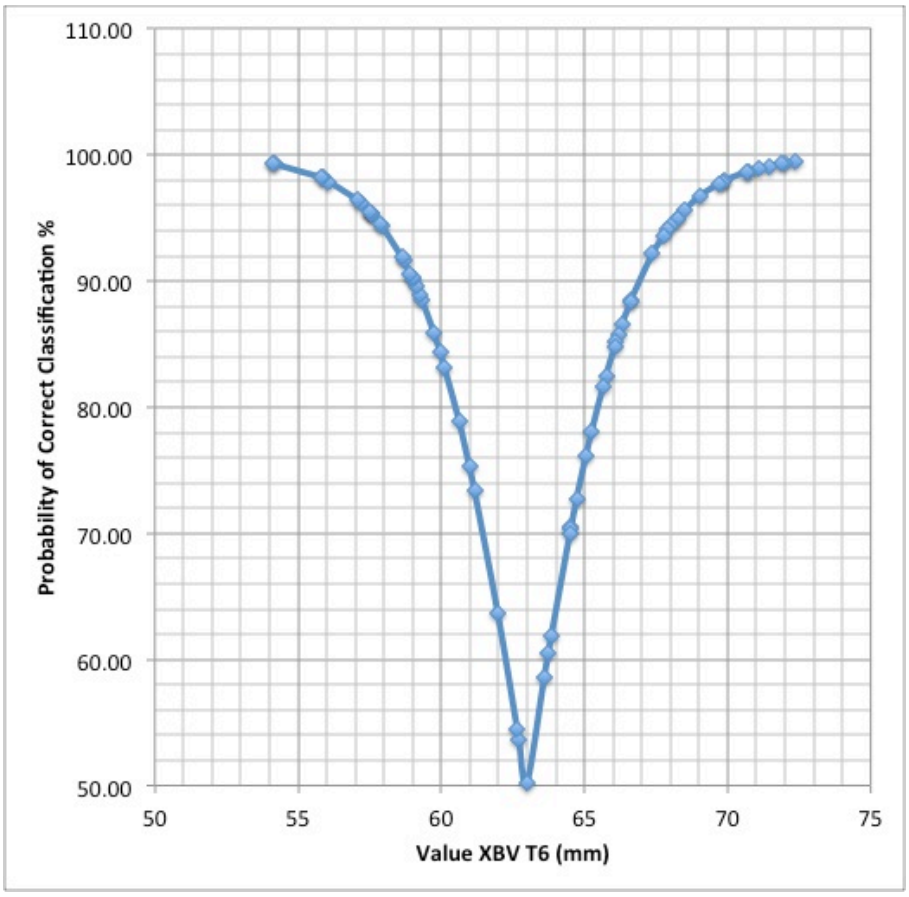

Posterior Probabilities T6 XBVBi:

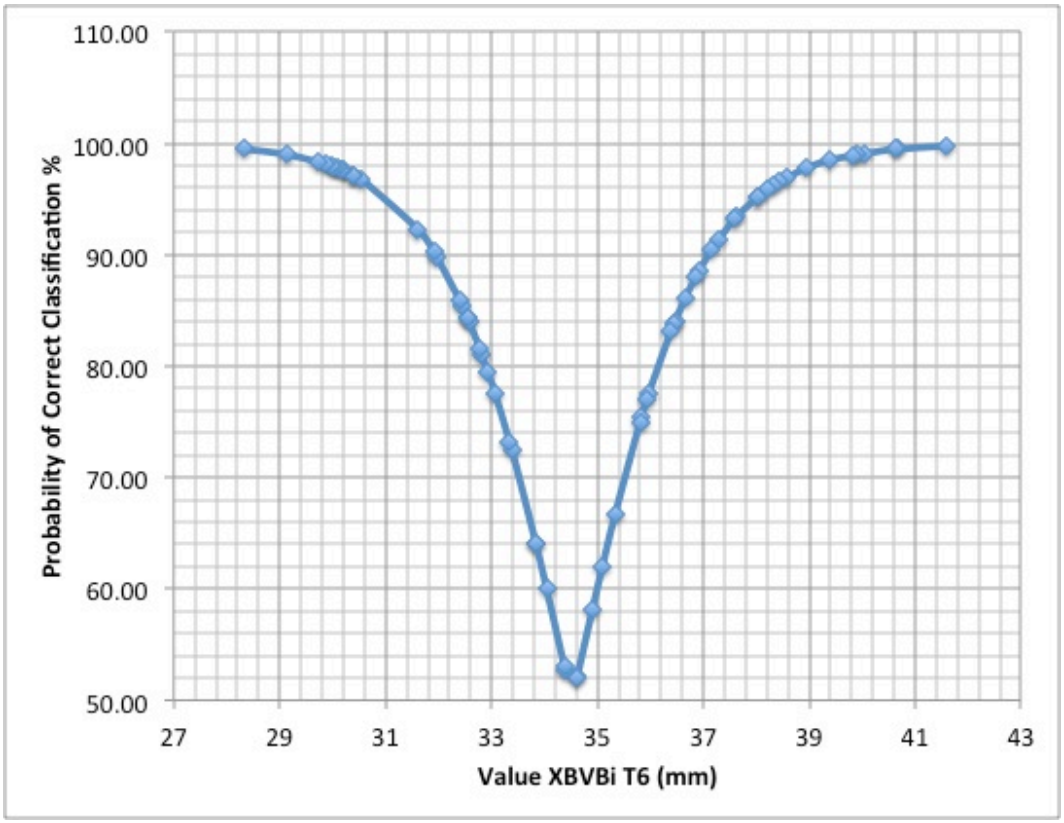

Posterior Probabilities T6 XLV:

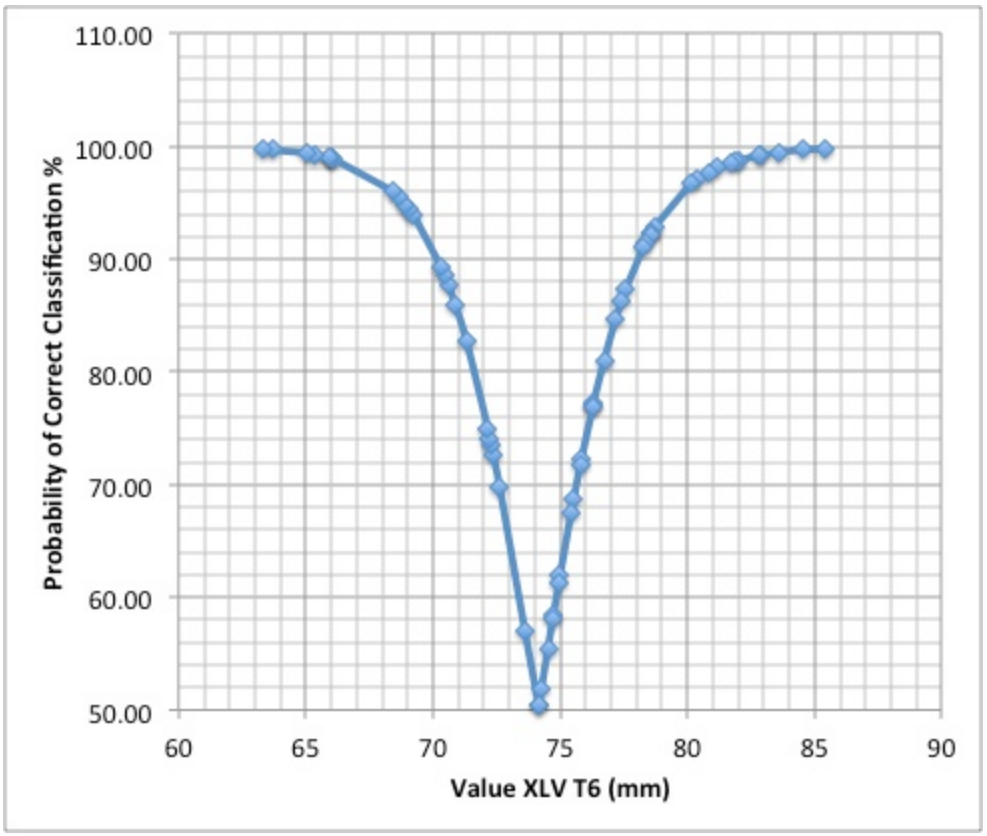

Posterior Probabilities T7 XBV:

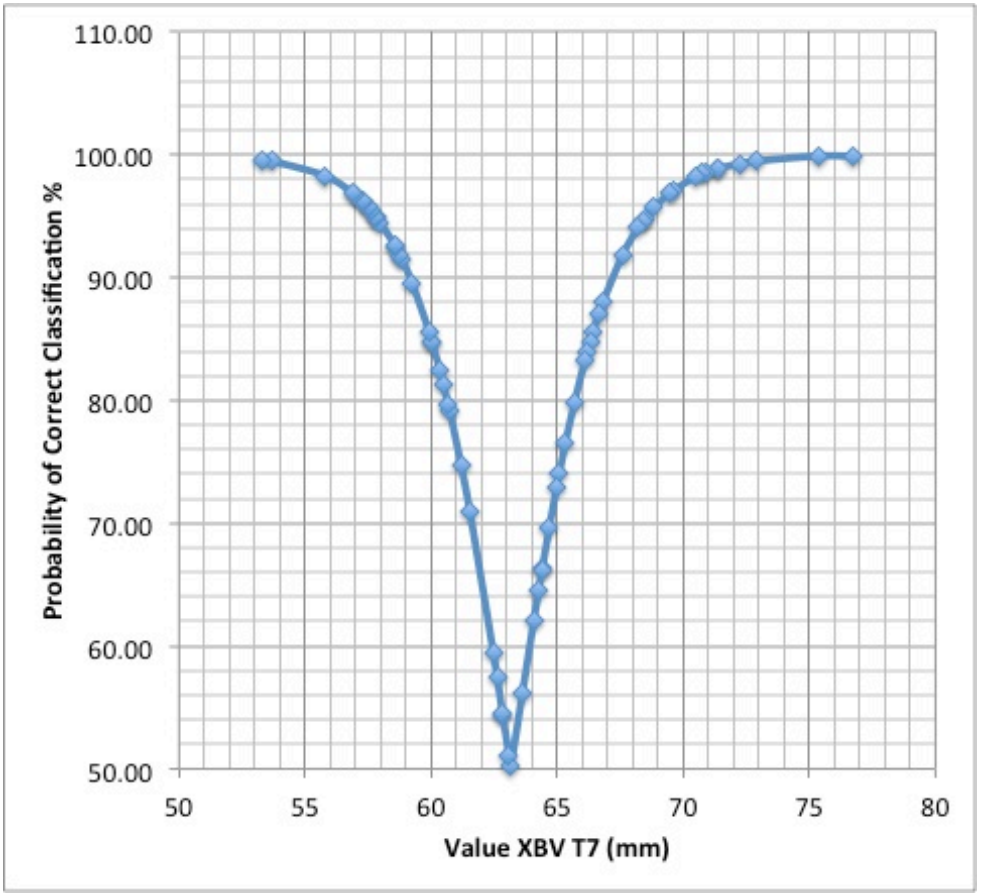

Posterior Probabilities T7 XBVBi:

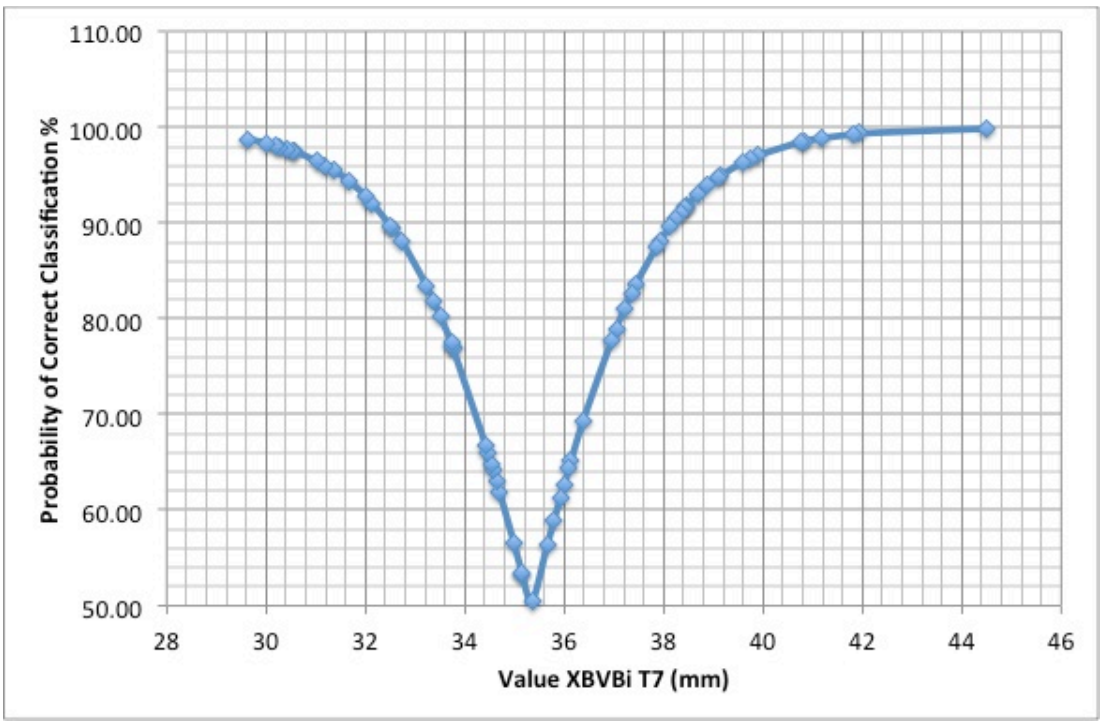

Posterior Probabilities T7 XDSF:

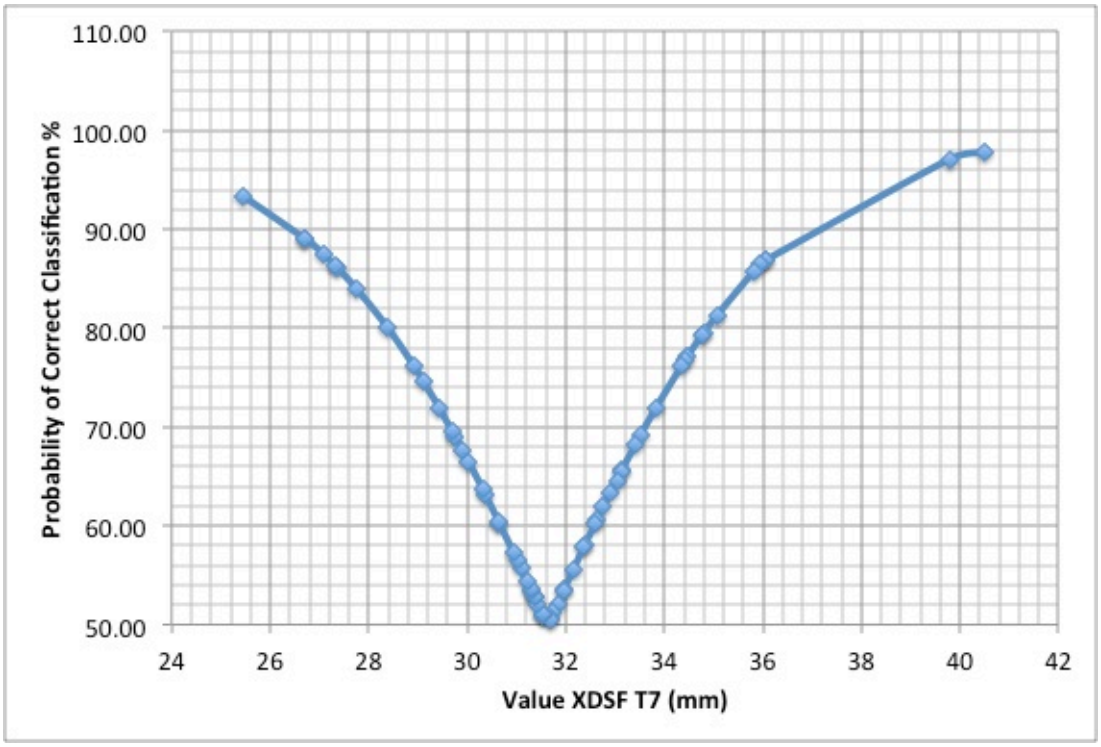

Posterior Probabilities T8 XBVBi:

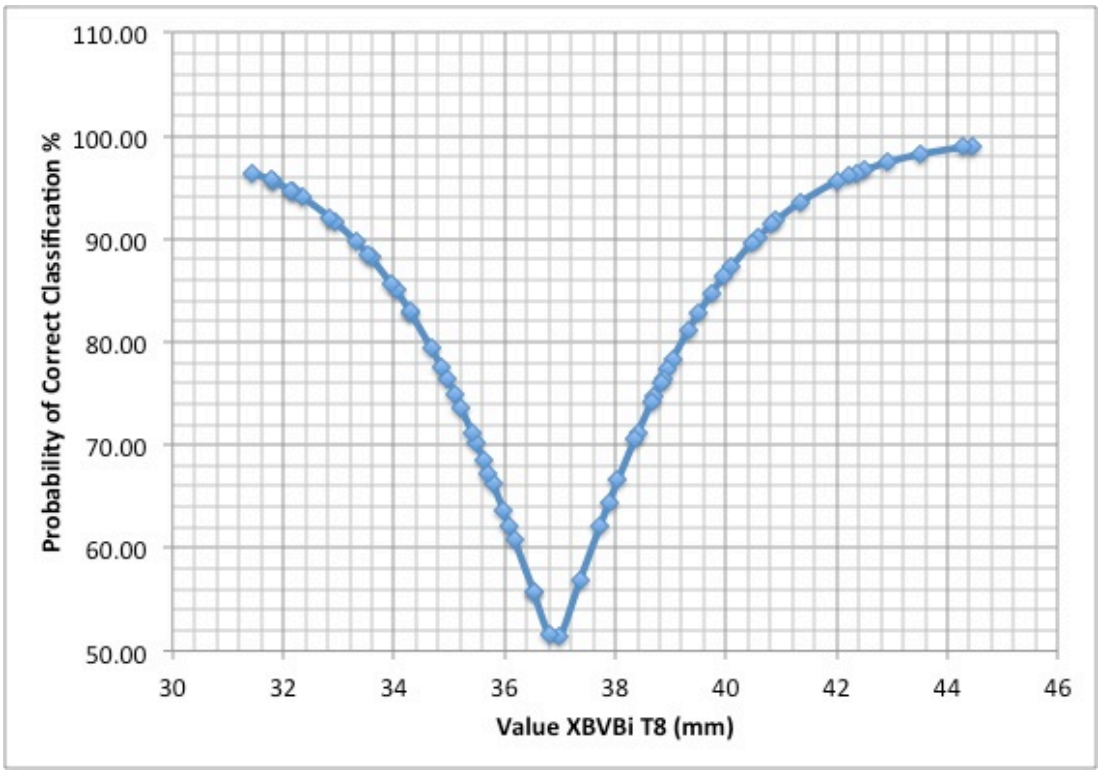

Posterior Probabilities T9 XBVBi:

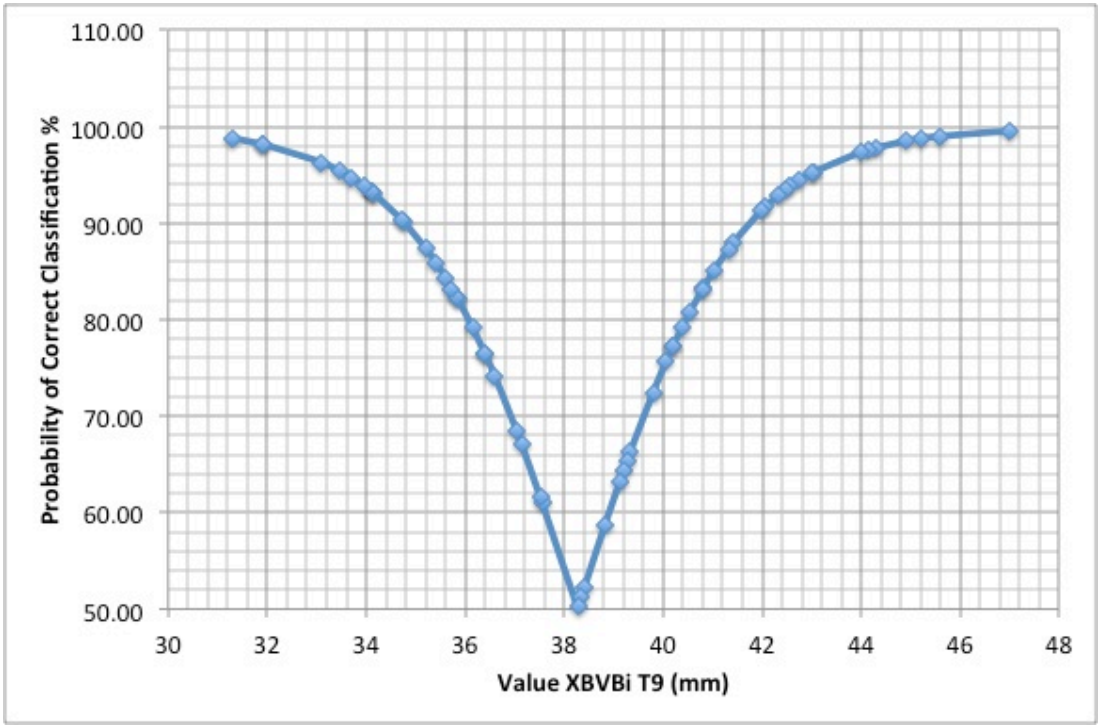

Posterior Probabilities T9 XLV:

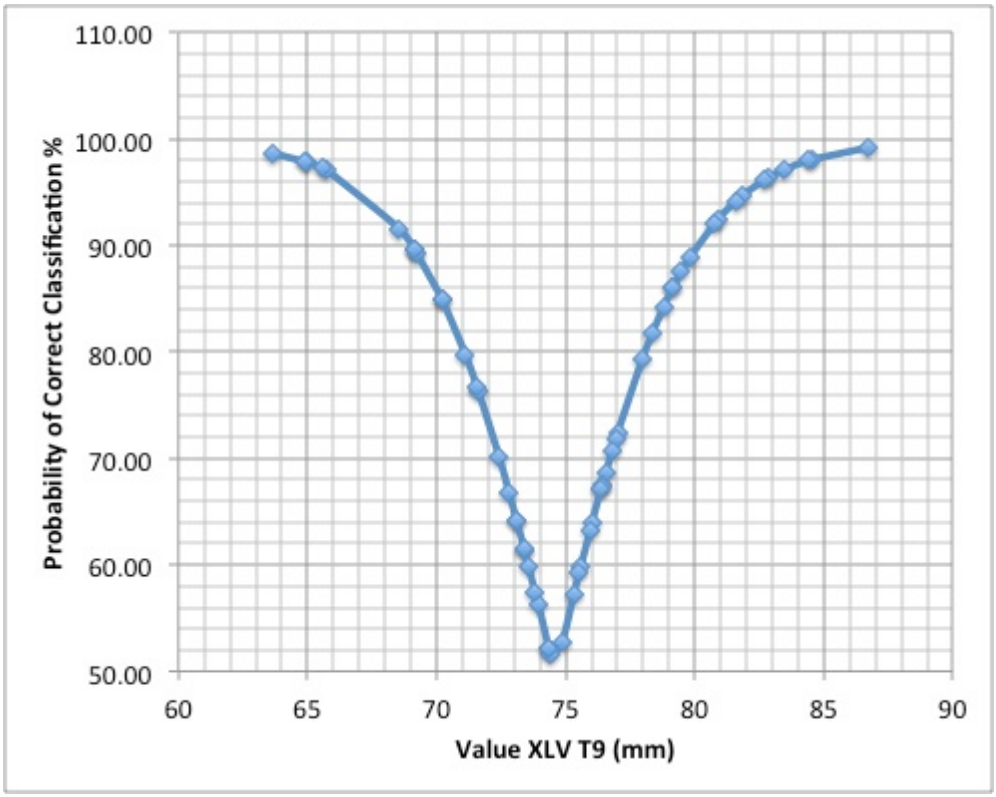

Posterior Probabilities T10 XDFc:

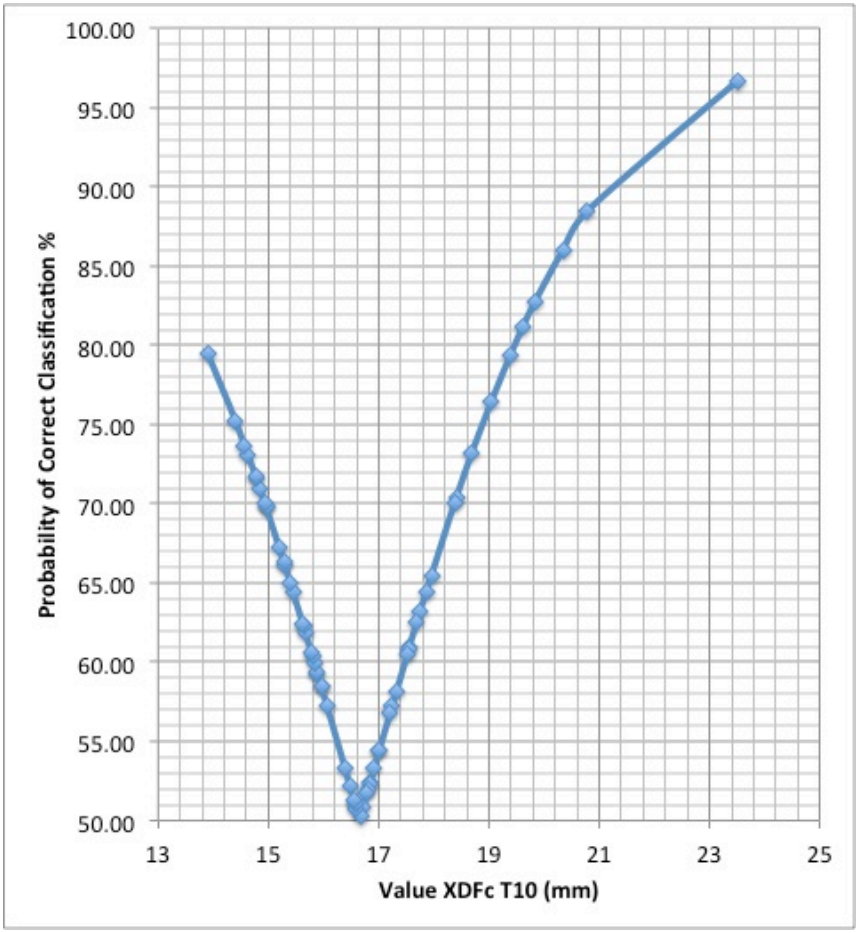

Posterior Probabilities T10 XLVBs:

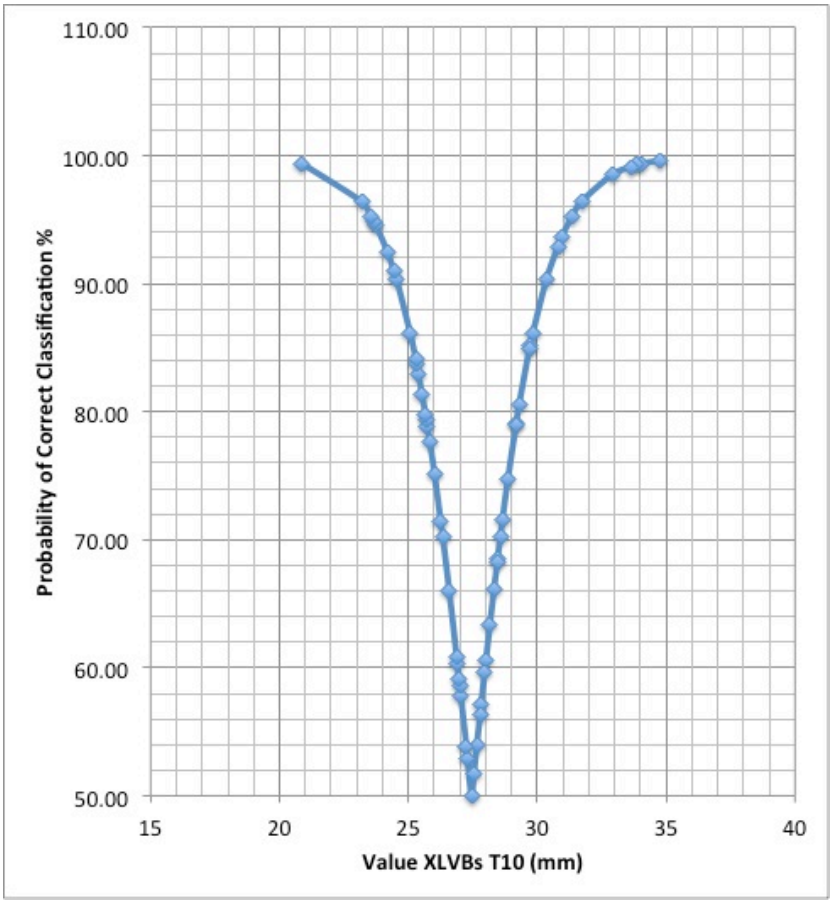

Posterior Probabilities T11 XBVBi:

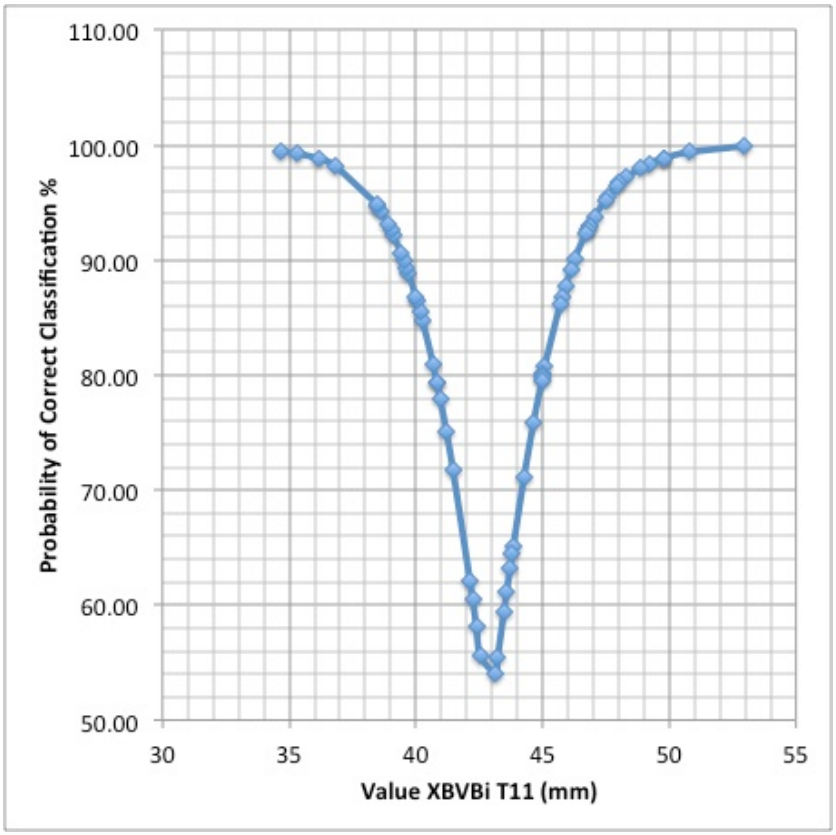

Posterior Probabilities T12 XBVBi

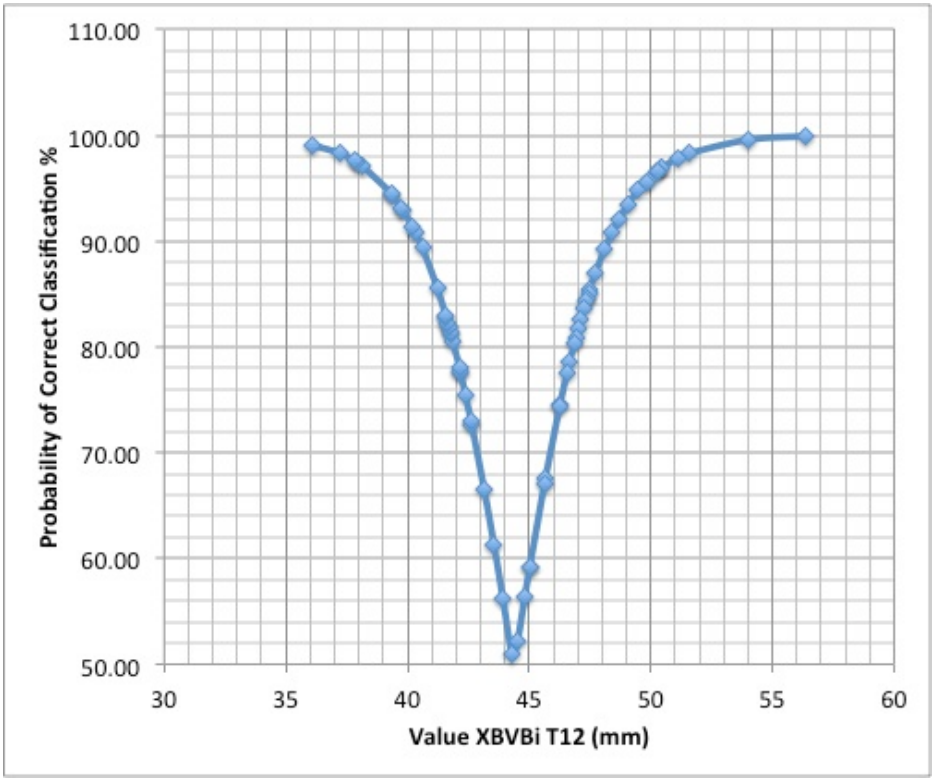

Posterior Probabilities T12 XLV:

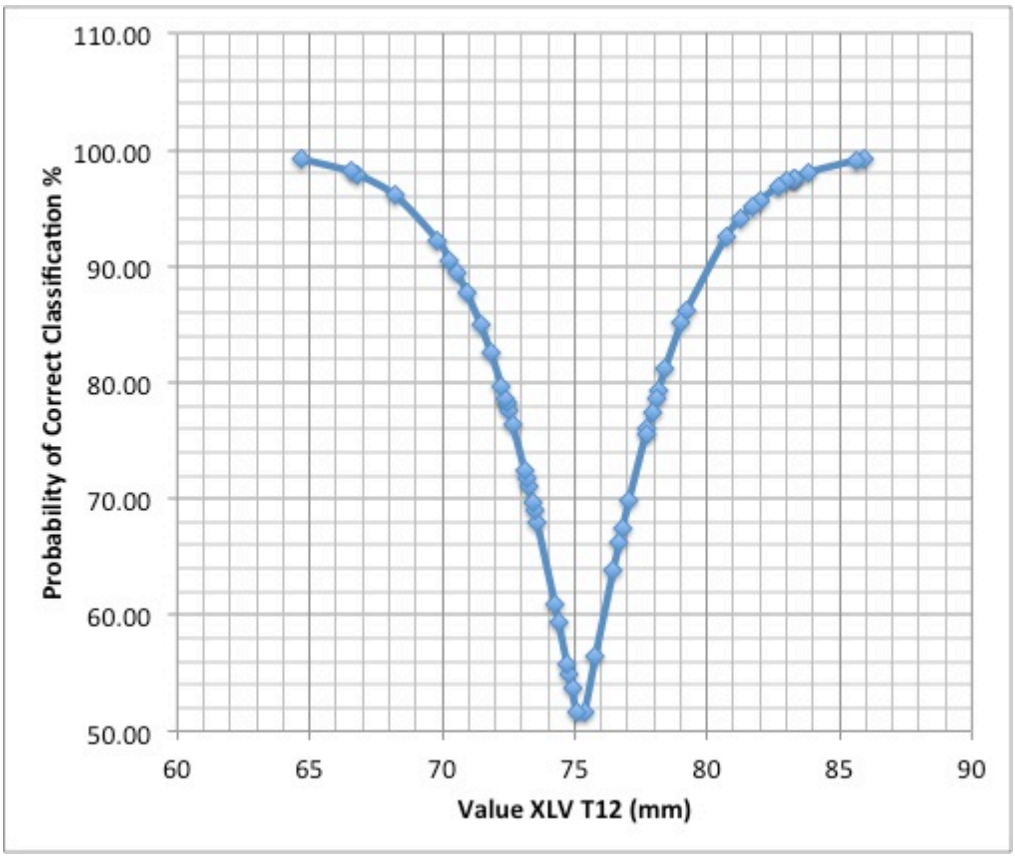

APPENDIX D: Performances above the 95% confidence level

Vertebra	Function	Accuracy %	n cases >95%
T1	Stepwise	90.6	38/64
	XBV	87.7	39/65
	XLV	87.5	22/64
	XLVBi	81.3	8/64
	XLVBs	80.0	13/65
T2	Stepwise	89.5	35/57
	XBV	83.1	27/65
	XDSF	82.5	10/63
	XBVBi	81.3	26/67
T3	Stepwise	86.4	35/66
	XBV	89.4	28/66
	XBVBi	86.6	26/67
	XDSF	83.1	7/65
	XHTP	82.1	7/67
T4	Stepwise	84.5	29/58
	XLV	85.0	17/60
	XBVBi	83.3	22/60
	XBV	82.5	8/63
	XLVBs	80.6	8/62
	XLVBi	80.4	9/56
T5	Stepwise	86.5	26/52
	XLV	86.8	14/53
	XBVBi	81.3	22/64
	XBV	80.0	11/65
T6	Stepwise	88.1	31/59
	XBV	84.8	23/66
	XBVBi	84.4	26/64
	XLV	82.2	22/61
T7	Stepwise	84.4	27/64
	XBV	87.5	21/64
	XBVBi	83.1	19/65
	XDSF	80.6	2/62
T8	XBVBi	82.3	15/57
T9	Stepwise	82.5	19/57
	XBVBi	83.3	14/60
	XLV	80.4	11/56
T10	XLVBs	81.0	10/58
	XDFc	30.3	1/61
T11	XBVBi	81.0	15/63
T12	XBVBi	83.3	15/66
	XLV	81.5	14/54